DESIGN SYNCHRONIZED TRANSCEIVER SYSTEM BASED ON FREQUENCY HOPPING SPREAD SPECTRUM

ISBN: 978-93-90753-97-0

Authored by
Khalid Awaad Humood
Ali Abbas Ali
Omar Abdulkareem Mahmood
Tahreer Mahmood

Published by
Novateur Publication
466, Sadashiv Peth, M.S.India-411030

Design Synchronized Transceiver System Based on Frequency Hopping Spread Spectrum

Authored By

Khalid Awaad Humood [1]

Ali Abbas Ali [2]

Omar Abdulkareem Mahmood [3]

Tahreer Mahmood [4]

[1,4]Department of Electronic Engineering, University of Diyala, Iraq
[2]Former Professor of Communication & Signal Processing, Isra University/Jordan
[3]Department of Communication Engineering, University of Diyala, Iraq

Acknowledgments

First of all, our deepest gratitude goes to ALLAH, the Compassionate, the Merciful for everything. I would like to express my sincere gratitude and thanks to my research group for the continuous support of my work. study. their patience and guidance helped us in all my time of research and the writing of this book. It was a great privilege to work and study under their guidance. My sincere thanks also go to all those helped and supported me during this work. Without their support it would not be possible to conduct this research book.

I am extremely grateful to my mother for her prayers, love and sacrifices. I am very much thankful to my wife and my sons for their love, understanding, prayers and continuing support to complete this work. Also, I express thanks to my friends for their support, without them I could have never completed this book. I express my special thanks to the department of electronic engineering college of engineering university of Diyala for their honest support throughout this research work.

Last but not the least, I would especially like to thank my country for their continuous support, represented by my sponsor, the university of Diyala.

Abstract

Frequency hopping spread spectrum (FH/SS) communication system has played a growing role in modern communication systems for both military and civil applications due to its unique features. It is one of the avoidances spread spectrum (SS) communication which is used in the jamming and interference environments. In FH/SS system, a synchronization reception with the code at the receiver is used for de-spreading the received signal and then a subsequent data recovery is followed. There are many available synchronization techniques that can be used in FH/SSS. Most of these techniques require complex search operations and hence need complex hardware.

In this book: a contiguous and noncontiguous parallel digital BPF banks for FH/SS transceiver system has been designed and implemented in real time successfully using MATLAB-Simulink. The above designed bank of filters is used as a simple and efficient approach for synchronization of the FH/SS transceiver system. Four FFH/SS transceiver systems using contiguous and noncontiguous BPF banks are proposed to transmitting at data rate 160 k bit/sec for frequency hopping rate of 160 k hop/sec. Four systems have been used to spread the transmitted data in the HF band, 18 MHz (3-21MHz), 37.2 MHz (3-40.2MHz) for ASK and BFSK FH/SSS using contiguous digital BPF banks respectively, 9.6 MHz (3-12.6 MHz), 19.2MHz (3-22.2MHz) for ASK and BFSK FH/SSS using noncontiguous digital BPF banks respectively.

Noncoherent detector is designed and simulated in the receiver due to Doppler effect. Two models of the jamming MTJ and HJ were designed and simulated. The proposed systems were examined in the presence of noise and two type of jamming: multitone and hopper. The obtained results proved that the proposed systems were passed these tests successfully.

Contents

Chapter Four
Design and Simulation of ASK FFH/SS Transceiver

Chapter Five
Design and Simulation FSK FFH SS Transceiver System

List of Abbreviations

AWGN	Additive White Gaussian Noise
ASK	Amplitude Shift Keying
AJ	Anti-Jamming
BFSK	Binary Frequency Shift Keying
BER	Bit Error Rate
BPF	Band Pass Filter
CDMA	Code Division Multiple Access
D/A	Digital-to-Analogue Converter
DFF	D Flip-Flop
DDFS	Direct Digital Frequency Synthesizer
DPLL	Digital Phase Locked Loop
DS	Direct Sequence
DS/SS	Direct Sequence Spread Spectrum
erfc	Complementary error function
FCC	Federal Communication Commission
FFH	Fast Frequency Hopping
FH	Frequency Hopping
FH/SS	Frequency Hopping /Spread Spectrum
FFH/SS	Fast Frequency Hopping /Spread Spectrum
FH/SSS	Frequency Hopping Spread Spectrum System
FFH/SSS	Fast Frequency Hopping Spread Spectrum System
FIR	Finite Impulse Response
FM	Frequency Modulation
FPGA	Field Programmable Gate Array
FSK	Frequency Shift Keying
FSRF	Frequency Selective Rayleigh Fading
GPS	Global Position System
HF	High Frequency
HJ	Hopper Jamming
HPF	High pass filter
IIR	Infinite Impulse Response
ISM	Industrial Scientific Medicine
LPF	Low Pass Filter
LPI	Low Probability of Intercept
MTJ	Multitone Jamming
NC	Noncoherent
PCS	Personal Communication System
PN	Pseudo-Noise
PLL	Phase Locked Loop
SFH	Slow Frequency Hopping
SFH/SS	Slow Frequency Hopping / Spread Spectrum

SFH/SSS	Slow Frequency Hopping / Spread Spectrum System
RF	Radio Frequency
SJR	Signal-to-Jamming Ratio S/J (dB)
SNR	Signal-to-Noise Ratio S/N (dB)
Sqrt	Square Root
SSS	Spread Spectrum System
TF	Transfer function
TH	Time-Hopping
PCS	Personal Communication System
VCO	Voltage Controlled oscillator

List of Symbol

B	Bandwidth
B_m	Message Bandwidth
B_{ss}	Spread spectrum signal Bandwidth
C	Channel capacity in bit per second (bps)
D	Division ratio
D_{JR}	Distance from the jammer to the receiver
D_{TJ}	Distance from the transmitter to the jammer
D_{TR}	Distance from the transmitter to the receiver
E_b	Average signal energy per data bit
F	Fraction
fc	Carrier Frequency
f_c	Center Frequency
f_{ct}	Cut off frequency
fg	Gurd band ($R_b/2$)
f_H	3dB Band Stop frequency
F_{IF}	Intermediate frequency
f_j	Frequency jamming
f_L	3dB Band Pass frequency
f_{m1}	The lower frequency modulations
f_{m2}	The upper frequency modulations
f_o	Frequency output
fr	Reference frequency
fs	Frequency sampling
G_P	Process gain
L	Diversity level
L_{SYS}	System implementation losses (in dB)
M	Level of FSK modulation
M_J	Jamming margin
ms	millisecond
n	Number of bits of maximum length linear feedback shift register
N	Noise Power
Ne	Number of errors bits during simulation time
N_f	Number of frequencies in total bandwidth
N_j	Number of jamming frequencies
N_0	Two-sided power spectral density of Gaussian noise
NT	Number of transmitted bits during simulation time
P_e	Probability of error
P(e/hi)	Conditional error probability
R_b	Data rate
R_h	Hopping rate

Rx	Receiver message
S	Signal Power
T_b	Data period
T_D	Time difference between the arrival of direct signal interference
T_J	Time for jammer
T_h	Hopping period
T_p	Processing time required by the follower jammer
Tx	Transmitter massage
V	Speed of the light
$F\Delta$	Frequency separation between successive carrier frequencies (For BFSK FH/SS) and it must be at least equal Bm for ASK FH /SS
α	Vector
η	Pulse duty factor
Z^{-1}	Time delay

Chapter one
Introduction

1.1 General Considerations.

The digital BPF is used in spread spectrum systems as ultra-wideband transceiver for low transmit power, low immunity to noise and interference, high data rate. Also, it is used in spread spectrum systems narrow band wireless transceiver for high selectivity, high immunity to noise and interference low data rate [1]. It is also used as basic element of a matched filter in tracking system for synchronization. Digital BPF is also used as adaptive or variable filter to cancel the noise or to make a parallel digital filter banks with adjustable cut off frequency [2]. In general, the digital BPF is used in spread spectrum system in three areas. Firstly, in transmitter to reject the one sideband of FSK modulator after spread the data [3]. Secondly in receiver, it is used to reject unwanted signals before de-spreading. Thirdly it is used in unit of synchronization as one part of matched filter, to achieve the tracking [4]. In this work design and simulate bank contiguous and noncontiguous parallel digital BPF banks for FFH/SS system receiver to achieve synchronization is presented.

1.2 Spread Spectrum Concepts.

Spread spectrum communications systems are often used when there is a need for message security and confidentiality, or when it is a requirement that the message be received error free [5]. A spread spectrum system is able to offer a very high degree of message security in a number of ways, depending on the system implementation. Such a system may spread the data over a very wide bandwidth, making it almost impossible for a narrow band receiver to decipher any useful information. Along a similar vein, the same system may be able to offer a very high degree of interference rejection, both from intentional and unintentional sources [6].

A spread spectrum communications system is usually characterised as one in which the transmission bandwidth is much greater than that necessary to transmit the required information. In addition, demodulation must be accomplished by correlating the received signal with a replica of the signal used to spread the information [7]. Spread spectrum modulation system was initially designed to permit digital data transmission under the difficult condition of very low signal-to-noise ratio (SNR) due to the low signal level and the presence of intentional or unintentional co-channel interference [8]. To be classified as spread spectrum, the modulation signal bandwidth must be at least 10 to 100 times the information rate, and must be independent of information bit rate [9]. Spread spectrum systems have many features, such as: selective addressing capability, CDMA, low power spectral density, message screening from eavesdroppers, navigation and high-resolution ranging, interference rejection and improved reliability in frequency selective fading and multipath environment [10]. There are several basic spread spectrum techniques available for use in digital data communication, these are:

a- DS: in which the energy of the required baseband transmission spreads over the required bandwidth by multiplication with a pseudo-random digital code sequence at an appropriate rate.

b- FH: in which the instantaneous frequency of the baseband transmission is changed in pseudo-random manner over the required bandwidth.

c- Pulsed FM or chirp: in which the instantaneous frequency of the transmission is swept across the required bandwidth in an appropriate manner.

d- TH: in which high-power bursts of wideband transmission occur at pseudo-random intervals of time.

e- Hybrid techniques: in which two of above-mentioned techniques are combined (e.g. DS/FH, DS/TH…etc.).

1.3 Spread Spectrum Technique.

Spread spectrum uses wide band, noise-like signals. Because spread spectrum signals are noise-like; they are hard to be detected. Spread spectrum signals are also hard to be intercepted or demodulated. Further, spread spectrum signals are harder to jam than narrow band signals.

These LPI and AJ features are why the military has used spread spectrum for so many years. Spread signals are intentionally made to be much wider band than the information they are carrying to make them more noise-like [11]. These special "spreading" codes are called "pseudo random" or "pseudo noise" codes. Spread spectrum transmitters use similar transmit power levels to narrow band transmitters. Because spread spectrum signals are so wide, they transmit at a much lower spectral power density, measured in watts per hertz, than narrow band transmitters. This lower transmitted power density characteristic gives spread signals a big plus. Spread and narrow band signals can occupy the same band, with little or no interference. This capability is the main reason for all the interest in spread spectrum today [12].

1.4 Channel Capacity of Spread Spectrum

The basis for spreading the spectrum of an information bearing signal is Shannon's well-known theory which suggests the following exchange between SNR and bandwidth technology can be derived from channel capacity as follows [12,13]:

$$C = B \ \mathrm{Log}2\left(1+\frac{S}{N}\right) \tag{1.1}$$

where:

C: channel capacity in bit per second (bps).

B: bandwidth in Hertz.

N: noise power in watt.

S: signal power in watt.

This equation shows the relationship between the ability of the channel to transfer error-free information in comparison with the signal-to-noise

power ratio existing in the channel and the bandwidth used to transmit the information.

Thus, for any given noise-to-signal power ratio (N/S), it can be seen that a low information-error rate can be achieved by increasing the bandwidth used to transfer the information. It is not possible by any encoding method to send at a higher rate and have an arbitrarily low frequency of errors. Shannon's expression for channel capacity represents the theoretical upper limit on data rate where arbitrarily small probability of bit error can be achieved with coding. In practical systems it is difficult to transmit at or near the capacity limit because the system complexity increases in proportion to the complexity of the coding scheme; and, the randomness of the system noise will tend to limit the number of discrete subdivisions of the signal that can be distinguished reliably [13].

1.5 Literature Survey.

Most of the previous works dealt with the design or analysis of a particular part of the frequency hopping system like the synthesizer, synchronization, modulation, demodulation and interference the previous works related to the present work are:

Scholtz, [14] introduced the Wozencraft Iterated Coding System (WICS) which is one of the earliest FH communication systems. This teletype FH system was developed in mid-1950 s. It employs 155 different tones in a 10 kHz band to communicate at 50 words/minute.

Mundy and Pinches, [15], designed and implemented the Jaguar-V frequency hopping radio system which was developed by Racal Electronics Ltd for the British Army in the early 1980s. The hop rate was 50-500 hops/sec and the frequency synthesizer is based on a conventional single loop PLL with use of a dual modulus presacral.

AL-Muraab [16] implemented a frequency hopping transmitter and receiver connected back-to-back. The modulation was FSK, the PN sequence length

was $15(2^4-1)$, the frequency synthesizer was a DPLL with settling time of 250 msec, and the transmitted frequencies were in the range of 145 kHz-211 kHz, with low data rate.

Meng [17] designed and analyzed of a coherent FH/SSS operating in the presence of both jamming and a nonideal channel response.

Glisic [18] achieved a new tracking approach for SFH/SS signal based on utilization of additional synch data carrying information for FH signal tracking purpose, which is added to the digital data stream.

Glisic [19] introduced a new algorithm for discrete tracking of SFH/SS signals. Each group of hopping is completely used for transmission of synchronization data. The motivation for introducing this algorithm is that it allows a large degree of flexibility with respect to trade of system performance, complexity and the redundancy introduced for tracking purposes.

Miller and lee [20] used parallel matched filter with adaptive threshold to reduce the acquisition time.

Borth [21], proposed an SFH personal communication system (PCS). In that system, the carrier hops at a rate of 500 hops/ sec. The hopping frequency synthesizer is based on a PLL and achieved a settling time of 0.6 msec.

Chen [22] analyzed the detectability of the frame synchronization codes with such frame scheme under additive white Gaussian noise channel, applying decorrelation method to perform once observed detection, major decision detection and accumulation posterior detection. The analyses showed accumulation posterior detection method can give better performance under the strict restrictions.

Samuel [23], analyzed and designed a FH/SS transceiver for wireless personal communications. This design proposes SFH-CDMA transceiver with hop rate of 20 k hop/sec and data rate of 80 k bit/sec. The hopping frequency synthesizer is based on a PLL and achieved a settling time of 600 μ sec. Subhi [24], implemented a wireless FH system by using a programmable transceiver and a microcontroller to test the proposed synchronization method. The system was intended at a low hopping rate.

Hammed [25], designed and implemented a frequency hopping communication system for both speech and data signal with hopping rate 9.6 k hop/sec and data rate 9.6 k bit/sec. Chail [26], designed and implemented a branch hopping wavelet packet system instead of implementing FH/SS, in the first part of this work the synchronization had been assumed perfect and the system working in low frequency band. Al-Fhaam [27], designed fast and multi carrier frequency hopping signals over Frequency Selective Rayleigh Fading channel (FSRF). This work proposed only theory without any numerical data for input or output results and without synchronizations between transmitter and receiver.

Evaluation of different quantization resolution levels on the BER performance of massive MIMO systems under different operating scenarios and An efficient technique to PAPR reduction for LTE uplink using Lonzo's resampling technique in both SC-LFDMA and SC-DFDMA systems [28, 29, 30, 31].

The above works suffer from one or more of the following drawbacks which are: -

1. Some of the above works are not study the jamming effect on those presented systems.
2. All the above works deal with slow settling time such as 250 m sec, 600 μ sec.
3. Some of above works assume there are perfect synchronization between transmitter and receiver.
4. All the above works do not mention anything about contiguous and non-contiguous filters techniques.
5. All the above works do not show the shapes of the signals at different stages of the work.
6. All the above works deal with low data rate such as 10 k bit/sec, 20 k bit/sec.
7. Most of the above works do not work in real time operation.
8. All the above works are not given clear idea about modulation or demodulation, such coherent or noncoherent, related with that works.

1.6 Aims of The Work.

The aims of the present work are to:

1. design and simulate a parallel digital BPF banks for FH/SS transceiver system using MATLAB-Simulink.
2. design and simulate a wireless transceiver for ASK and BFSK FH system using MATLAB-simulink with following properties:
   a. the system spreads transmitted data in high frequency (HF) band with hopping rate 160 k hop/sec and data rate 160 k bit/sec.
   b. design and simulate ASK demodulator to achieve the detection of data for ASK FH/SS system.
   c. design and simulate BFSK modulator to modulate the data for BFSK FH/SS system.
   d. design and simulate noncoherent demodulator to achieve the diction of data for FSK FH/SS system.
3. design and simulate two type of jamming model MTJ and HJ.
4. investigate the performance of the proposed systems in the presence of two model of jammers (MTJ and HJ) and noise.
5. investigate the performance of FH/SS by seeing the shape of the signals at different sequent stages of the designed systems.

1.7 Book Layout.

This book consists of six chapters:

- **Chapter one**: includes general consideration, spread spectrum concept, how spread spectrum works, channel capacity of spread spectrum, literature survey, aim of the work, and book outline.
- **Chapter two**: presents a review for the frequency hopping system and the related theory.

- **Chapter three**: covers the proposed design and simulation of contiguous and noncontiguous digital BPF banks for ASK and FSK FH/SS systems.
- **Chapter four**: is concerned with the proposed design and simulation of ASK FH/SS transceiver systems using contiguous and noncontiguous digital BPF banks.
- **Chapter five:** presents the proposed design and simulation of BFSK FH/SS transceiver systems using contiguous and noncontiguous digital BPF bank filters.
- **Chapter six:** gives the conclusions, recommendations and suggestions for future work.

CHAPTER TWO

Frequency Hopping Spread Spectrum

2.1 Introduction.

This chapter a concentrate on giving FH system, therefore many topics related to the FH are presented such as why it is preferred to the DS especially in secure applications. A comparison is made between SFH and FFH. Also, this chapter state the following: system background, parameter of FH, performance of FH in the presence of noise and jamming. A review to other topics related to the work is presented such as DDFS, indirect DDFS and synchronization of FH.

2.2 System Background

A FH communications system differs markedly from a DS system. Whereas in a DS system, the carrier frequency remains constant, and the data is spreading over a wide band of frequencies, in a FH system, the data is transmitted using a conventional narrow band technique, but the carrier frequency is changed in discrete hops over a wide bandwidth. A typical FH spectrum is shown in Figure (2.1). Note that the bandwidths of each individual carrier may or may not overlap depending on the system design [32]. This technique is also very secure in that a narrow band receiver will be unable to detect any useful information, receiving just a short burst of information on odd occasions. FH systems also have the ability to reject both intentional and unintentional interference, although somewhat more involved than the direct sequence case [33] .

A FH transmitter is shown diagrammatically in Figure (2.2). The receiver uses the same technique as the transmitter, but in reverse, along a similar line to the DS/SS transmit/receive pair. Note that although a second mixer stage and RF oscillator are shown, their application depends on the desired carrier frequency.

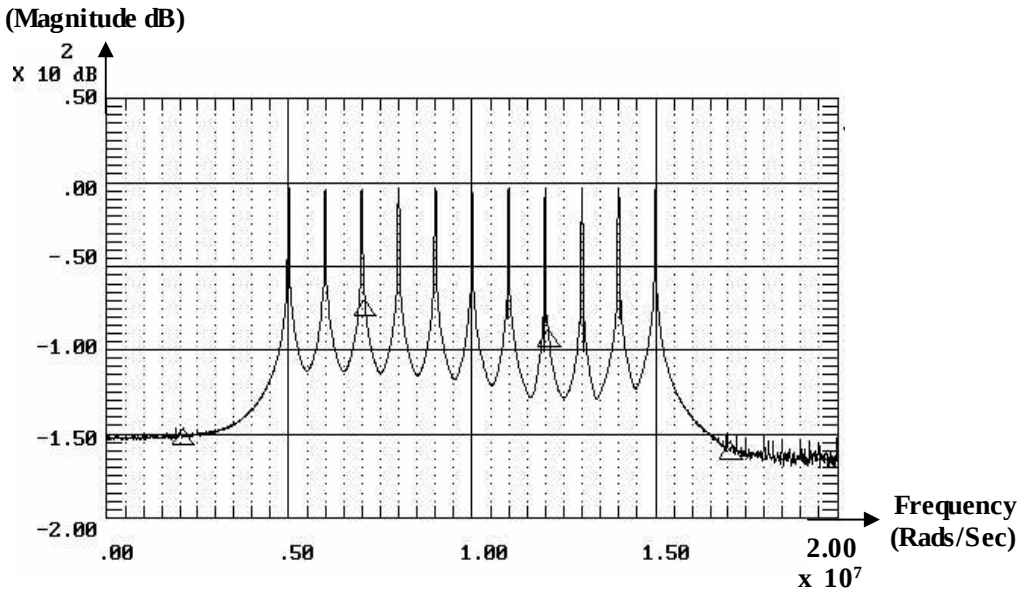

Figure (2.1) A typical frequency hopping spectrum.

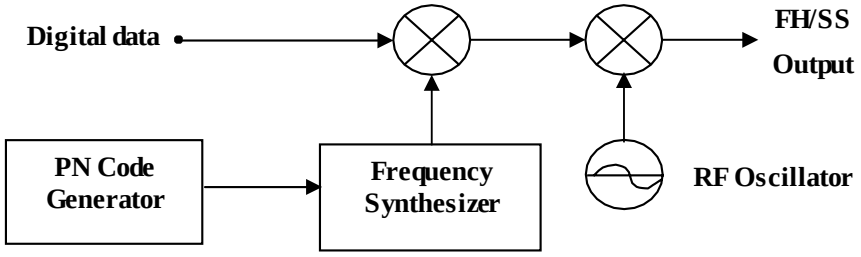

Figure (2.2): FH/SS transmitter.

If the synthesizer is able to function at the required rate and generate the appropriate frequencies, then there is no need for a subsequent mixing stage [34]. In FH/SS, the signal itself does not spread across the entire large bandwidth; instead, the wide bandwidth is divided into sub- bands, and the signalhops from one band to the next in a pseudorandom manner.

FH system is nothing more than FSK except that the set of frequency choice is greatly expanded [35]. A FH system consists basically of a code generator and a frequency synthesizer capable of responding to the coded output of the code generator [36] . Typically, each carrier frequency is chosen from a set of 2^n frequencies which are spaced approximately by the data rate [3,12]. The simplified block diagrams of ASK and FSK FH system, are shown in Figures (2.3) [26] and (2.4) respectively.

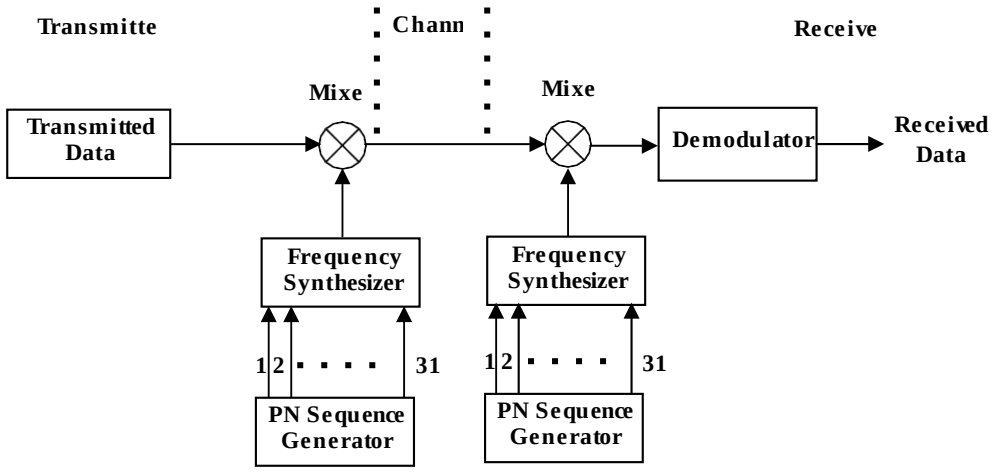

Figure (2.3): Simplified block diagram of ASK FH system.

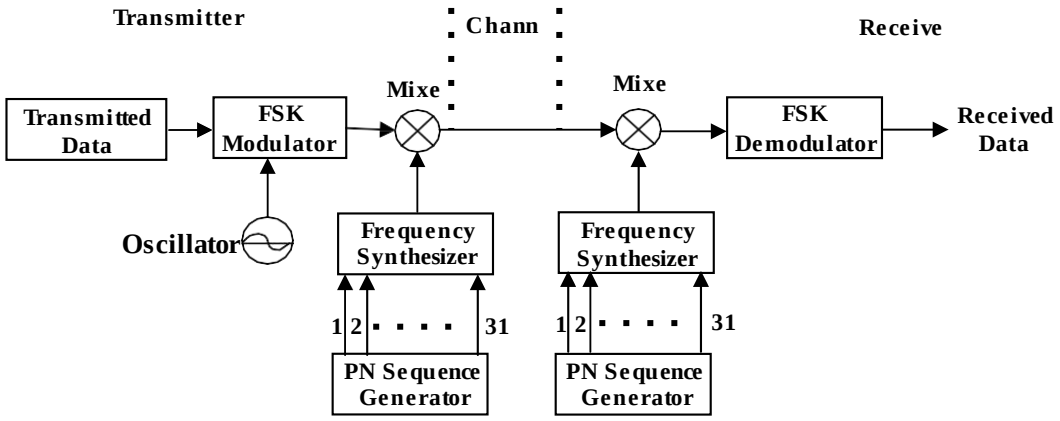

Figure (2.4): Simplified block diagram of FSK FH system.

The PN code generator is a sequence that consists of statistically independent symbols (pseudo-random one's and zeros) called chips. The PN sequences have the properties of random noise. The PN sequences used in spread spectrum communication is usually periodic. The PN sequence has the following properties [37]:

(a) they are easy to generate, (b) they have good statistical randomness properties, (c) they have long period, (d) they are difficult to reconstruct from short segments.

One of the most effective devices for generating a PN code is the maximum length linear feedback shift register.

The clock of the PN code is one of the basic factors which limit the settling time [38,39].

2.3 Parameters of FH System.

The important parameter is the processing gain (G_P), which is defined as the ratio of the bandwidth of spread spectrum signal (B_{SS}) to the information bandwidth (B_m) [13], and it is given by:

$$G_p = \frac{B_{ss}}{B_m} \tag{2.1}$$

$$B_{ss} = \left(2^n - 1\right)\Delta F \tag{2.2}$$

$$Bm = \Delta F \tag{2.3}$$

where:

ΔF: frequency separation between two successive carrier frequencies,

n : the number of bits of the maximum length linear feedback shift register

$$Gp = \left(2^n - 1\right)\frac{\Delta F}{\Delta F} \tag{2.4}$$

In the design of practical system P_G is not, by itself a measure of how well the system is capable of performing in jamming environment. For this purpose , the jamming margin is introduced .This margin (M_J) is the amount of interference that the receiver can withstand while operating and producing an acceptable output signal-to-noise ratio in the jamming environment [7]. It is defined as:

$$M_J\ (dB) = G_p\ (dB) - \left(\frac{S}{N}\right)_{min}\ (dB) - L_{sys}\ (dB) \tag{2.5}$$

where:

S/N : signal-to-noise ratio at output of the channel in (dB).

L_{sys} : system implementation losses in (dB).

It could not be expected to operate with interference more than jamming margin above the desired signal.

2.4 Slow Frequency Hopping (SFH).

When the hopping duration (T_h) is larger than the data duration (T_b) of one information bit, as shown in Figure (2.5), the FH system is called SFH

system. That allows many data bits to be transmitted at each frequency hop and the resulting transmitter and receiver equipment is simpler and less expensive than that of FFH system. The disadvantage of SFH is that any enemy can defeat the anti-jam protection by smart jammer which attempts to measure signal frequency and tune the interference to that portion of the band. If the jammer can adopt quickly enough, it may be able to follow the SFH. on the other hand, SFH can be used to interleave many frequencies multiplexed channels within the same frequency hop band. This would make it difficult for the jammer to detect the specific target signal, the signal would be lost among all others in the band [12,25]. As a consequence, SFH can be useful either against simple jammer or in conjunction with frequency division multiplexing of many signals. In many cases, these features, along with the relative low cost compared with FFH may make this technique attractive.

2.5 Fast Frequency Hopping (FFH)

When the hopping duration (T_h) is equal to or less than the data duration (T_b) of one information bit as shown in Figure (2.6), the FH system is called FFH system. This system is the better in avoiding both follower jammer and multitone jamming because the signal is hopped to a new frequency before the jammer can complete its measurement, retune and interference functions [40].

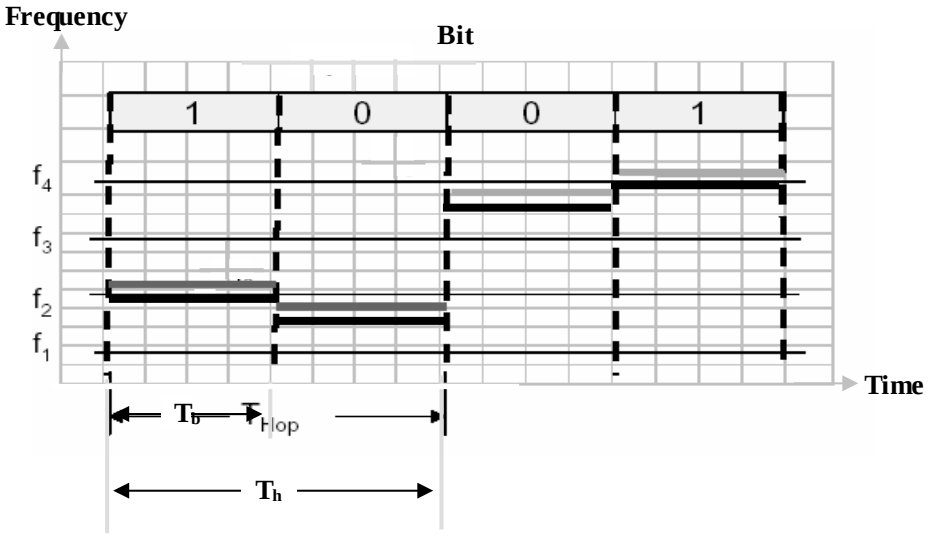

Figure (2.5) Time- frequency plane of SFH

In the FFH/SS system, the required hopping rate (R_h) is determined by considering time delays introduced by signal propagation to the receiver at the jammer, and time delays involved in processing and tuning at the jammer [12].

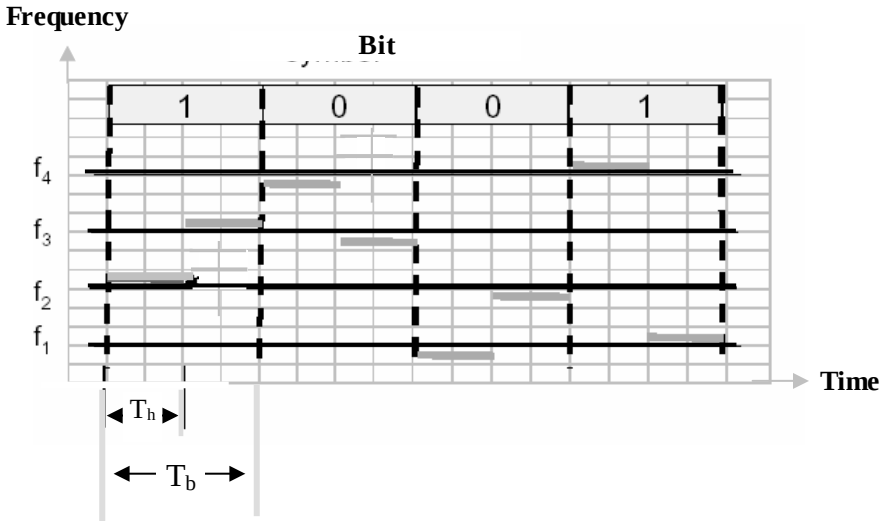

Figure (2.6): Time - frequency plane of FFH.

2.6 Performance of FH System Under Noise and Jamming.

FH system has good performance under noise and jamming. Probably the most important application of FH system is the resistance to jamming [41,42].

The effectiveness of FH system against sophisticated jamming depends upon the unpredictability of the hopping pattern.

2.6.1 Noise.

In the case of the noise, the transmission channel simply adds AWGN samples to transmitted data stream at the appropriate average power level to obtain the desired SNR at the receiver [3].

In a FH/SSS the received signal is corrupted by the additive white noise only and can be written as in following equation

$$r(t) = s(t) + n(t) \tag{2.6}$$

where:

r(t) is the received signal, s(t) is the transmitted FH/SS signal, and n(t) is the additive white noise.

The probability of error (p_e) for a FH /SSS employing ASK or coherent FSK detector is identical to the probability of conventional (unspread) ASK and FSK and can be written as [34,41].

$$Pe = \frac{1}{2} erfc \sqrt{\frac{E_b}{2N_0}} \quad (2.7)$$

While the probability of error in FSK system employing NC detections is given by

$$P_{e,FSK,NC} = \frac{1}{2} \exp\left(\frac{-E_b}{2N_0}\right) \quad (2.8)$$

where:

E_b: the energy per bit, erfc: complementary error functions.

N_o: the two-sided power spectral density of Gaussian noise.

2.6.2 Multitone Jamming (MTJ).

MTJ is also called fixed tone jamming. The suitable method for this jamming is to place multiple tones along the transmission band. This causes an interfering with the hopping frequency and so the information is missing.

The probability of error in case of hitting a certain frequency may be represented by [43].

$$P\left(\frac{e}{hit}\right) = \frac{(M-1)}{M} \quad (2.9)$$

where, p(e/hit) is the error probability conditional on a jamming tone being in a receiver bandwidth and M, is the level of FSK modulation. The probability of hit any frequency among the total number of frequencies used is.

$$P(hit) = N_j / N_f / M \quad (2.10)$$

where: N_j: the number of jamming frequencies, N_f: the number of frequencies in total bandwidth. The probability of error is

2.6.3 Hopper Jamming (HJ).

It is the same as the MTJ except that the HJ is driven by PN code generator with high rate to spread the adjacent tones with spacing equal to the message bit rate [34].

2.6.4 Partial Band Jamming.

Partial band jamming is characterized by a MTJ covering a fraction of the total bandwidth. This jamming is more effective as causing a large degradation to a fraction of the transmitted symbols rather than a little degradation of all symbols [44]. It is clearly understood that during each hop, FH signal is simply as FSK signal and hence. It has equivalent probability of error, which for noncoherent system is given by equation (2.9). It is obvious that the system is error free in bands not affected by partial band jamming of the spectrum, and is an FSK system in the jammed bands, which are of the spectrum [26].

2.6.5 Pulse Jamming.

The performance of frequency hopping system is affected by jamming pulse, with duration more than the symbol time. The probability of error may be calculated by the following formula [34]: -

$$Pe = \frac{1}{2\eta} \tag{2.12}$$

where η : is the pulse duty factor.

2.6.6 Follower Jamming.

A follower jammer also known as repeater or transponder jammer. It is a device that, intercepts a signal, processes it and then transmits jamming at the same center frequency. To be effective against a FH system, the jamming energy must reach the victim receiver before it hops to a new set of a frequency channels. Thus the greater the hop rate, the more protected the FH system against a repeater jammer [45]. Figure (2.7) illustrates the geometrical configuration of transceiver and jammer [41,46]. For a follower jammer to be effective:-

$$d_{TJ} + d_{JR} \le \left(FT_h - T_p\right) V + d_{TR} \tag{2.13}$$

D_{TJ},D_{JR},D_{TR} : distances from the transmitter to the jammer, from the jammer to the receiver, and from the transmitter to the receiver respectively, and V is the speed of the light, T_p: processing time required by the repeater, T_h:hopping period , F : fraction.

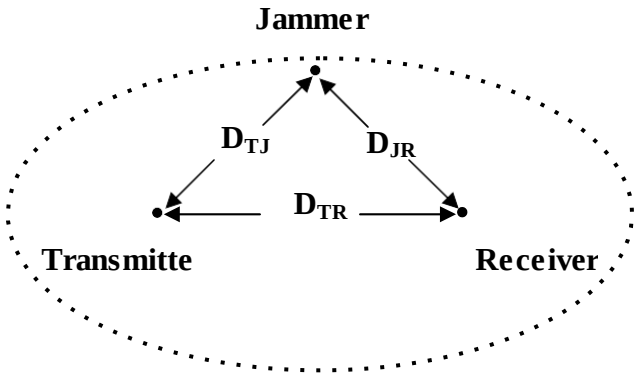

Figure (2.7): Geometrical configuration of transceiver and a jammer.

Equation, (2.15) states that the time delay of jamming relative to the intended signal must not exceed a certain fraction of the T_h if the jamming is to be effective.

2.7 Frequency Synthesizers.

A frequency synthesizer is a device that generates a large number of precise frequencies from a highly stable reference frequency [38]. The frequency synthesizer is the heart and the critical part of the system, because the settling time of the synthesizer determines the hop rate of the frequency hopping system. Recent advances in integrated-circuit design include the development of inexpensive frequency synthesizers and their subsequent application in most communication receivers [35,46].

A frequency synthesizer can replace the expensive array of crystal resonators in a multichannel radio receiver. A single-crystal oscillator provides reference frequency, and the frequency synthesizer generates the other frequencies [47]. The oldest synthesis method, first described by Finden , is referred to as direct frequency synthesis; it utilizes mixers , multipliers , dividers ,and BPF , direct synthesis has been superseded in almost all application by in direct (coherent) synthesis , with utilizes a PLL that may be analogue or digital. The newest

method is DDFS, it uses a digital computer and D/A converter to generate the signal [48]. Each of these methods has advantages as well as disadvantage ; and if the specifications are sufficiently stringent , it may be necessary to incorporate all three methods in to the synthesis design, the three methods are :-

2.7.1 Direct Frequency Synthesis.

Is the oldest of the frequency synthesis methods, it synthesizes a specified frequency from one or more reference frequency mixers. The oscillators are usually easier to realize than the BPFs. Figure (2.8) illustrates a method of generating 99 desecrate frequencies from 18 crystal oscillators. One switch selects one of the nine oscillators that cover the frequency range one to 9 khz in 1-khz steps. The two signals are then combined in a frequency mixer, and the BPF selects the higher of the two mixer output frequencies. Direct frequency synthesis refers to the generation of new frequencies from one or more reference frequencies by using a combination of multipliers, dividers , BPF, and mixers [38].

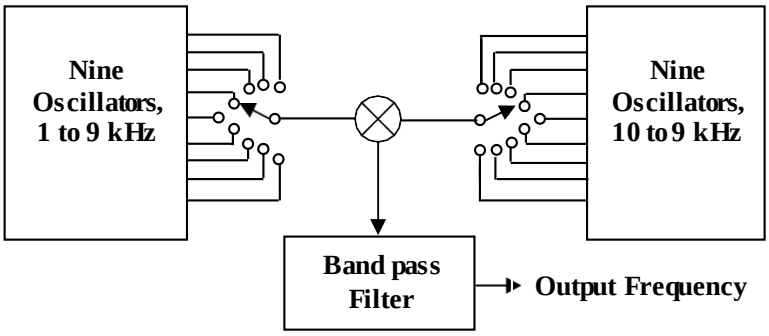

Figure (2.8): A two-decade direct frequency

2.7.2 Indirect Frequency Synthesis.

The disadvantages associated with direct synthesis are greatly diminished with the frequency synthesis by phase look technique that employs a PLL. A simple PLL is illustrated in Figure (2.9). It is sufficient to state that when the PLL is functioning properly, the two phase-detector input frequencies are equal. That is, the output frequency must therefore be:

$$f_0 = D f_r \qquad (2.14)$$

where:

D: division ratio, f_r : reference frequency, f_o: frequency output.

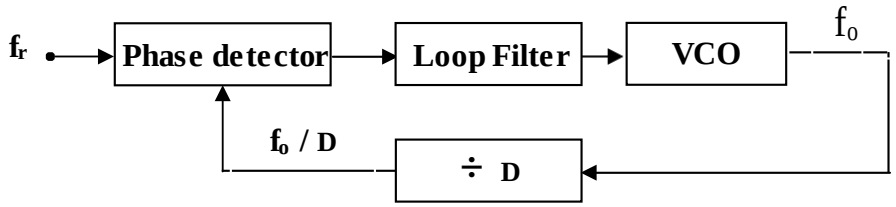

Figure (2.9): An indirect frequency synthesizer

Therefore, the output frequency (f_o) is an integer multiple of the reference [25,49] this technique differs from direct synthesis in many respects. The system analysis of indirect synthesis centers on an investigation of PLL stability and acquisition, not on spurious outputs. Indirect synthesizers usually require small hardware size, light weight, and low dc power consumption compared to direct type, but require more time to switch from one frequency to another [39].

2.8 Synchronization in FH system

The synchronization process in FH system consists of two operations, acquisition and tracking. Acquisition is the operation by which the phase of the locally generated sequence is brought to within a fraction of the sequence. The synchronization error is further reduced or at least maintained within certain bound as a result of the tracking operation [50].

Acquisition problem is the most difficult task of synchronization. A code start without prior knowledge of timing, or at best very minimal knowledge, is the usual rule rather than knowing the proper time for achieving synchronization with the desired transmitter and receiver [18].

Serial search and matched filtering are usually the most effective acquisition techniques. The first type provides the acquisition of a long hopping pattern and for short hopping pattern, the second method is used. In the serial search acquisition system, the PN code generator operates at a rate different from the transmitter code generator. The receiver configuration for acquisition is illustrated in Fig. (2.11). The purpose of the matched filter, envelope detector,

and the threshold detector is to detect the autocorrelation signal approximately when the peak amplitude is reached [19, 51, 52, 53].

Figure (2.12) shows a matched filter acquisition system, the frequency synthesizer produce tone frequencies ($f_1, f_2, \ldots\ldots, f_n$) which are offset by the intermediate frequency (F_{IF}) from the consecutive of the frequencies of the transmitted hopping pattern.

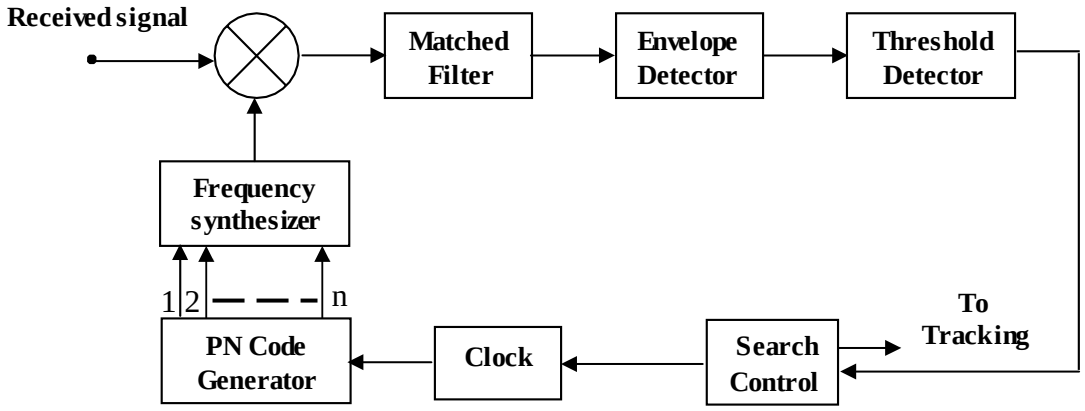

Figure (2.11): Serial search acquisition system

A significant point in the use of matched filter acquisition system is that they must accurately represent the clock period of the signal to be detected. Doppler shift, clock frequency drift can cause the delay element periods in the filter to be mismatched with the incoming signal [24].

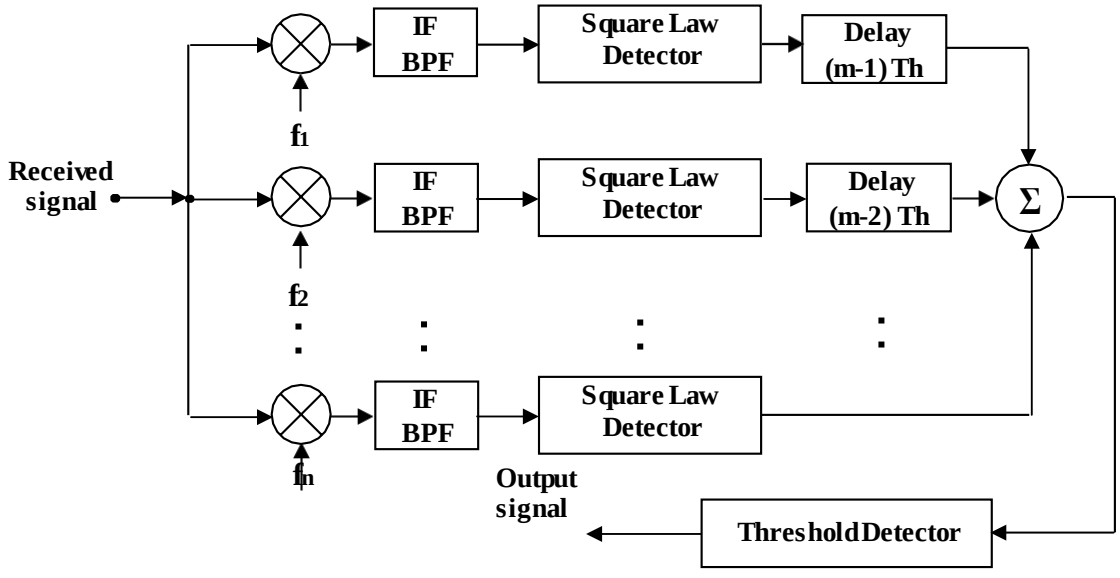

Figure (2.12): Matched filter acquisition system.

Chapter Three

Design and Simulation of Contiguous and Noncontiguous Digital BPF Banks for FFH/SS Receiver

3.1 Introduction.

MATLAB-Simulink is an attractive simulation tool that provides the designer many facilities to rapidly design, implement and test the desired system. Also, it gives the designer a clear imagination to the system parameters required to complete the design. This information's gained from MATLAB-Simulink implementation [54]. Parallel contiguous and noncontiguous digital BPF banks are designed and simulated. This design used for spread spectrum receiver to achieve synchronization.

There are two main classes of digital filter FIR and IIR. In the proposed system, IIR filter is used because this type needs less number of coefficients and order than FIR [55].

IIR is sensitive to number coefficients and is not suitable for prefect linear phase response [56,57].

3.2 Design IIR BPF

The design of a digital filter is a task of determined a TF which is a rational function in Z^{-1} in the case of recursive (IIR) filters. This TF function must meet certain performance specifications.

The designed individual BPF of the proposed system is considered as TF with two zeros and two conjugate poles are shown in Figure (3.1).

X : pole

○ : zero

ϕ_i : angle in degree (i = 1, 2, … , 31)

α : vector (| z | $\angle\phi_i$, 0.9 > z > 1)

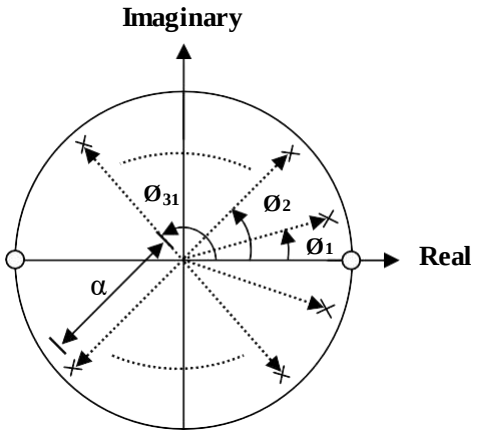

Figure (3.1) : Pole zero configuration for the designed BPF banks

Then the TF of proposed designed for BPF banks is given as fallow:

$$H(Z)=\frac{1-Z^{-2}}{(1-\alpha e^{j\phi})(1-\alpha e^{-j\phi})} \tag{3.1}$$

$$\phi_i=\omega_{ci}\,T_{si} \tag{3.2}$$

Where:

ω_{ci} : center frequency (radian per second), (i = 1, 2, ……, 31)

T_{si} : sampling time, i = 1, 2, ……, 31)

From equation (3.1):

$$H(Z)=\frac{(1-Z^{-1})(1+Z^{-1})}{1-2\alpha\cos\phi i Z^{-1}+\alpha^2 Z^{-2}} \tag{3.3}$$

The general recursive filter TF can be given by the following formula [58].

$$H(Z)=\left(\sum_{k=0}^{L} b_k Z^k\right)/\left(1+\sum_{k=1}^{R} a_k Z^k\right) \tag{3.4}$$

where:

L and R: are integer numbers and must satisfy the inequality $L \le R$.

a_k and b_k: are coefficient numbers.

By using MATLAB-Simulink version 7 and depending on equation (3.3), the IIR second order Butterworth BPF01 with (f_L 3 MHz, f_H 3.6 MHz, f_c 3.3 MHz and f_S 60 MHz) have been designed and so for the others BPFs. Its realization is shown in Figure (3.2) and the magnitude response, pole zero configurations of

IIR second order Butterworth BPF01 for ASK FFH/SSS specified (f_L 3 MHz, f_H 3.6 MHz, f_c 3.3 MHz and f_S 60 MHz) using contiguous technique are shown in Figures (3.3) and (3.4) respectively.

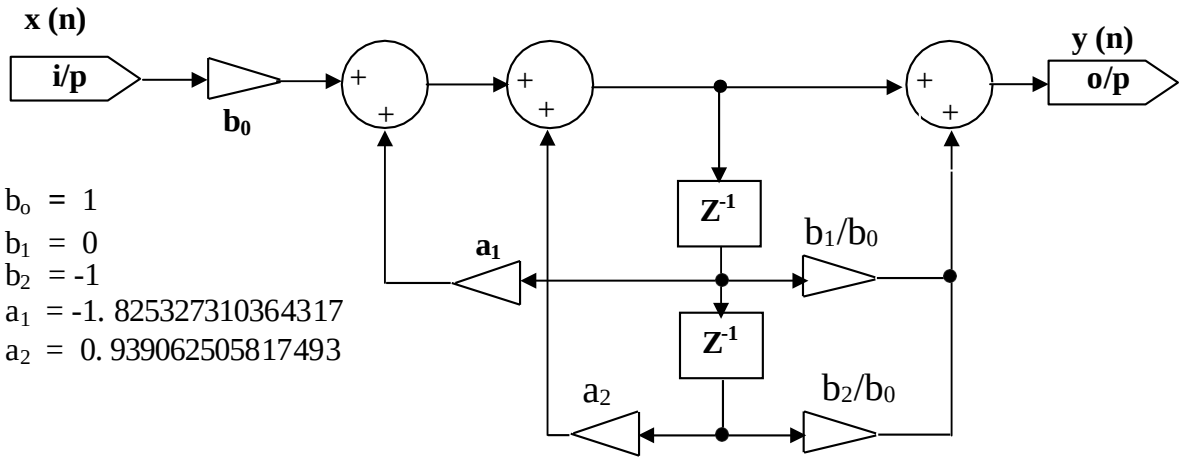

Figure (3.2): IIR Second order Butterworth BPF realization.

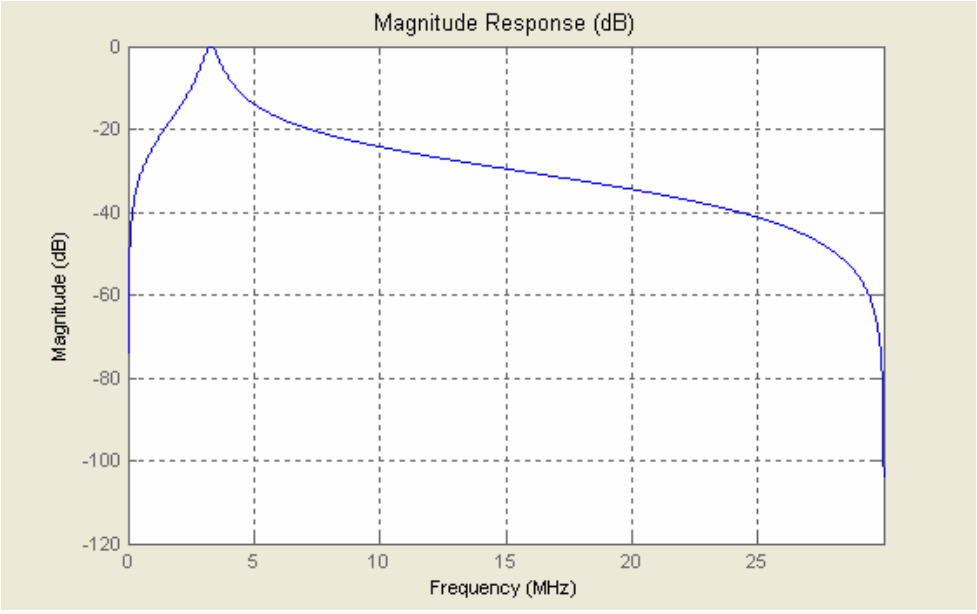

Figure (3.3): The magnitude response of IIR second order BPF01 for ASK FFH/SSS using contiguous technique.

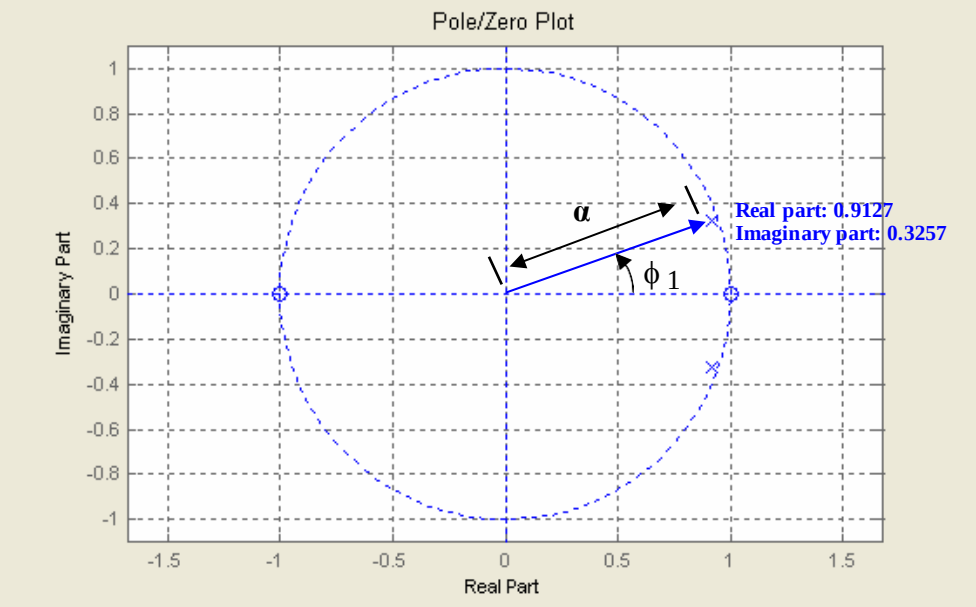

Figure (3.4): The pole zero configuration of IIR second order BPF01 for ASK FFH/SSS using contiguous technique.

An important special case that is used as a building block occurs when L = R =2. Thus H (z) is a ratio two quadratics in z^{-1}, called a biquadratic section, and given by:

$$H(Z) = \frac{(b_o + b_1 Z^{-1} + b_2 Z^{-2})}{1 + a_1 Z^{-1} + a_2 z^{-2}} = \frac{b_o\,((1 + (b_1 / b_o) Z^{-1} + (b_2 / b_o) Z^{-2}))}{1 + a_1 Z^{-1} + a_2 Z^{-2}} \qquad (3.5)$$

The direct form II and alternative realization of the biquadratic H (z) are shown in Figures (3.7) and (3.8). The alternative realization has been shown to be useful for amplitude scaling for improving performance of filter operation.

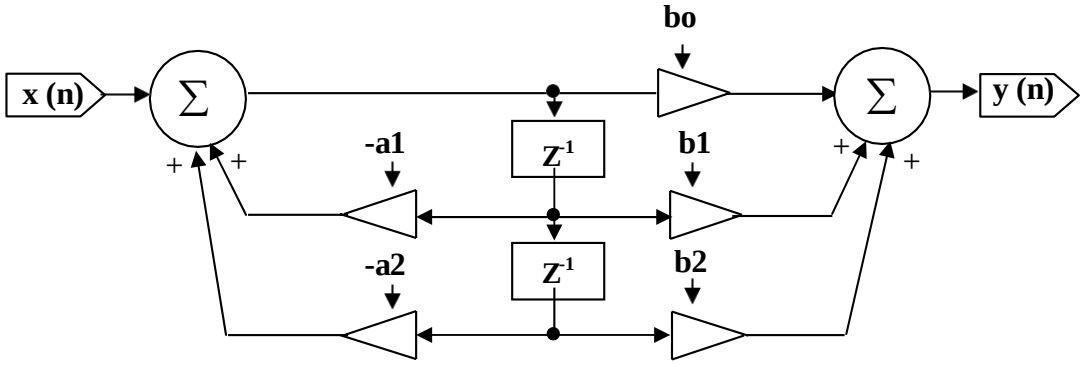

Figure (3.5): The direct form II realization of the biquadratic section. (H (z) = (b_0 + $b_1.z^{-1}$+ $b_2.z^{-2}$) / (1 + $a_1.z^{-1}$+ $a_2.z^{-2}$))

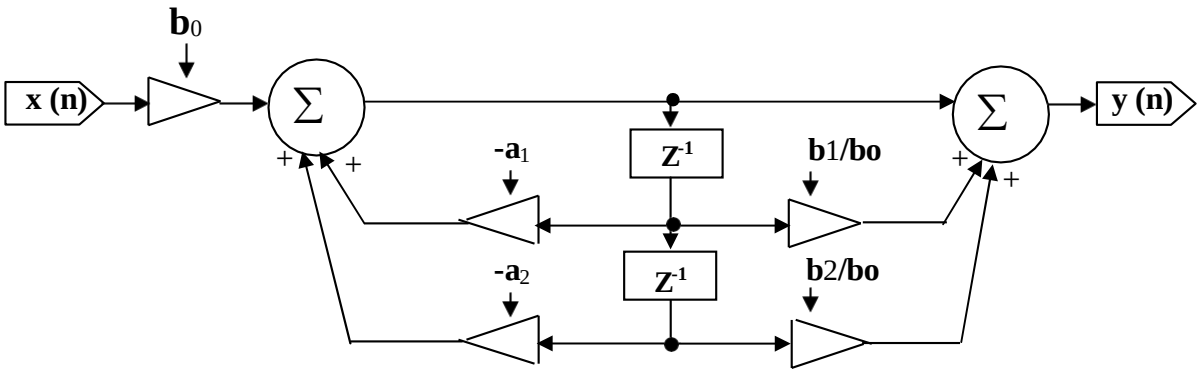

Figure (3.6): An alternative realization of the biquadratic section. ($H(z) = b_0 (1+ (b_1/b_0) z^{-1}+ (b_2/b_0) z^{-2}) / (1 + a_1.z^{-1}+ a_2.z^{-2})$)

Finally the TF of the designed BPF01 IIR second order Butterworth is:

$$H(Z) = \frac{1 - Z^{-2}}{1 + 1.825327310364317\ Z^{-1} + 0.939062505817493\ Z^{-2}}$$

3.3 Design of Parallel IIR Second Order Butterworth BPF Banks for ASK FFH/SSS.

It is designed using two techniques:

3.3.1 Contiguous Filters

In section (3.2) the design of individual IIR second order Butterworth BPF is done. The proposed system needs to design contiguous parallel IIR second order Butterworth BPF banks as shown in Figures (3.7) and (3.8) using MATLAB-Simulink, which consists of 31 filters. Table (3.1) shows the TF for each filter which is found by the same procedure as in section (3.2). In this proposed system, the center frequency of each filter is shown in Table (3.2). The relation between f_c , f_H and f_L is [59, 60, 61] :

$$f_c = (f_H + f_L)/2 \qquad (3.6)$$

where:

f_c : center frequency, f_H : 3dB band stop frequency, f_L : 3dB band pass frequency.

$$\frac{1}{Tb} = 200 \text{ K bits / sec}$$

where:

$1 / T_b$: data rate.

The bandwidth of each filter is approximately twice of data rate (R_b) [62].

$$R_b = 1 / T_b \quad (3.7)$$

$$\Delta F = 2 / T_b + f_g \quad (3.8)$$

where:

ΔF : 3dB bandwidth of BPF, f_g : guard band.

$$f_g = R_b / 2 \quad (3.9)$$

$$B_{ss} = (2^n - 1)\Delta F \quad (3.10)$$

where:

B_{SS} spread spectrum bandwidth.

:

n: integer number (number of DFF of the PN code).

The design steps of this contiguous filters type are the same as those stated in section (3.2). Figure (3.9) shows the distribution of the frequencies over the ASK FFH/SSS band (3MHz – 21.6MHz) used in this system. The magnitude response and pole zero configurations for BPF01 are shown in Figures (3.3) and (3.4) respectively which is stated in section (3.2). Figures (3.10) and (3.11) show the magnitude response and pole zero configurations respectively for BPF31 ASK FFH/SSS specified (f_L = 21 MHz, f_H = 21.6 MHz , fs = 60 MHz, f_c 21.3 MHz)**,** using contiguous technique.

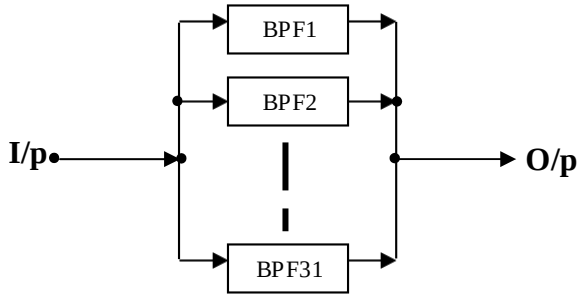

Figure (3.7): Parallel IIR second order Butterworth BPF Banks.

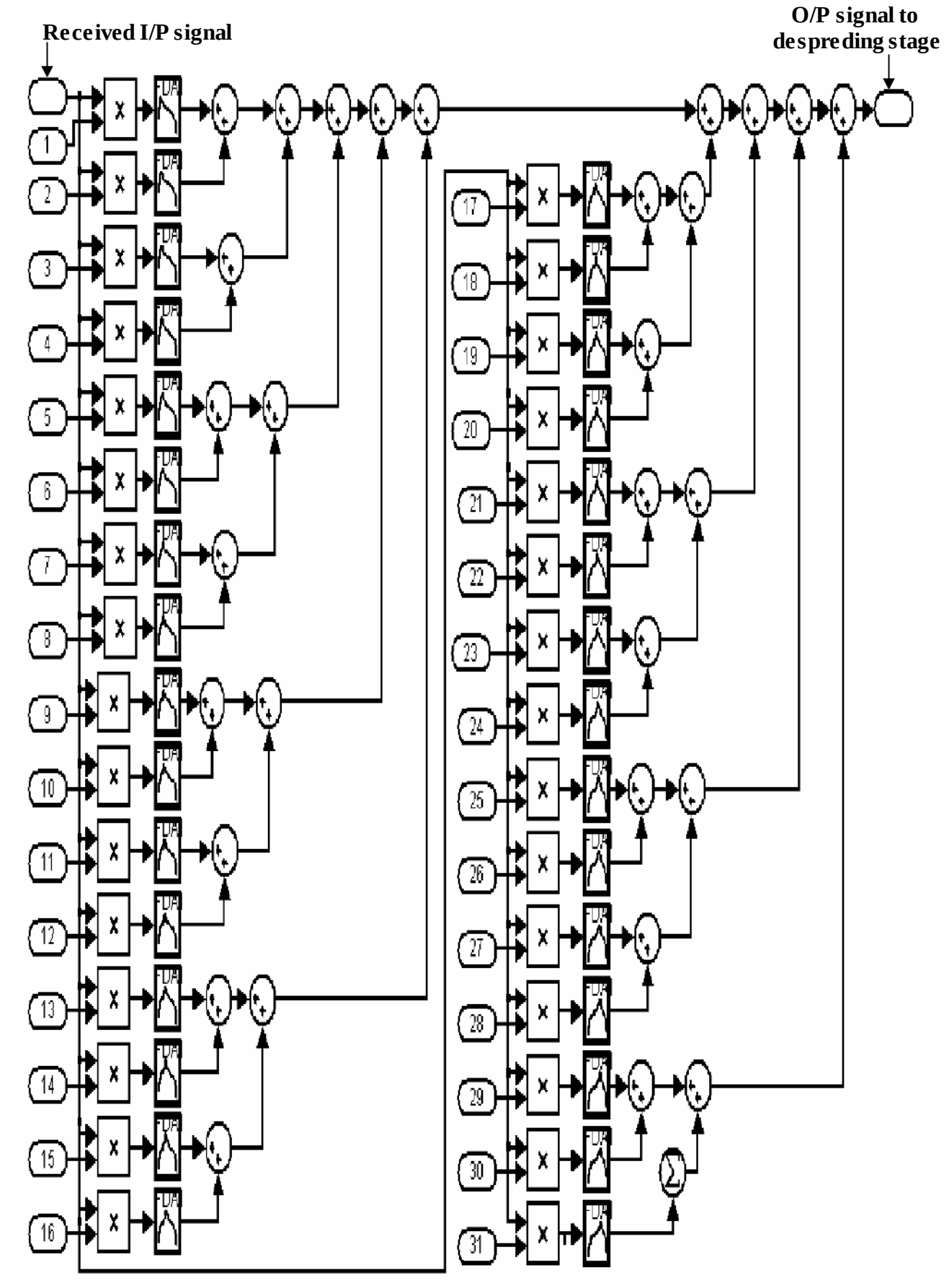

Figure (3.8): Design and simulation parallel IIR second order Butterworth BPF banks for FH/SSS. [(1,2, …… , 31) is the digital I/P used for controlling of BPFs]

Table (3.1): The TF of Contiguous IIR second order Butterworth BPF banks for ASK FFH/SSS

Filter	*Numerator*	*Denominator*
BPF01	$1-Z^{-2}$	$1- 1.825327310364317\ Z^{-1} + 0.939062505817493\ Z^{-2}$
BPF02	$1-Z^{-2}$	$1- 1.780462134788994\ Z^{-1} + 0.939062505817492\ Z^{-2}$
BPF03	$1-Z^{-2}$	$1- 1.728570288583437\ Z^{-1} + 0.939062505817493\ Z^{-2}$
BPF04	$1-Z^{-2}$	$1- 1.669856565157487\ Z^{-1} + 0.939062505817493\ Z^{-2}$
BPF05	$1-Z^{-2}$	$1- 1.604552680763758\ Z^{-1} + 0.939062505817493\ Z^{-2}$
BPF06	$1-Z^{-2}$	$1- 1.532916359969485\ Z^{-1} + 0.939062505817492\ Z^{-2}$
BPF07	$1-Z^{-2}$	$1- 1.455230318635282\ Z^{-1} + 0.939062505817492\ Z^{-2}$
BPF08	$1-Z^{-2}$	$1- 1.371801148064918\ Z^{-1} + 0.939062505817492\ Z^{-2}$
BPF09	$1-Z^{-2}$	$1- 1.282958105079473\ Z^{-1} + 0.939062505817493\ Z^{-2}$
BPF10	$1-Z^{-2}$	$1- 1.189051812581083\ Z^{-1} + 0.939062505817493\ Z^{-2}$
BPF11	$1-Z^{-2}$	$1- 1.090452875804537\ Z^{-1} + 0.939062505817492\ Z^{-2}$
BPF12	$1-Z^{-2}$	$1- 0.987550419707721\ Z^{-1} + 0.939062505817492\ Z^{-2}$
BPF13	$1-Z^{-2}$	$1- 0.880750553273190\ Z^{-1} + 0.939062505817493\ Z^{-2}$
BPF14	$1-Z^{-2}$	$1- 0.770474766781543\ Z^{-1} + 0.939062505817493\ Z^{-2}$
BPF15	$1-Z^{-2}$	$1- 0.657158268381848\ Z^{-1} + 0.939062505817492\ Z^{-2}$
BPF16	$1-Z^{-2}$	$1- 0.541248266523904\ Z^{-1} + 0.939062505817493\ Z^{-2}$
BPF17	$1-Z^{-2}$	$1- 0.423202205030802\ Z^{-1} + 0.939062505817492\ Z^{-2}$
BPF18	$1-Z^{-2}$	$1- 0.303485957777140\ Z^{-1} + 0.939062505817492\ Z^{-2}$
BPF19	$1-Z^{-2}$	$1- 0.182571990097678\ Z^{-1} + 0.939062505817492\ Z^{-2}$
BPF20	$1-Z^{-2}$	$1- 0.060937494182508\ Z^{-1} + 0.939062505817492\ Z^{-2}$
BPF21	$1-Z^{-2}$	$1+0.060937494182508\ Z^{-1} + 0.939062505817492\ Z^{-2}$
BPF22	$1-Z^{-2}$	$1+0.182519900976780\ Z^{-1} + 0.939062505817492\ Z^{-2}$
BPF23	$1-Z^{-2}$	$1+0.303485957777140\ Z^{-1} + 0.939062505817492\ Z^{-2}$
BPF24	$1-Z^{-2}$	$1+0.423202205030802\ Z^{-1} + 0.939062505817493\ Z^{-2}$
BPF25	$1-Z^{-2}$	$1+0.541248266523903\ Z^{-1} + 0.939062505817492\ Z^{-2}$
BPF26	$1-Z^{-2}$	$1+0.657158268381847\ Z^{-1} + 0.939062505817492\ Z^{-2}$
BPF27	$1-Z^{-2}$	$1+0.770474766781542\ Z^{-1} + 0.939062505817492\ Z^{-2}$
BPF28	$1-Z^{-2}$	$1+0.880750553273190\ Z^{-1} + 0.939062505817492\ Z^{-2}$
BPF29	$1-Z^{-2}$	$1+0.987550419707721\ Z^{-1} + 0.939062505817492\ Z^{-2}$
BPF30	$1-Z^{-2}$	$1+1.090452875804536\ Z^{-1} + 0.939062505817492\ Z^{-2}$
BPF31	$1-Z^{-2}$	$1+1.189051812581083\ Z^{-1} + 0.939062505817492\ Z^{-2}$

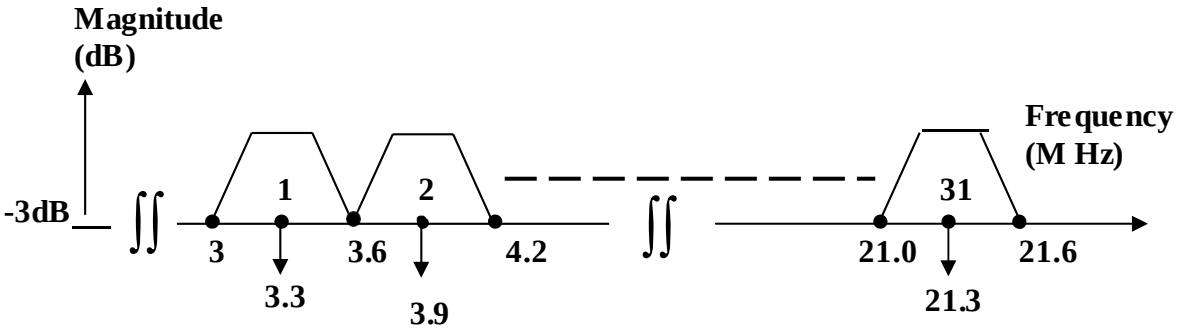
Magnitude
(dB)
-3dB
Frequency
(M Hz)
1
2
31
3
3.3
3.6
3.9
4.2
21.0
21.3
21.6

Figure (3.9): The distribution of the frequencies over the band of spread spectrum when using contiguous filters for ASK FFH/SSS.

Table (3.2): Center frequency of contiguous digital BPF banks for ASK FFH/SSS

Filter	*Frequency (MHz)*	*Filter*	*Frequency (MHz)*
BPF01	03.3	BPF17	12.9
BPF02	03.9	BPF18	13.5
BPF03	04.5	BPF19	14.1
BPF04	05.1	BPF20	14.7
BPF05	05.7	BPF21	15.3
BPF06	06.3	BPF22	15.9
BPF07	06.9	BPF23	16.5
BPF08	07.5	BPF24	17.1
BPF09	08.1	BPF25	17.7
BPF10	08.7	BPF26	18.3
BPF11	09.3	BPF27	18.9
BPF12	09.9	BPF28	19.5
BPF13	10.5	BPF29	20.1
BPF14	11.1	BPF30	20.7
BPF15	11.7	BPF31	21.3
BPF16	12.3		

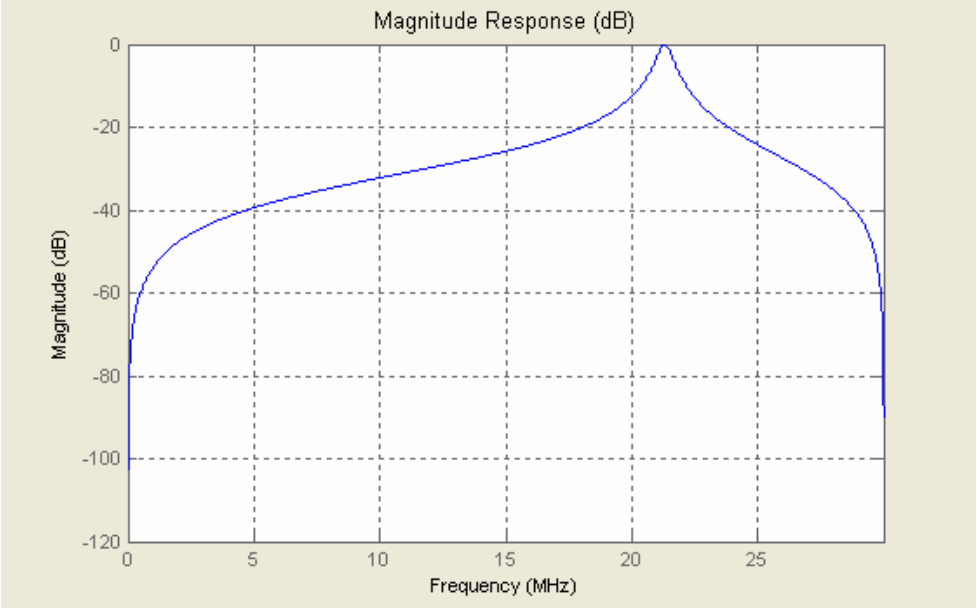

Figure (3.10): The magnitude response of IIR second order BPF31 for ASK FH/SSS specified using contiguous technique.

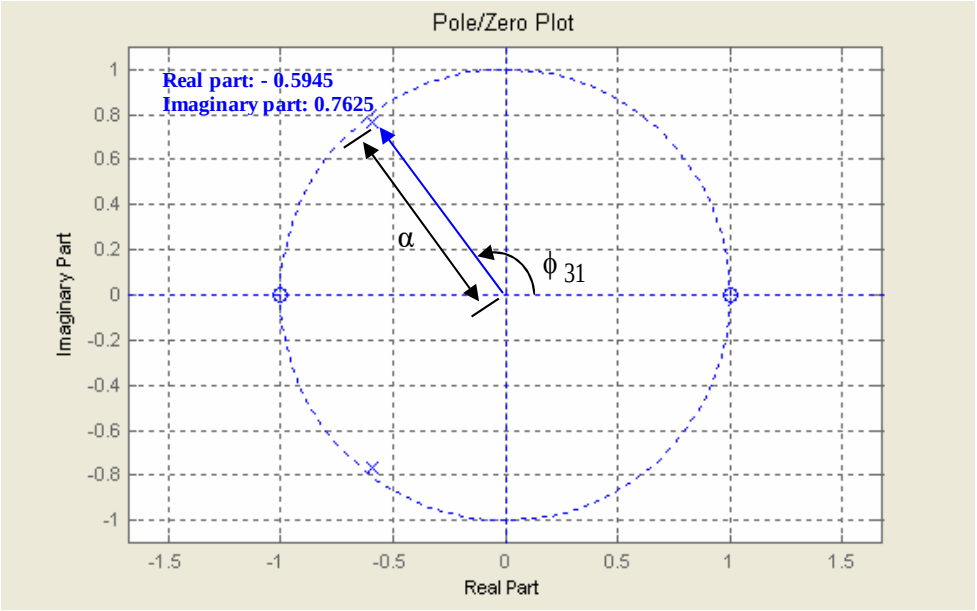

Figure (3.11): The pole zero configuration of IIR second order BPF31 for ASK FH/SSS specified using contiguous technique.

3.3.2 Noncontiguous Filters

In this design noncontiguous technique is used to make the overall bandwidth of FH/SS signal smaller than that used in contiguous technique. This compression can make the system has good benefits. As shown in section (3.3) the proposed system needs to design noncontiguous parallel IIR second order Butterworth BPF banks as shown in Figure (3.8). It consists of 31 noncontiguous filters. Table (3.4) shows the TF for each filter which found by the design using MATLAB-Simulink. The center frequency of each filter is shown in Table (3.4). The relation between f_c , f_H and f_L was stated in section (3.1). The other steps design is the same as that stated in section (3.3). The realization of each filter is the same as that shown in Figure (3.4) except that the coefficient values are different. Figure (3.12) shows the distribution of frequencies over the band of ASK FFH/SS used in this system. Figures (3.13),(3.14),(3.15) and (3.16) show the magnitude response and pole zero configuration for BPF01 specified (f_L = 3 MHz, f_H = 3.6 MHz, f_S = 30 MHz, f_c 3.3 Mhz) and BPF31 specified (f_L = 12 MHz, f_H = 12.6 MHz, f_S = 30 MHz, f_c 12.3 MHz) respectively of IIR second order Butterworth noncontiguous BPF banks for ASK FFH/SSS.

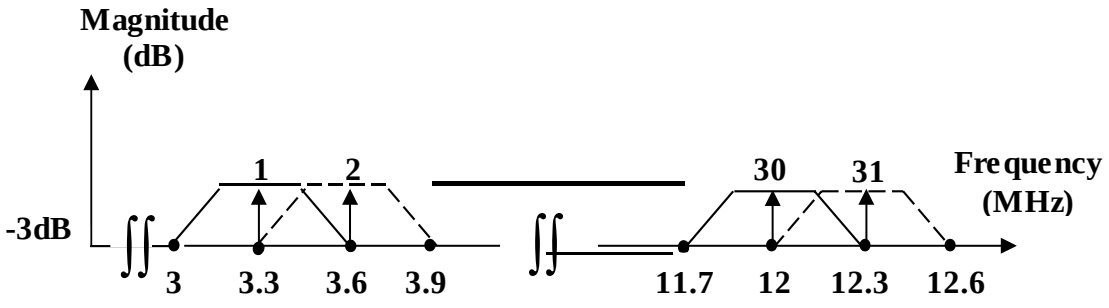

Figure (3.12): The distribution of the frequencies over the band of spread spectrum noncontiguous filters for ASK FFH/SSS.

Table (3.3): The TF of noncontiguous IIR second order Butterworth BPF banks for ASK FFH/SSS

Filter	*Numerator*	*Denominator*
BPF01	**$1-Z^{-2}$**	**$1- 1.452678572599146\ Z^{-1} + 0.881618592363189\ Z^{-2}$**
BPF02	**$1-Z^{-2}$**	**$1- 1.374352894101055\ Z^{-1} + 0.881618592363189\ Z^{-2}$**
BPF03	**$1-Z^{-2}$**	**$1- 1.290603272612059\ Z^{-1} + 0.881618592363189\ Z^{-2}$**
BPF04	**$1-Z^{-2}$**	**$1- 1.201760229626613\ Z^{-1} + 0.881618592363189\ Z^{-2}$**
BPF05	**$1-Z^{-2}$**	**$1- 1.108174388046856\ Z^{-1} + 0.881618592363189\ Z^{-2}$**
BPF06	**$1-Z^{-2}$**	**$1- 1.010215088434197\ Z^{-1} + 0.881618592363189\ Z^{-2}$**
BPF07	**$1-Z^{-2}$**	**$1- 0.908268931390862\ Z^{-1} + 0.881618592363189\ Z^{-2}$**
BPF08	**$1-Z^{-2}$**	**$1- 0.802738251823930\ Z^{-1} + 0.881618592363189\ Z^{-2}$**
BPF09	**$1-Z^{-2}$**	**$1- 0.694039531113274\ Z^{-1} + 0.881618592363189\ Z^{-2}$**
BPF10	**$1-Z^{-2}$**	**$1- 0.582601753449814\ Z^{-1} + 0.881618592363189\ Z^{-2}$**
BPF11	**$1-Z^{-2}$**	**$1- 0.468864712530910\ Z^{-1} + 0.881618592363189\ Z^{-2}$**
BPF12	**$1-Z^{-2}$**	**$1- 0.353277277394375\ Z^{-1} + 0.881618592363189\ Z^{-2}$**
BPF13	**$1-Z^{-2}$**	**$1- 0.236295617941000\ Z^{-1} + 0.881618592363189\ Z^{-2}$**
BPF14	**$1-Z^{-2}$**	**$1- 0.118381407636811\ Z^{-1} + 0.881618592363189\ Z^{-2}$**
BPF15	**$1-Z^{-2}$**	**$1- 0.000000000000000\ Z^{-1} + 0.88168592363189\ Z^{-2}$**
BPF16	**$1-Z^{-2}$**	**$1+0.118381407636811\ Z^{-1} + 0.881618592363189\ Z^{-2}$**
BPF17	**$1-Z^{-2}$**	**$1+0.236295617941000\ Z^{-1} + 0.881618592363189\ Z^{-2}$**
BPF18	**$1-Z^{-2}$**	**$1+0.353277277394375\ Z^{-1} + 0.881618592363189\ Z^{-2}$**
BPF19	**$1-Z^{-2}$**	**$1+0.468864712530910\ Z^{-1} + 0.881618592363189\ Z^{-2}$**
BPF20	**$1-Z^{-2}$**	**$1+0.582601753449814\ Z^{-1} + 0.881618592363189\ Z^{-2}$**
BPF21	**$1-Z^{-2}$**	**$1+0.694039531113274\ Z^{-1} + 0.881618592363189\ Z^{-2}$**
BPF22	**$1-Z^{-2}$**	**$1+0.802738251823931\ Z^{-1} + 0.881618592363189\ Z^{-2}$**
BPF23	**$1-Z^{-2}$**	**$1+0.908268931390862\ Z^{-1} + 0.881618592363189\ Z^{-2}$**
BPF24	**$1-Z^{-2}$**	**$1+1.010215088434197\ Z^{-1} + 0.881618592363189\ Z^{-2}$**
BPF25	**$1-Z^{-2}$**	**$1+1.108174388046856\ Z^{-1} + 0.881618592363189\ Z^{-2}$**
BPF26	**$1-Z^{-2}$**	**$1+1.201760229626614\ Z^{-1} + 0.881618592363189\ Z^{-2}$**
BPF27	**$1-Z^{-2}$**	**$1+1.290603272612059\ Z^{-1} + 0.881618592363189\ Z^{-2}$**
BPF28	**$1-Z^{-2}$**	**$1+1.374352894101055\ Z^{-1} + 0.881618592363189\ Z^{-2}$**
BPF29	**$1-Z^{-2}$**	**$1+1.452678572599145\ Z^{-1} + 0.881618592363189\ Z^{-2}$**
BPF30	**$1-Z^{-2}$**	**$1+1.525271192436898\ Z^{-1} + 0.881618592363189\ Z^{-2}$**
BPF31	**$1-Z^{-2}$**	**$1+1.591844263708227\ Z^{-1} + 0.881618592363189\ Z^{-2}$**

Table (3.4): Center frequency of noncontiguous digital BPF banks for ASK FFH/SSS

Filter	*Frequency (MHz)*	*Filter*	*Frequency (MHz)*
BPF01	**3.3**	**BPF17**	**8.1**
BPF02	**3.6**	**BPF18**	**8.4**
BPF03	**3.9**	**BPF19**	**8.7**
BPF04	**4.2**	**BPF20**	**9.0**
BPF05	**4.5**	**BPF21**	**9.3**
BPF06	**4.8**	**BPF22**	**9.6**
BPF07	**5.1**	**BPF23**	**9.9**
BPF08	**5.4**	**BPF24**	**10.2**
BPF09	**5.7**	**BPF25**	**10.5**
BPF10	**6.0**	**BPF26**	**10.8**
BPF11	**6.3**	**BPF27**	**11.1**
BPF12	**6.6**	**BPF28**	**11.4**
BPF13	**6.9**	**BPF29**	**11.7**
BPF14	**7.2**	**BPF30**	**12.0**
BPF15	**7.5**	**BPF31**	**12.3**
BPF16	**7.8**		

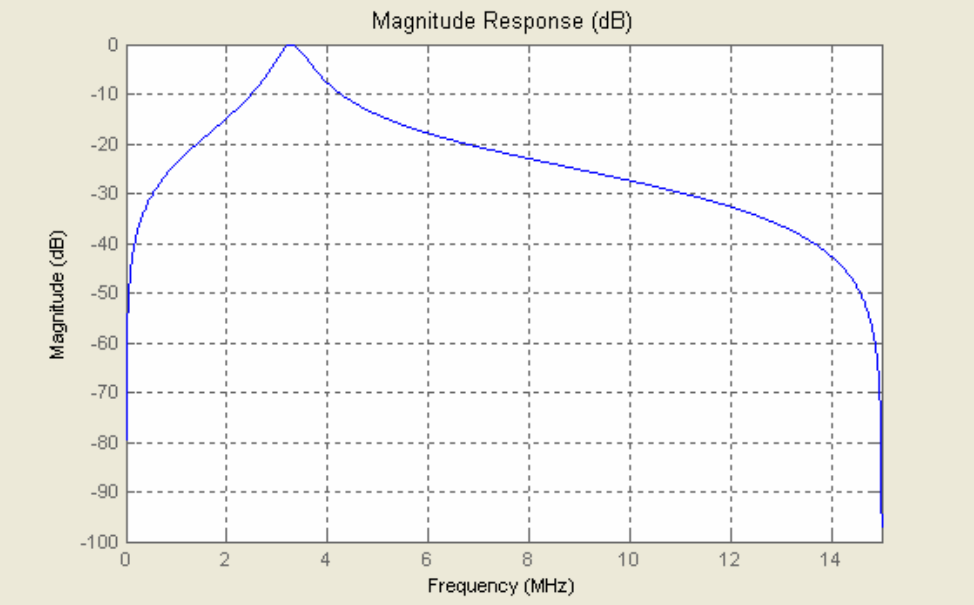

Figure (3.13): The magnitude response of IIR second order BPF01 for ASK FFH/SSS using noncontiguous technique.

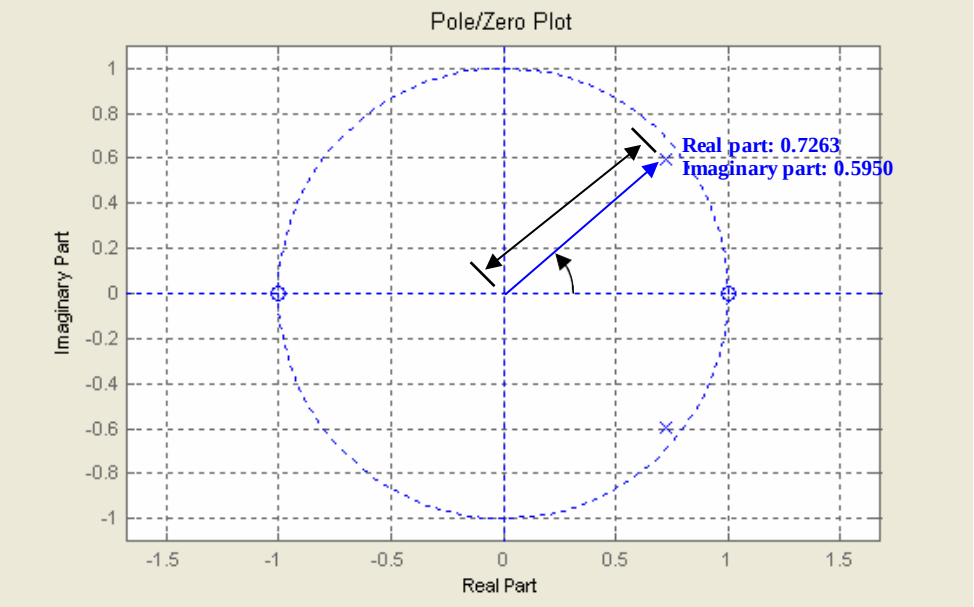

Figure (3.14): The pole zero configuration of IIR second order BPF01 for ASK FFH/SSS using noncontiguous technique.

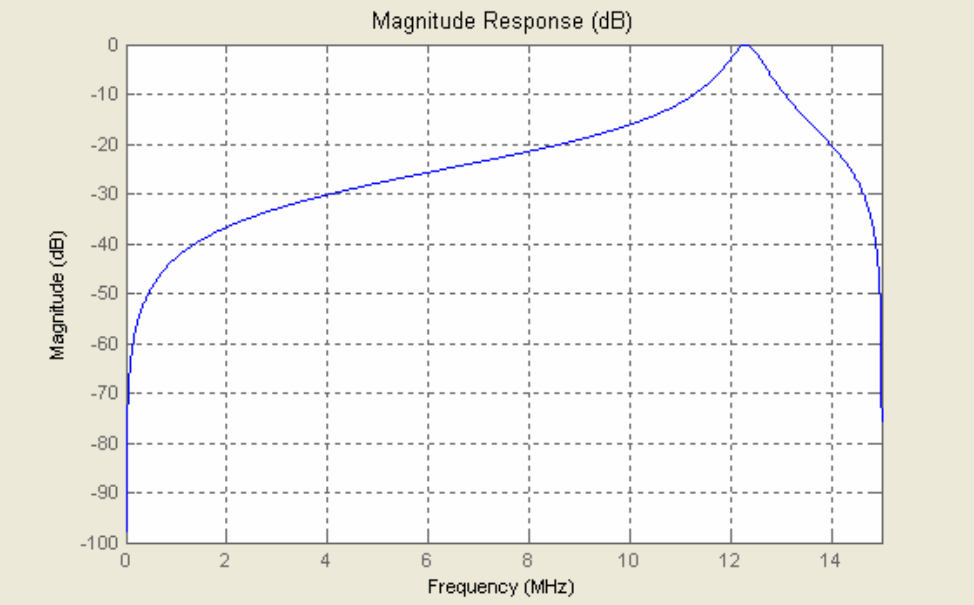

Figure (3.15): The magnitude response of IIR second order BPF31 for ASK FFH/SSS using noncontiguous technique.

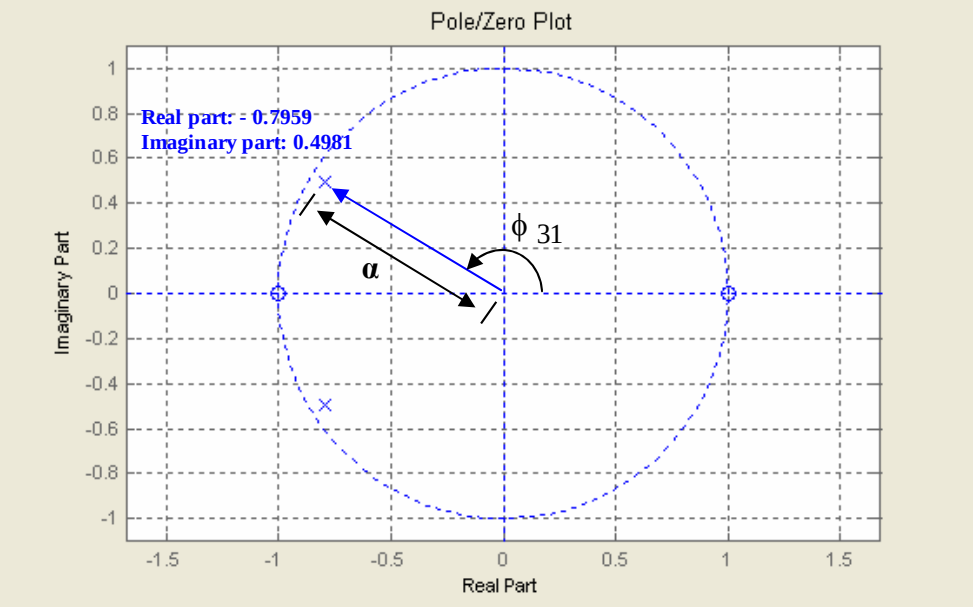

Figure (3.16): The pole zero configuration of IIR second order BPF31 for ASK FFH/SSS using noncontiguous technique.

3.4 Design of Parallel IIR Second Order Butterworth BPF banks for FSK FH/SSS.

It is designed using two techniques:

3.4.1 Contiguous Filters

In section (3.3) the design of individual IIR second order BPF is done. The proposed system needs to design parallel IIR second order Butterworth BPF banks as shown in Figure (3.8). It consists of 31 contiguous filters. Table (3.5) shows the TF for each filter is found by the same procedure as in section (3.2). The center frequency of each filter is shown in Table (3.6). These center frequencies values are corresponding to that of DDFS. The relation between f_c, f_{m1}, f_{m2}, R_b, R_h and f_L is [62]:

$$f_c = (f_{m1} + f_{m2}) / 2 + f_L \quad (3.10)$$

$$\frac{1}{Tb} \leq f_{m2} - f_{m1} \quad (3.11)$$

where:

f_c : center frequency.

f_{m1} : 3dB the lower frequency modulation.

f_{m2} : 3dB the upper frequency modulation.

f_L : 3dB lower frequency edge of each BPF from the band of FSK FFH/SS (3dB band pass frequency).

$\frac{1}{T_b}$:data rate (R_b)

$$f_{m1} = 1 / T_h \quad (3.12)$$

$$f_{m2} = 2 / T_h \quad (3.13)$$

where: T_h : hop period, $\frac{1}{T_h}$: hop rate (R_h)

The 3dB bandwidth of each filter is approximately is:

$$\Delta F = f_H - f_L = 2f_g + 2 / T_h \quad (3.14)$$

$$f_g = \frac{2}{T_b} \quad (3.15)$$

where: f_g : guard band.

In the designed proposed system, the hop rate are taken equal data rate (200kbit/sec), f_{m1} 400 KHz, f_{m2} 800 KHz to make the separation between adjacent FSK symbol frequencies be at least $\frac{1}{T_h}$ [63] therefore the 3dB bandwidth (ΔF) of each filters is 1.2 MHz.

$$\frac{1}{T_b} = \frac{1}{T_h} \quad (3.16)$$

$$L = \frac{T_h}{T_b} = 1 \quad (3.17)$$

where: L: diversity level.

Figure (3.17) shows the distribution of the frequencies over the band (3 MHz-40.2 MHz) used in FSK FFH/SSS using contiguous techniques.

The realization of each filter is the same as that shown in Figure (3.2) except that the coefficient values are different. Figures (3.18) and (3.19) show the magnitude response and pole zero configurations respectively for specified (f_L = 3 MHz, f_H =4.2 MHz, f_S = 120 MHz, f_c 3.6 MHz) BPF01 for FSK FFH/SSS. And Figures (3.20) and (3.21) show the magnitude response and pole zero configuration respectively for specified (f_L = 39 MHz, f_H =40.2 MHz,

f_S = 120 MHz, f_c 39.6 MHz) BPF31 for FSK FFH/SSS using contiguous techniques.

Table (3.5): The TF of contiguous IIR second order Butterworth BPF banks for FSK FFH/SSS

Filter	*Numerator*	*Denominator*
BPF01	**$1-Z^{-2}$**	**$1- 1.905656704377797\ Z^{-1} + 0.939062505817493\ Z^{-2}$**
BPF02	**$1-Z^{-2}$**	**$1- 1.879070499370685\ Z^{-1} + 0.939062505817492\ Z^{-2}$**
BPF03	**$1-Z^{-2}$**	**$1- 1.845068461568212\ Z^{-1} + 0.939062505817493\ Z^{-2}$**
BPF04	**$1-Z^{-2}$**	**$1- 1.803784781479528\ Z^{-1} + 0.939062505817493\ Z^{-2}$**
BPF05	**$1-Z^{-2}$**	**$1- 1.755382386929223\ Z^{-1} + 0.939062505817492\ Z^{-2}$**
BPF06	**$1-Z^{-2}$**	**$1- 1.700052300055639\ Z^{-1} + 0.939062505817493\ Z^{-2}$**
BPF07	**$1-Z^{-2}$**	**$1- 1.638012883433751\ Z^{-1} + 0.939062505817492\ Z^{-2}$**
BPF08	**$1-Z^{-2}$**	**$1- 1.569508978297854\ Z^{-1} + 0.939062505817492\ Z^{-2}$**
BPF09	**$1-Z^{-2}$**	**$1- 1.494810938265061\ Z^{-1} + 0.939062505817492\ Z^{-2}$**
BPF10	**$1-Z^{-2}$**	**$1- 1.414213562373095\ Z^{-1} + 0.939062505817492\ Z^{-2}$**
BPF11	**$1-Z^{-2}$**	**$1- 1.328034931643161\ Z^{-1} + 0.939062505817492\ Z^{-2}$**
BPF12	**$1-Z^{-2}$**	**$1- 1.236615137594800\ Z^{-1} + 0.939062505817493\ Z^{-2}$**
BPF13	**$1-Z^{-2}$**	**$1- 1.140315020819634\ Z^{-1} + 0.939062505817492\ Z^{-2}$**
BPF14	**$1-Z^{-2}$**	**$1- 1.039514585452992\ Z^{-1} + 0.939062505817492\ Z^{-2}$**
BPF15	**$1-Z^{-2}$**	**$1- 0.934611660926607\ Z^{-1} + 0.939062505817492\ Z^{-2}$**
BPF16	**$1-Z^{-2}$**	**$1- 0.826020521157996\ Z^{-1} + 0.939062505817492\ Z^{-2}$**
BPF17	**$1-Z^{-2}$**	**$1- 0.714168916830822\ Z^{-1} + 0.939062505817493\ Z^{-2}$**
BPF18	**$1-Z^{-2}$**	**$1- 0.599499084061659\ Z^{-1} + 0.939062505817493\ Z^{-2}$**
BPF19	**$1-Z^{-2}$**	**$1- 0.482463302292784\ Z^{-1} + 0.939062505817492\ Z^{-2}$**
BPF20	**$1-Z^{-2}$**	**$1- 0.363523458286276\ Z^{-1} + 0.939062505817492\ Z^{-2}$**
BPF21	**$1-Z^{-2}$**	**$1- 0.243148953267983\ Z^{-1} + 0.939062505817492\ Z^{-2}$**
BPF22	**$1-Z^{-2}$**	**$1- 0.121814850415330\ Z^{-1} + 0.939062505817492\ Z^{-2}$**
BPF23	**$1-Z^{-2}$**	**$1- 0.000000000000000\ Z^{-1} + 0.939062505817492\ Z^{-2}$**
BPF24	**$1-Z^{-2}$**	**$1+0.1218148504153300\ Z^{-1} + 0.939062505817492\ Z^{-2}$**
BPF25	**$1-Z^{-2}$**	**$1+0.2431489532679820\ Z^{-1} + 0.939062505817492\ Z^{-2}$**
BPF26	**$1-Z^{-2}$**	**$1+0.3635234582862760\ Z^{-1} + 0.939062505817493\ Z^{-2}$**
BPF27	**$1-Z^{-2}$**	**$1+0.482463302292784\ Z^{-1} + 0.939062505817492\ Z^{-2}$**
BPF28	**$1-Z^{-2}$**	**$1+0.5994990840616590\ Z^{-1} + 0.939062505817492\ Z^{-2}$**
BPF29	**$1-Z^{-2}$**	**$1+0.7141689168308220\ Z^{-1} + 0.939062505817493\ Z^{-2}$**
BPF30	**$1-Z^{-2}$**	**$1+0.8260202511579960\ Z^{-1} + 0.939062505817493\ Z^{-2}$**
BPF31	**$1-Z^{-2}$**	**$1+0.9346116609266070\ Z^{-1} + 0.939062505817493\ Z^{-2}$**

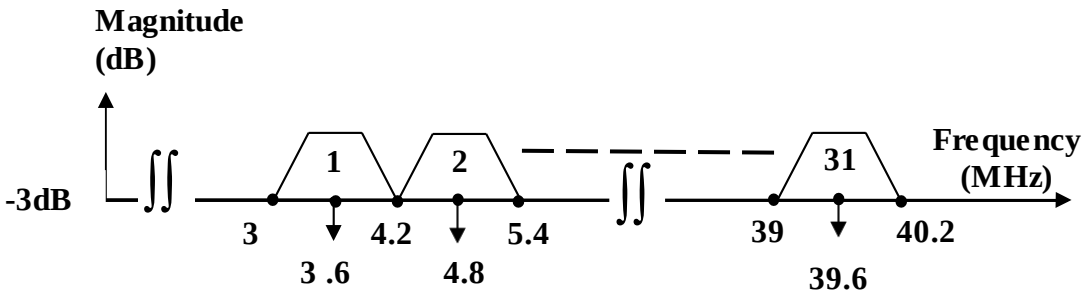

Figure (3.17): Distribution of the frequencies over the band of FSK FFH/SSS contiguous filters.

Table (3.6): Center frequency of contiguous digital BPF banks for BSK FFH/SSS

Filter	*Frequency (MHz)*
BPF01	03.6
BPF02	04.8
BPF03	06.0
BPF04	07.2
BPF05	08.4
BPF06	09.6
BPF07	10.8
BPF08	12.0
BPF09	13.2
BPF10	14.4
BPF11	15.6
BPF12	16.8
BPF13	18.0
BPF14	19.2
BPF15	20.4
BPF16	21.6

Filter	*Frequency (MHz)*
BPF17	22.8
BPF18	24.0
BPF19	25.2
BPF20	26.4
BPF21	27.6
BPF22	28.8
BPF23	30.0
BPF24	31.2
BPF25	32.4
BPF26	33.6
BPF27	34.8
BPF28	36.0
BPF29	37.2
BPF30	38.4
BPF31	39.6

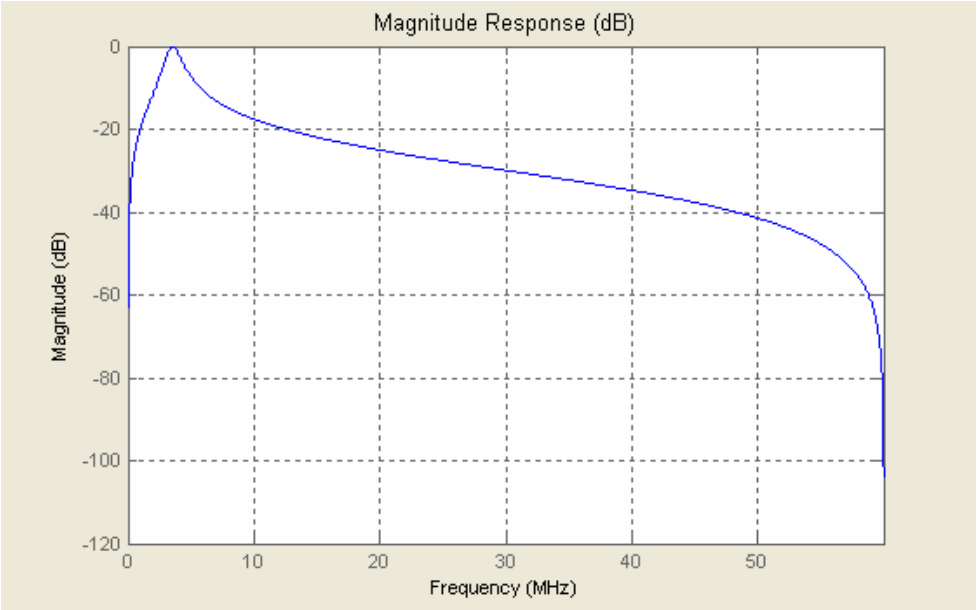

Figure (3.18): The magnitude response of IIR second order BPF01 for FSK FFH/SSS using contiguous technique

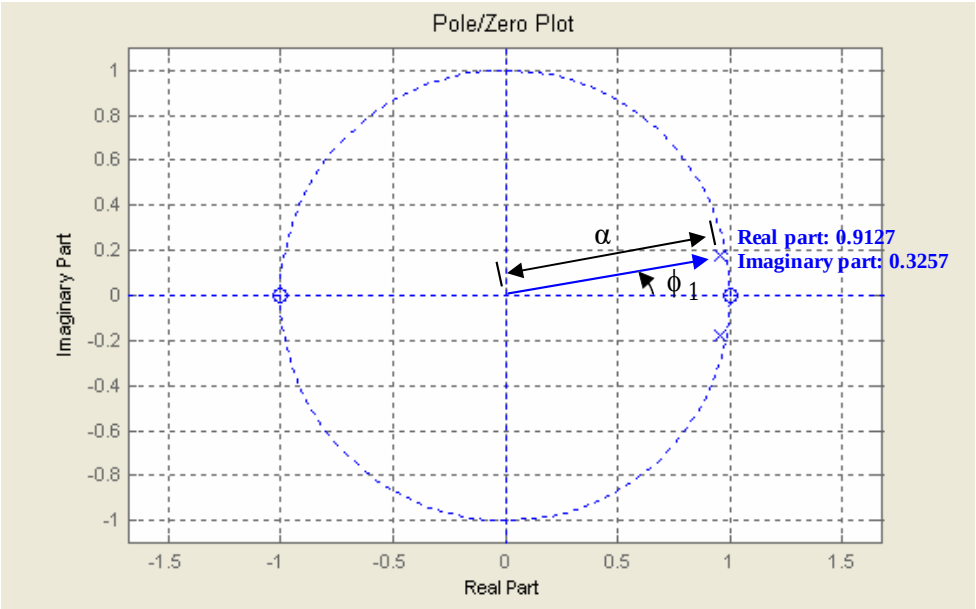

Figure (3.19): The pole zero configuration of IIR second order BPF01 for FSK FFH/SSS using contiguous technique.

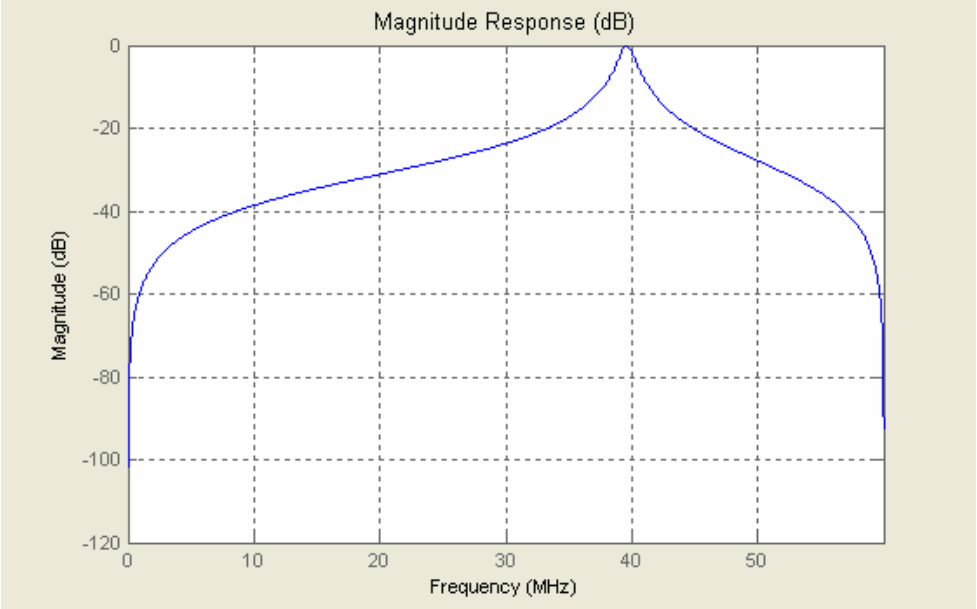

Figure (3.20): The magnitude response of IIR second order BPF31 for FSK FFH/SSS using contiguous technique

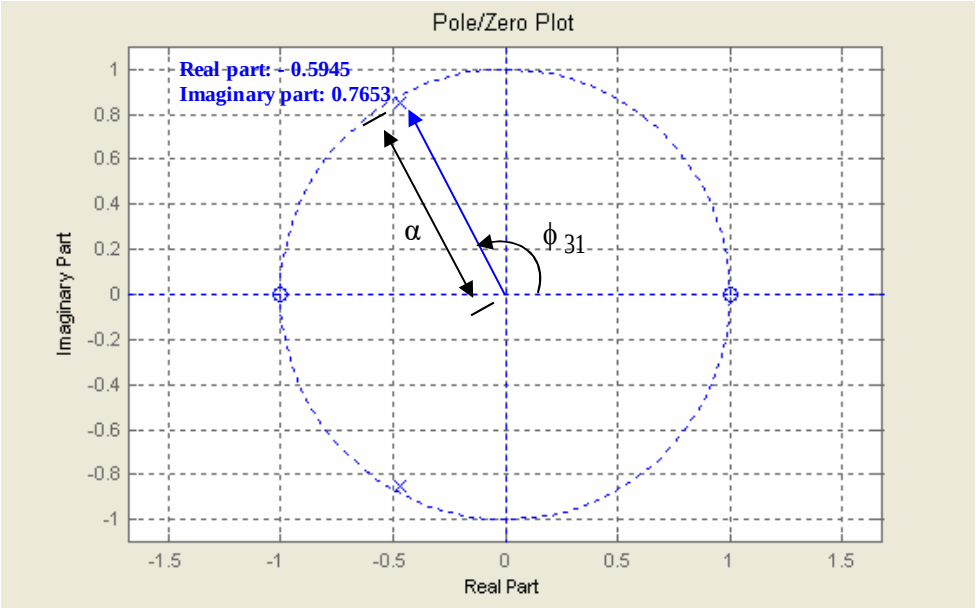

Figure (3.21) The pole zero configuration of IIR second order for BPF31 for FSK FFH/SSS using contiguous technique

3.4.2 Noncontiguous Filters

In this design the noncontiguous technique is used to make the overall bandwidth of FH /SS signal smaller than that used in contiguous technique. This compression can make the system have good benefits. As shown in section (3.4) the proposed system needs to design parallel IIR second order Butterworth BPF banks as shown in Figure (3.8) which consists of 31 Butterworth noncontiguous filters, Table (3.7) shows the TF for each filter which is found by the same procedure as in section (3.2). The center frequency of each filter is shown in Table (3. 8). These center frequencies values are corresponding to that of DDFS. The relation between f_c , f_{m1} , f_{m2} and R_b with the other step of the design is the same as that stated in section (3.4.1). The realization of each filter is the same as that shown in Figure (3.2) except that the coefficient values are different. Figure (3.22) shows the distribution of frequencies over the band (3 MHz-22.2 MHz) of FSK FFH/SSS used in the system using noncontiguous technique. Figures (3.23) and (3.24) show the magnitude response and pole zero configuration respectively for specified (f_L = 3 MHz, f_H = 4.2 MHz, f_s = 60 MHz, f_c 3.6 MHz) BPF01 for FSK FFH/SSS. Figures (3.25) and (3.26) show the magnitude response and pole zero configuration respectively for specified (f_L = 21 MHz, f_H = 22.2 MHz, f_s = 60 MHz, f_c 21.6MHz), BPF01 for FSK FFH/SSS using noncontiguous technique.

Table (3.7): The TF of noncontiguous IIR second order Butterworth BPF banks for FSK FFH/SSS

Filter	*Numerator*	*Denominator*
BPF01	$1-Z^{-2}$	$1 - 1.752943756671322\ Z^{-1} + 0.881618592363189\ Z^{-2}$
BPF02	$1-Z^{-2}$	$1 - 1.705905619856961\ Z^{-1} + 0.881618592363189\ Z^{-2}$
BPF03	$1-Z^{-2}$	$1 - 1.652135052915168\ Z^{-1} + 0.881618592363189\ Z^{-2}$
BPF04	$1-Z^{-2}$	$1 - 1.591844263708228\ Z^{-1} + 0.881618592363189\ Z^{-2}$
BPF05	$1-Z^{-2}$	$1 - 1.525271192436899\ Z^{-1} + 0.881618592363189\ Z^{-2}$
BPF06	$1-Z^{-2}$	$1 - 1.452678572599146\ Z^{-1} + 0.881618592363189\ Z^{-2}$
BPF07	$1-Z^{-2}$	$1 - 1.374352894101055\ Z^{-1} + 0.881618592363189\ Z^{-2}$
BPF08	$1-Z^{-2}$	$1 - 1.290603272612059\ Z^{-1} + 0.881618592363189\ Z^{-2}$
BPF09	$1-Z^{-2}$	$1 - 1.201760229626613\ Z^{-1} + 0.881618592363189\ Z^{-2}$
BPF10	$1-Z^{-2}$	$1 - 1.108174388046856\ Z^{-1} + 0.881618592363189\ Z^{-2}$
BPF11	$1-Z^{-2}$	$1 - 1.010215088434197\ Z^{-1} + 0.881618592363189\ Z^{-2}$
BPF12	$1-Z^{-2}$	$1 - 0.908268931390862\ Z^{-1} + 0.881618592363189\ Z^{-2}$
BPF13	$1-Z^{-2}$	$1 - 0.802738251823931\ Z^{-1} + 0.881618592363189\ Z^{-2}$
BPF14	$1-Z^{-2}$	$1 - 0.694039531113274\ Z^{-1} + 0.881618592363189\ Z^{-2}$
BPF15	$1-Z^{-2}$	$1 - 0.582601753449814\ Z^{-1} + 0.881618592363189\ Z^{-2}$
BPF16	$1-Z^{-2}$	$1 - 0.468864712830910\ Z^{-1} + 0.881618592363189\ Z^{-2}$
BPF17	$1-Z^{-2}$	$1 - 0.353277277394375\ Z^{-1} + 0.881618592363189\ Z^{-2}$
BPF18	$1-Z^{-2}$	$1 - 0.236295617941000\ Z^{-1} + 0.881618592363189\ Z^{-2}$
BPF19	$1-Z^{-2}$	$1 - 0.118381407636811\ Z^{-1} + 0.881618592363189\ Z^{-2}$
BPF20	$1-Z^{-2}$	$1 - 0.000000000000000\ Z^{-1} + 0.881618592363189\ Z^{-2}$
BPF21	$1-Z^{-2}$	$1 + 0.118381407636811\ Z^{-1} + 0.881618592363189\ Z^{-2}$
BPF22	$1-Z^{-2}$	$1 + 0.236295617941000\ Z^{-1} + 0.881618592363189\ Z^{-2}$
BPF23	$1-Z^{-2}$	$1 + 0.353277277394375\ Z^{-1} + 0.881618592363189\ Z^{-2}$
BPF24	$1-Z^{-2}$	$1 + 0.468864712830910\ Z^{-1} + 0.881618592363189\ Z^{-2}$
BPF25	$1-Z^{-2}$	$1 + 0.582601753449814\ Z^{-1} + 0.881618592363189\ Z^{-2}$
BPF26	$1-Z^{-2}$	$1 + 0.694039531113274\ Z^{-1} + 0.881618592363189\ Z^{-2}$
BPF27	$1-Z^{-2}$	$1 + 0.802738251823931\ Z^{-1} + 0.881618592363189\ Z^{-2}$
BPF28	$1-Z^{-2}$	$1 + 0.908268931390862\ Z^{-1} + 0.881618592363189\ Z^{-2}$
BPF29	$1-Z^{-2}$	$1 + 1.010215088434197\ Z^{-1} + 0.881618592363189\ Z^{-2}$
BPF30	$1-Z^{-2}$	$1 + 1.108174388046856\ Z^{-1} + 0.881618592363189\ Z^{-2}$
BPF31	$1-Z^{-2}$	$1 + 1.201760229626614\ Z^{-1} + 0.881618592363189\ Z^{-2}$

Table (3.8): Center frequency of contiguous digital BPF banks for BSK FFH/SSS

Filter	*Frequency (MHz)*
BPF01	**03.6**
BPF02	**04.2**
BPF03	**04.8**
BPF04	**05.4**
BPF05	**06.0**
BPF06	**06.6**
BPF07	**07.2**
BPF08	**07.8**
BPF09	**08.4**
BPF10	**09.0**
BPF11	**09.6**
BPF12	**10.2**
BPF13	**10.8**
BPF14	**11.4**
BPF15	**12.0**
BPF16	**12.6**

Filter	*Frequency (MHz)*
BPF17	**13.2**
BPF18	**13.8**
BPF19	**14.4**
BPF20	**15.0**
BPF21	**15.6**
BPF22	**16.2**
BPF23	**16.8**
BPF24	**17.4**
BPF25	**18.0**
BPF26	**18.6**
BPF27	**19.2**
BPF28	**19.8**
BPF29	**20.4**
BPF30	**21.0**
BPF31	**21.6**

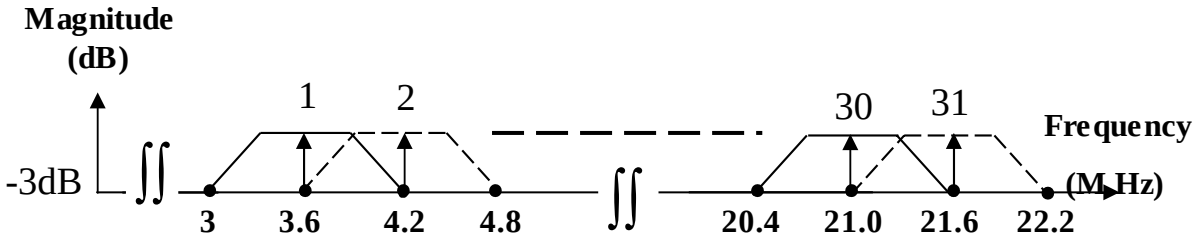

Figure (3.22): The distribution of the frequencies over the band of FSK FFH/SSS noncontiguous filters

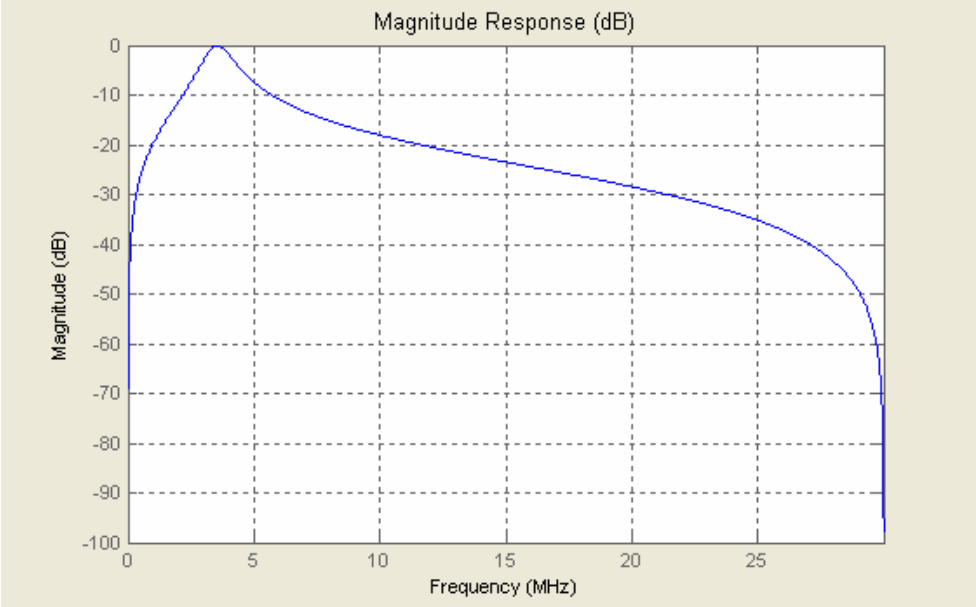

Figure (3.23): The magnitude response of IIR second order for BPF01 for FSK FFH/SSS using contiguous technique.

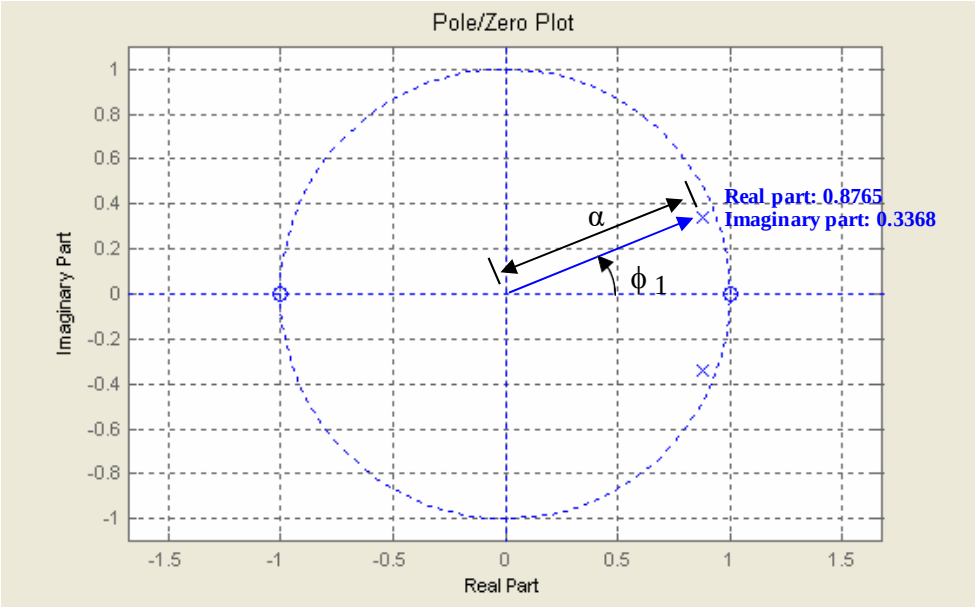

Figure (3.24): The pole zero configuration of IIR second order BPF01 for FSK FFH/SSS using contiguous technique

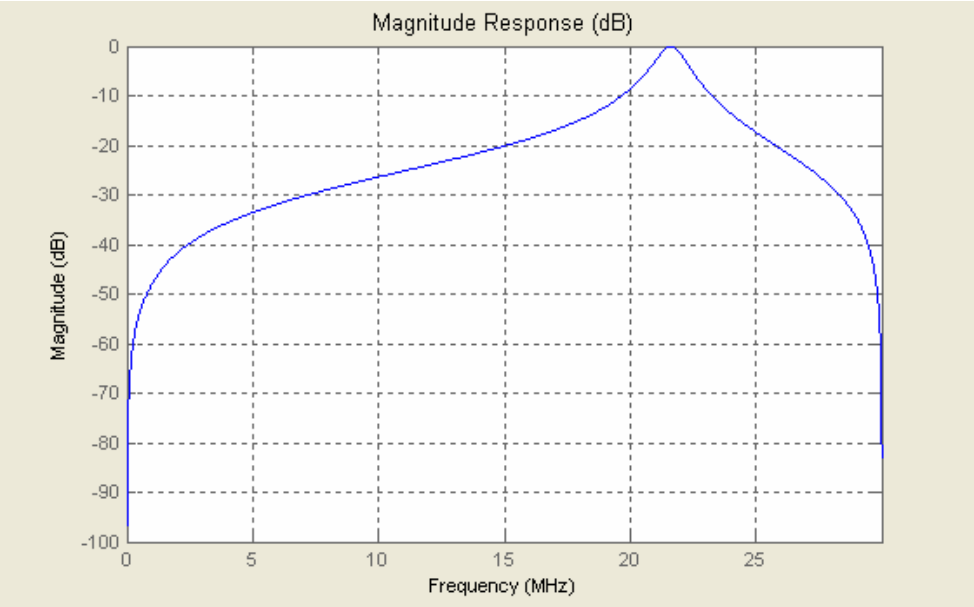

Figure (3.25): The magnitude response of IIR second order BPF31 for FSK FFH/SSS using noncontiguous technique

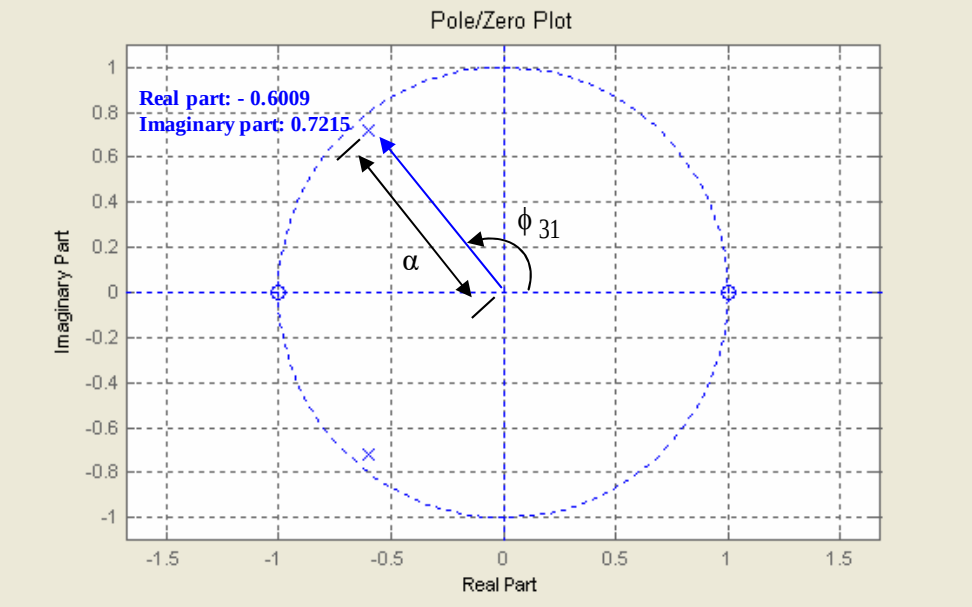

Figure (3.26) The pole zero configuration of IIR second order BPF31 for FSK FFH/SSS using noncontiguous technique.

Chapter Four

Design and Simulation of ASK FFH/SS Transceiver

4.1 Introduction

In this chapter ASK FFH/SS systems for hopping rate with 160 k hop/sec and 160 k bit/sec data rate using contiguous and noncontiguous IIR second order Butterworth BPF banks are designed using MATLAB-Simulink tool. These systems are designed and implemented successfully in real time in the presence of AWGN and two types of jamming.

4.2 The Proposed System

The block diagram of proposed system for contiguous and noncontiguous IIR second order Butterworth BPF banks for ASK FFH/SS systems is shown in Figure (4.1a) and it is implemented using MATLAB-Simulink version 7, as shown in Figure (4.1b). This contains, the transmitter, transmission channel, contiguous and noncontiguous digital BPF banks and receiver.

4.2.1 The Transmitter

The transmitter contains: data generator, spread code generator, serial/parallel converter, DDFS, mixer (spreading ASK signals) and digital HPF.

4.2.1.1 Data Generator

The binary data generator (Bernoulli Binary Generator) taken from communication block is set with a probability of zero 50 % and 50 % one's, to be used to transmit in data rate 160 k bit /sec. The waveform and spectrum of data are shown in Figures (4.2) and (4.3) respectively.

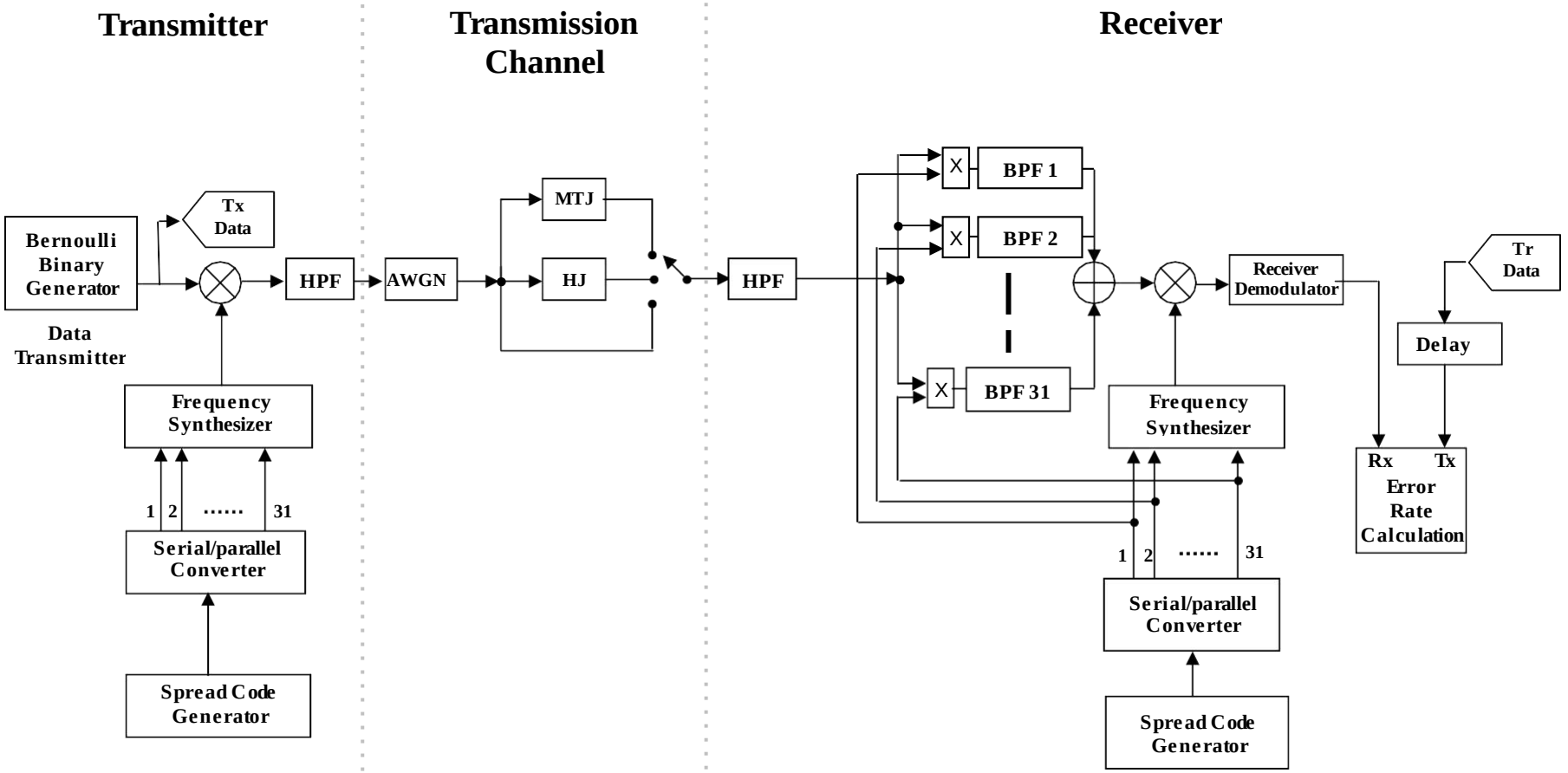

Figure (4.1a): Transceiver Block diagram of ASK FFH /SS system.

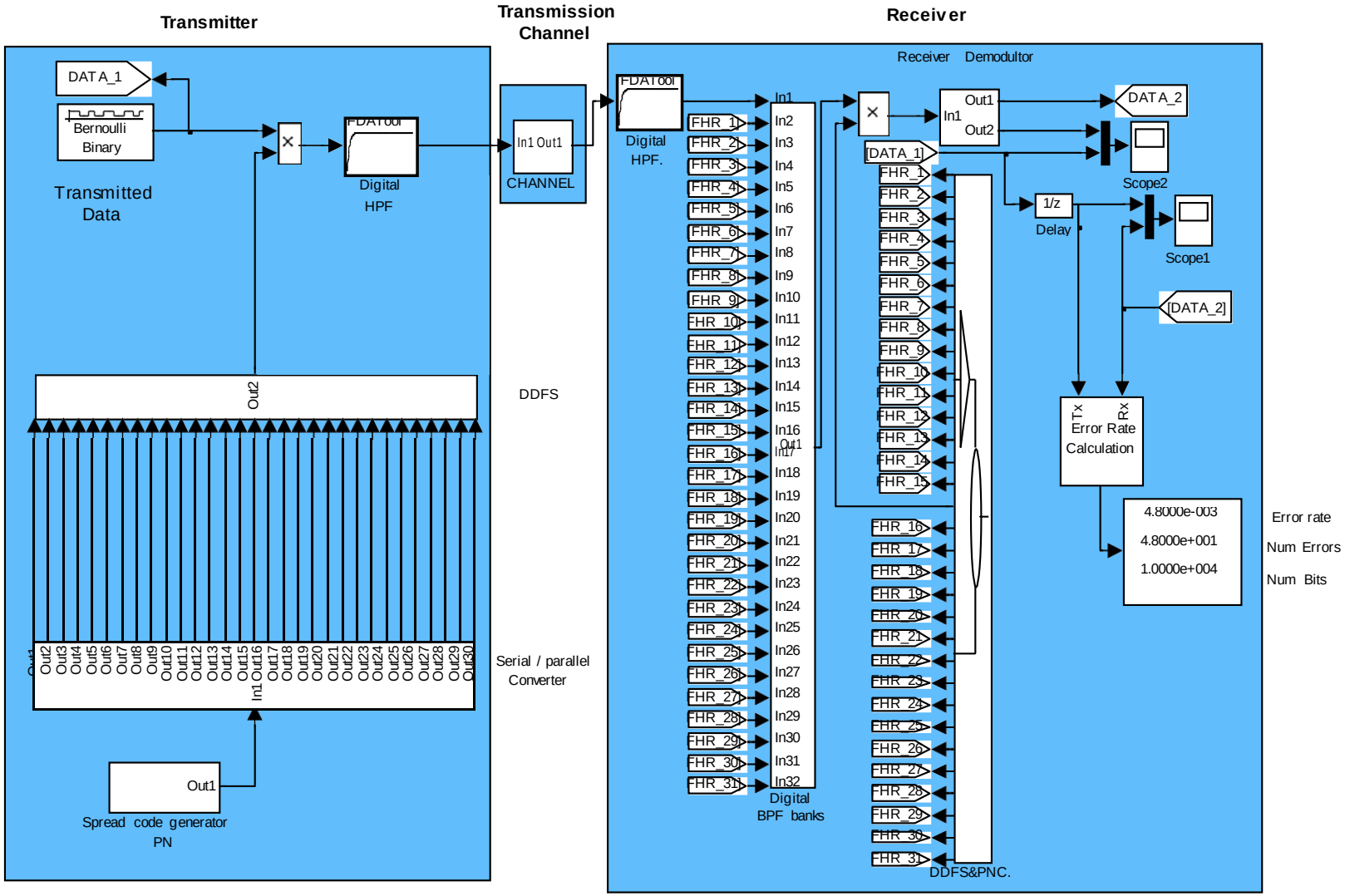

Figure (4.1b): Design and simulation of ASK FFH / SS transceiver system

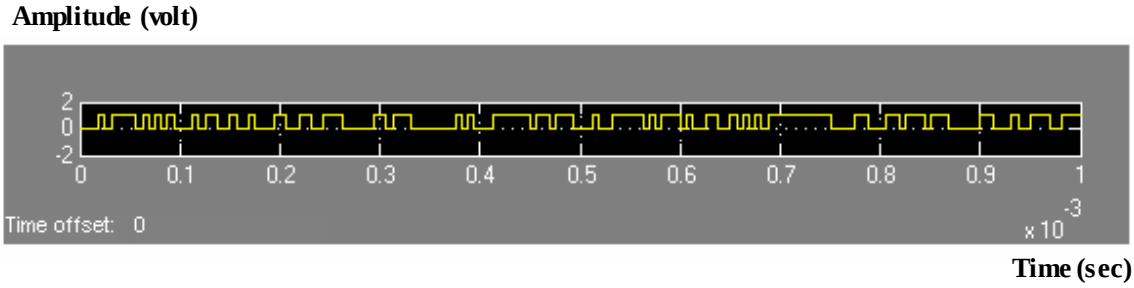

Figure (4.2): Waveform of data 160 k bit/sec

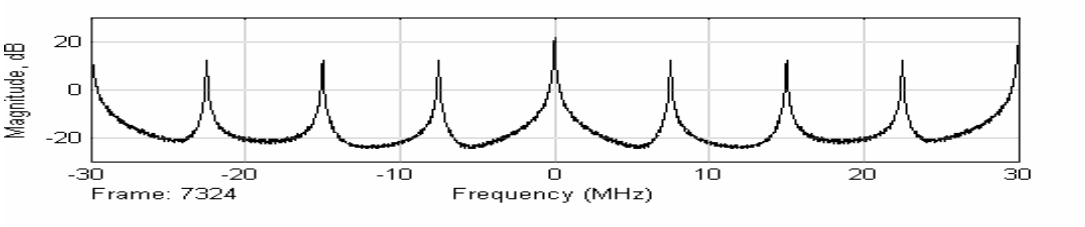

Figure (4.3): Spectrum of data 160 k bit/sec

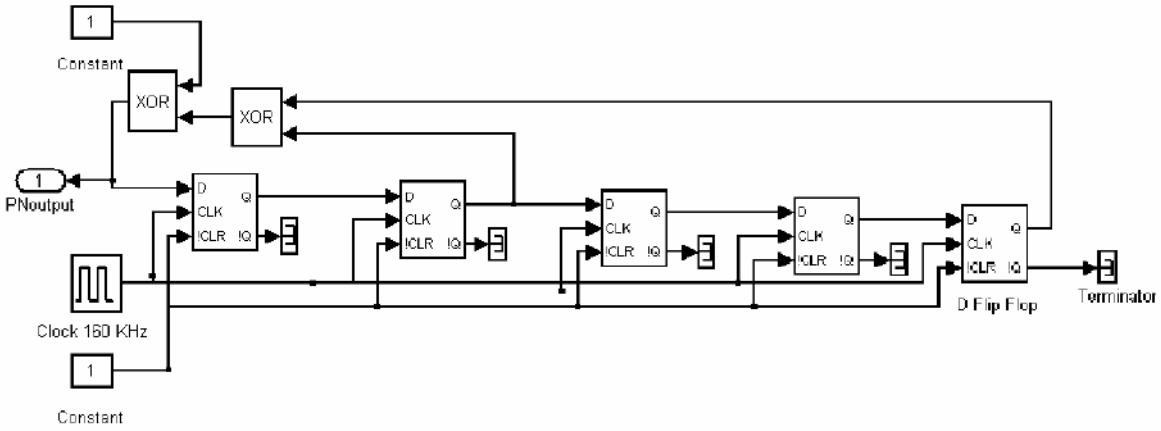

Figure (4.4): Design and simulation of PN code generator using Simulink.

4.2.1.2 Spread Code Generator.

The spreading code generator is a PN code. Its implementation design using Simulink are shown in Figure (4.4). PN sequence is generated as a maximal linear code with a polynomial, $f(x) = 1 + x^2 + x^5$. The PN sequence is generated by using five stages DFF from Simulink-Extras with two feedback taped (X^2, X^5) Ex-Ored to the input of the first stage, in order to get 31 bit length maximal linear code (2^n-1,n =5), the waveform of PN digital clock, 160 kHz is shown in Figure (4.5). The waveform and spectrum of 31 bit maximal liner code are shown in Figures (4.6) and (4.7), respectively, for ASK FFH/SSS using contiguous and noncontiguous technique.

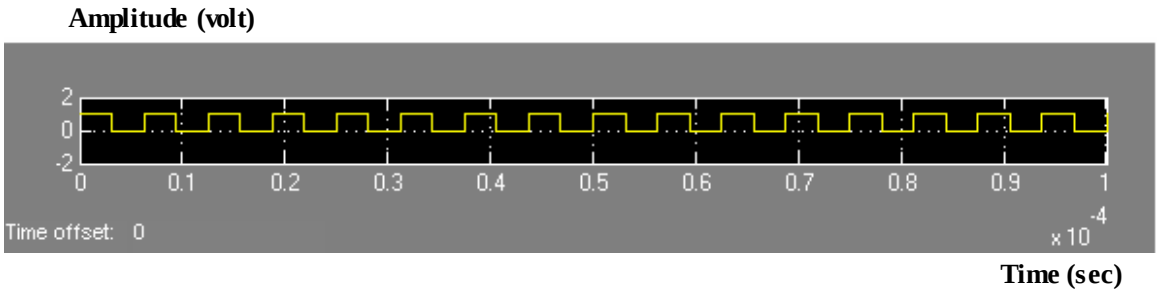

Figure (4.5): The waveform digital clock 160 KHz

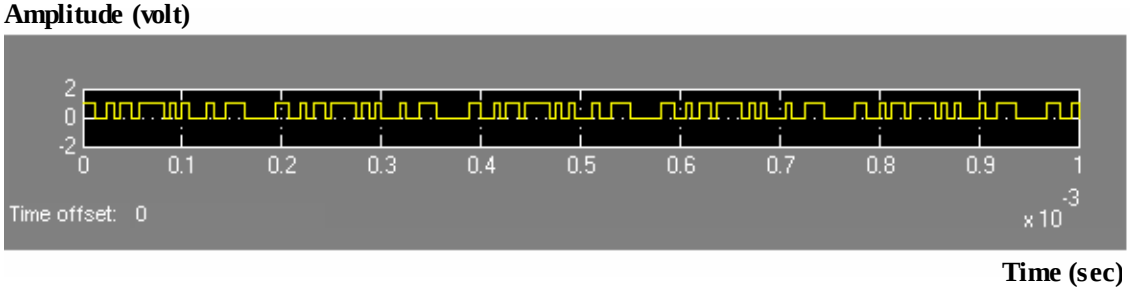

Figure (4.6): Waveform of 31 bit maximal liner code

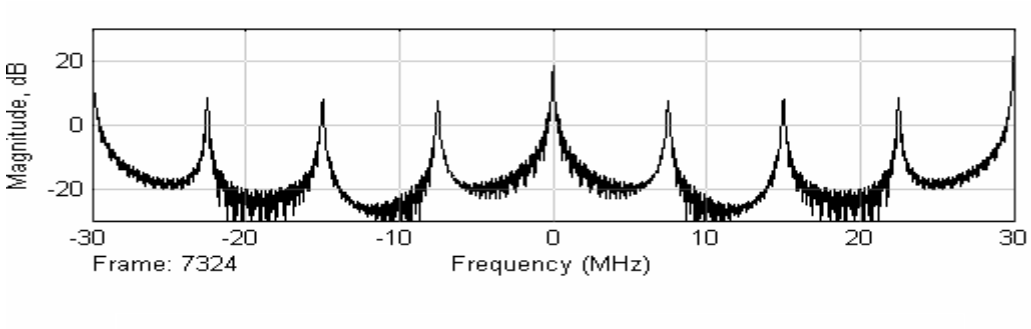

Figure (4.7) Spectrum of 31bit maximal liner code

4.2.1.3 Serial / Parallel Converter.

The implementation of the design using Simulink is shown in Figure (4.12). It is used to convert the serial output of spread code generator to parallel bits in order to control the DDFS. The serial / parallel converter is implemented using five stages DFF taken from Simulink- Extra and the output of the converter connected to the direct digital frequency synthesizer through special logic circuit.

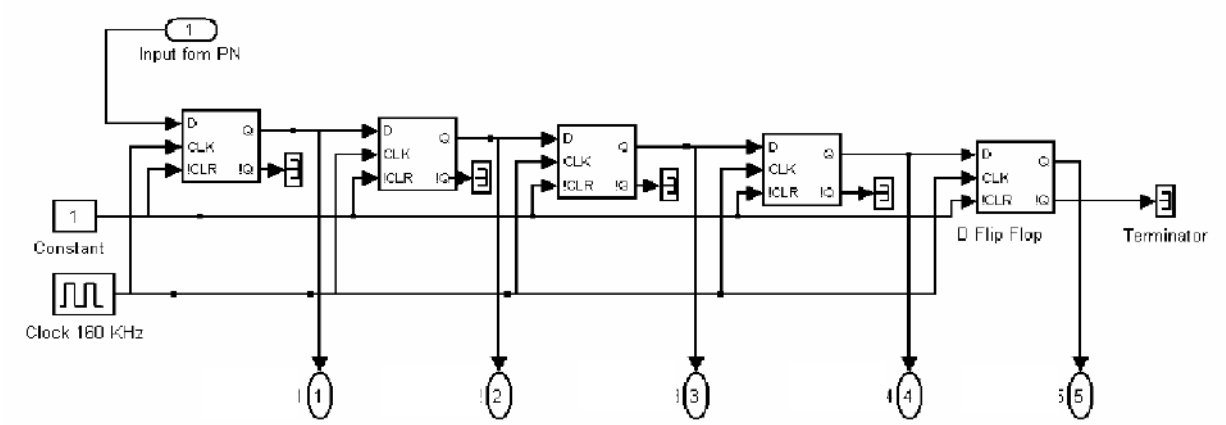

Figure (4.8) Design and simulation serial / parallel converter using simulink

4.2.1.4 Direct Digital Frequency Synthesizer (DDFS)

The block diagram of implementing it is shown in Figure (4.9). It is implemented by using 31 sinusoidal waves each one is taken from DSP signal processing block set (MATLAB-Simulink) and connected by special logic circuit to keep that only one signal at a time multiplied with data at each hop. Figures (4.10),(4.11),(4.12) and (4.13) show the output of DDFS waveforms and spectrums for ASK FFH/SSS using contiguous and noncontiguous technique respectively.

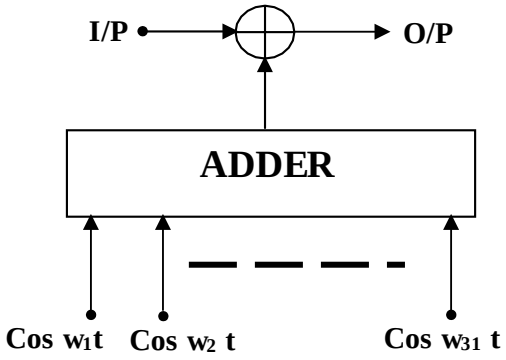

Figure (4.9)Direct Digital Frequency Synthesizer

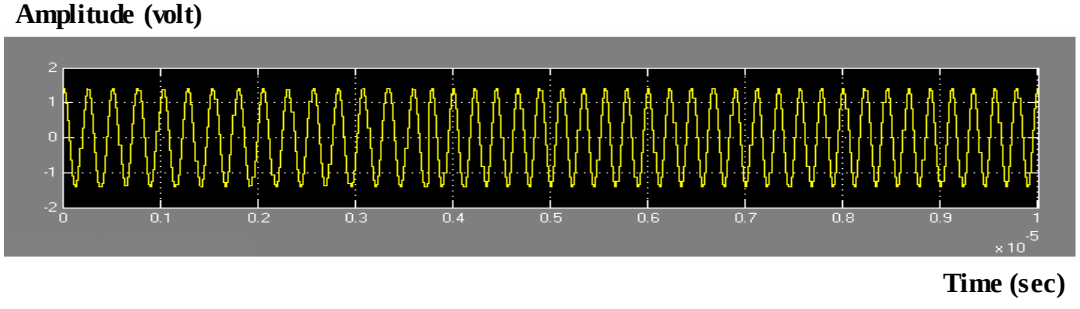

Figure (4.10): Waveform of some 31 signals of DDFS for ASK FFH/SSS using contiguous technique

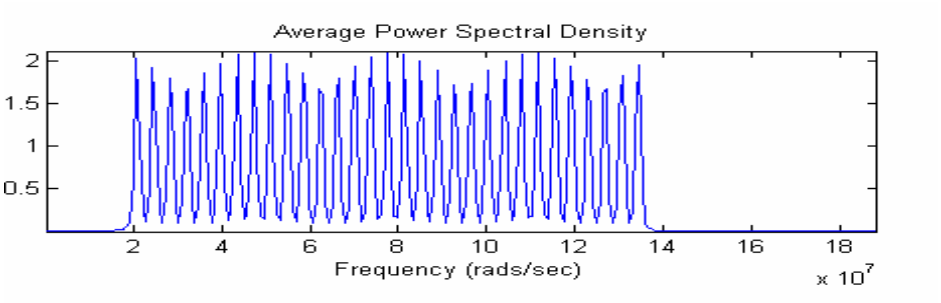

Figure (4.11): Spectrum of 31 signals of DDFS for ASK FFH/SSS using contiguous technique

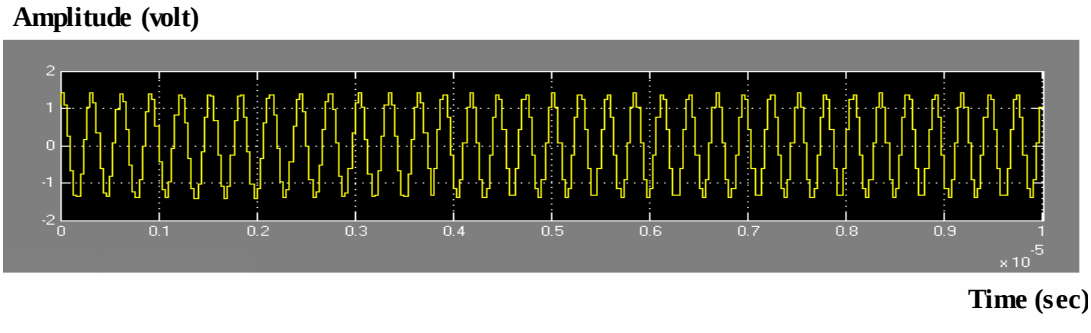

Figure (4.12): Waveform of some 31 signals of DDFS for ASK FFH/SSS using noncontiguous technique

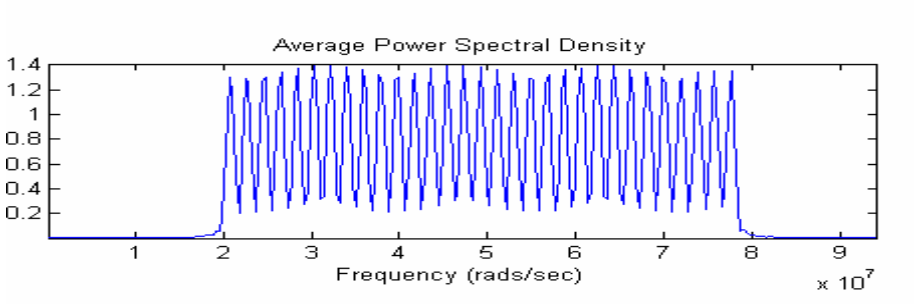

Figure (4.13): Spectrum of 31 signals of DDFS for ASK FFH/SSS using noncontiguous technique

4.2.1.5 Data Spreading for ASK FFH/SSS.

The basic idea of FH, and all types of spread spectrum are spreading the data over a wide bandwidth by mixing with local DDFS before transmitted. The spreading technique for FH in this system does not directly modulate the data modulated carrier but it is used to control the sequence of carrier frequencies. Because the transmitted signal appears as a data modulated carrier which is hopping from one frequency to the next, (FH spreader) this type of pread spectrum is called FH/SS. On the receiver side, the frequency hopping is

removed (FH despreader) by mixing with local oscillator DDFS, which is hopping synchronously with the received signal. Figure (4.14) shows the waveforms of transmitted data and DDFS signals and spreading transmitted data ASK FFH/SSS. Figure (4.15) shows spectrum of spreading transmitted data for ASK FFH/SSS.

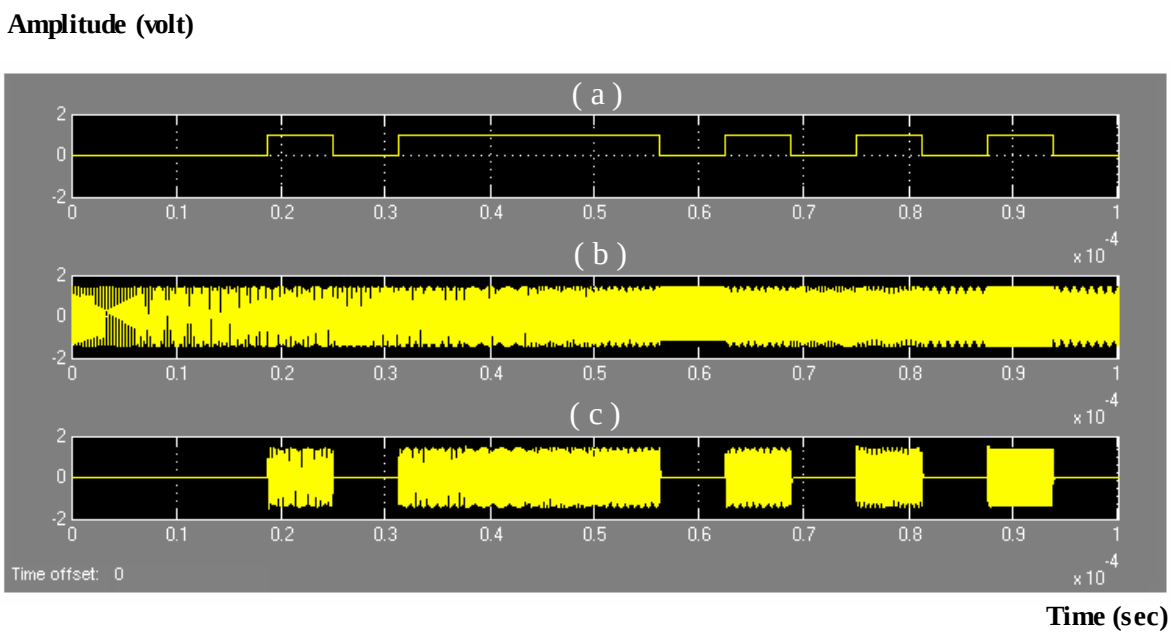

Figure (4.14): Waveforms of:
(a) Transmitted data 160 k bit/sec.
(b) DDFS signals.
(c) Spreading data (ASK) before channel.

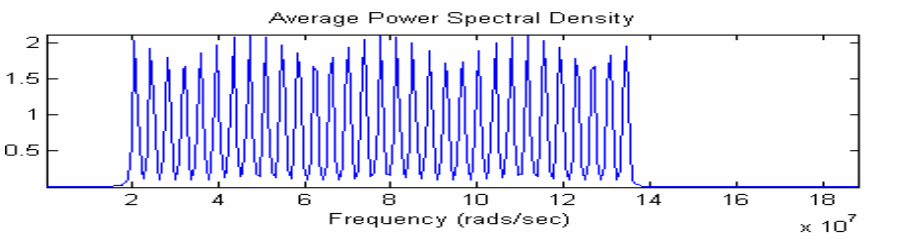

Figure (4.15): Spectrum of spreading data of ASK FFH signal transmitted

4.2.1.6 Digital High Pass Filter (HPF).

The digital HPF used in the proposed system is IIR second order Butterworth HPF designed with -3dB cut off frequency 3MHz. This filter is implanted using MATLAB-Simulink; it is used to reject unwanted signals.

4.3 The Channel

The FH/SSS which is shown in Figure (4.1) has been used to transmit data through transmission channel. The block diagram of the transmission channel contains: AWGN, MTJ and HJ.

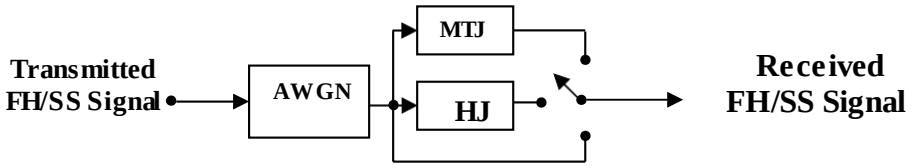

Figure (4.16): Transmission channel

4.3.1 AWGN

When the transmission channel uses only AWGN through the manual switch, it is added to the transmitted signal with signal to noise ratio (as selected). The waveform and spectrum of the transmitted signal under AWGN (SNR = -5 d B) are shown in Figures (4.17), (4.18), (4.19) and (4.20) for ASK FFH/SSS using contiguous and noncontiguous technique respectively.

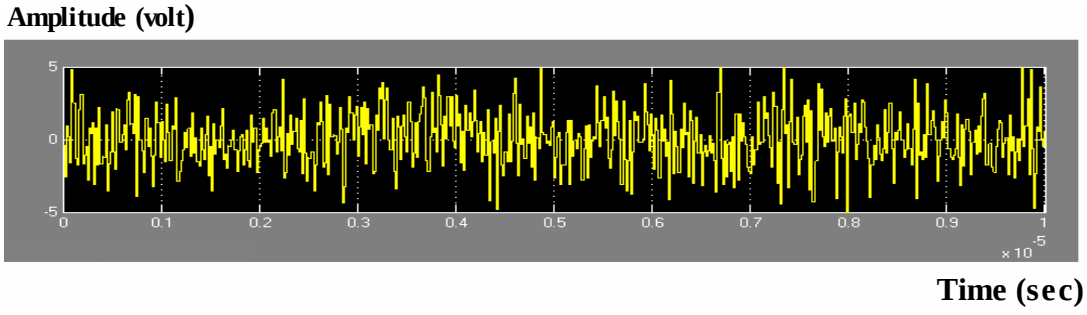

Figure (4.17): Waveform of transmitted ASK FFH/SS signals under AWGN (SNR = -5dB) using contiguous technique

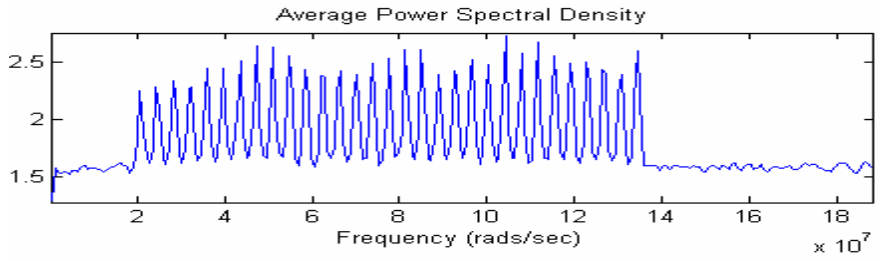

Figure (4.18): Spectrum of transmitted ASK FFH/SS signals under AWGN (SNR=-5 dB)

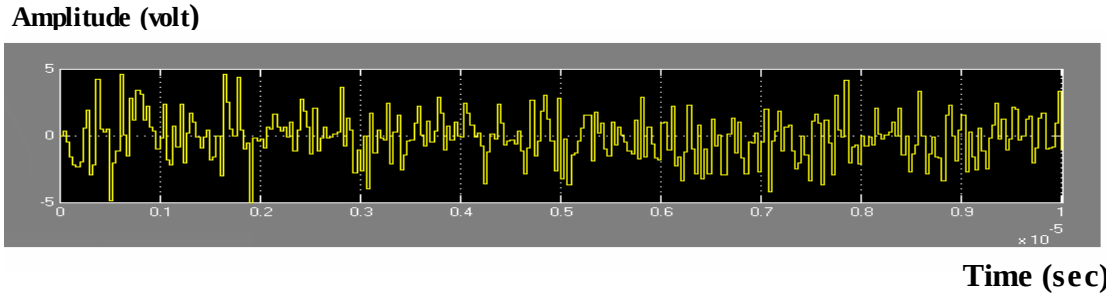

Figure (4.19): Waveform of transmitted ASK FFH/SS signals under AWGN (SNR = -5dB) using noncontiguous technique

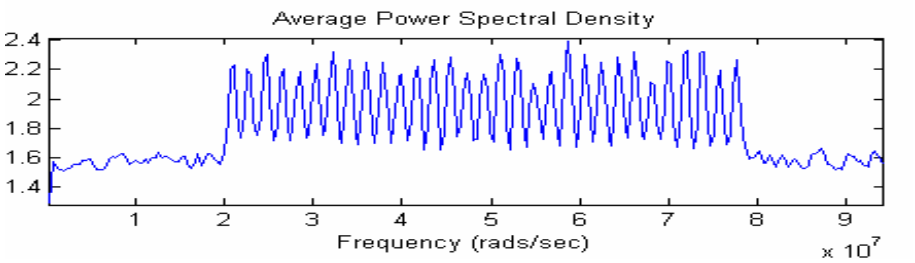

Figure (4.20): Spectrum of transmitted ASK FFH/SSS signals under AWGN (SNR = -5dB) using noncontiguous technique

4.3.2 Multitone Jamming (MTJ)

The block diagram of implementing it is shown in Figure (4.21). MTJ (f_j = 3.16 MHz, 3.32 MHz, 3.48 MHz, SJR = 2.181134486 dB) is added to the transmitted data with AWGN (for BER = 0.0001). The waveform and spectrum of transmitted signals under MTJ and AWGN are shown in Figures (4.22), (4.23),(4.24) and (4.26) for ASK FFH/SSS using contiguous and noncontiguous technique respectively.

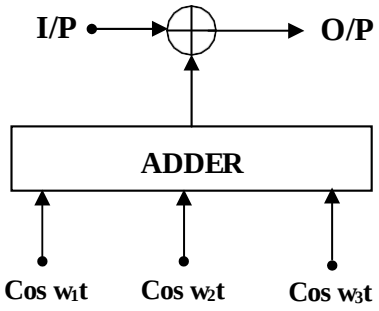

Figure (4.21): Block Diagram of MTJ

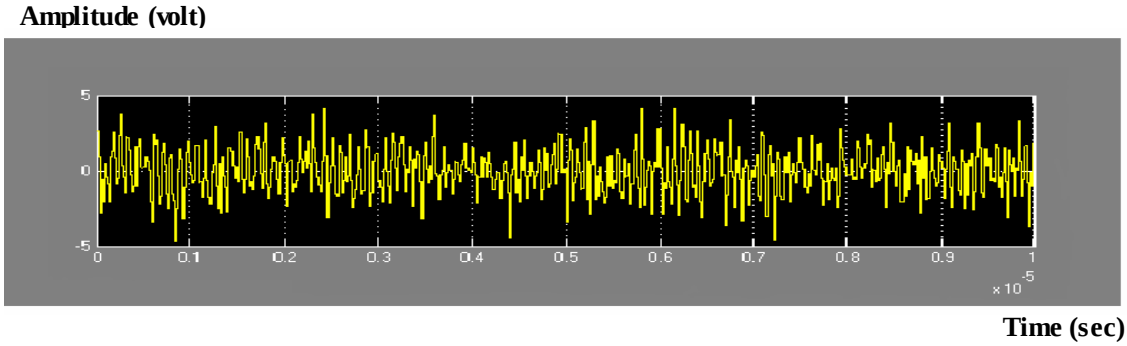

Figure (4.22): Waveform of transmitted ASK FFH/SS signals spreading data under MTJ using contiguous technique

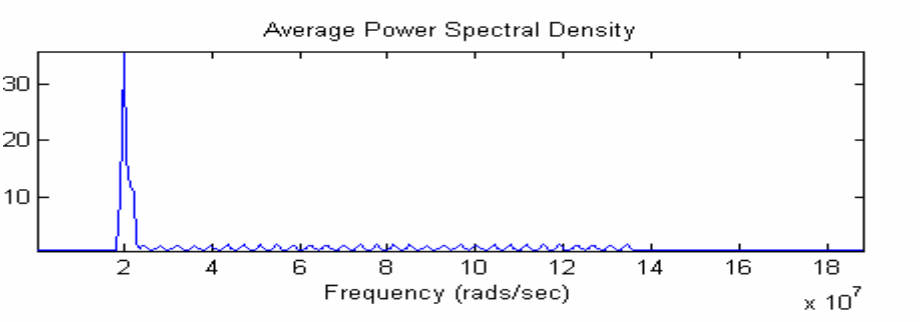

Figure (4.23): Spectrum of transmitted ASK FFH/SS signals under MTJ using contiguous technique

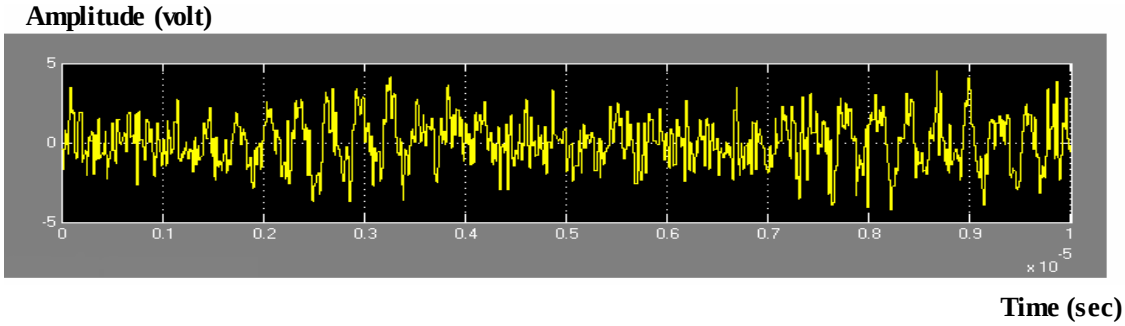

Figure (4.24): The waveform of transmitted ASK FFH/SS signals under MTJ using noncontiguous technique

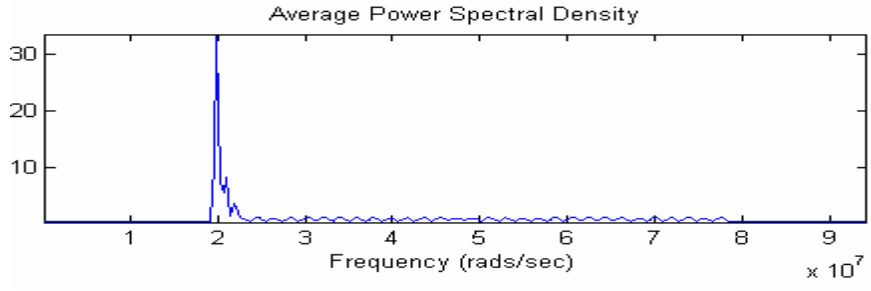

Figure (4.25): Spectrum of transmitted ASK FFH/SS signals under MTJ using noncontiguous technique

4.3.3 Hopper Jamming (HJ)

The block diagram of implementing it is shown in Figure (4.26). HJ is (f_j=3.16 MHz,3.32 MHz,3.48 MHz, SJR = 2.181134486 dB) added to the transmitted data with AWGN (BER = 0.00001). The waveform of transmitted signals under HJ and AWGN are shown in Figures (4.27), (4.28), (4.29) and (4.30) for contiguous and noncontiguous technique respectively.

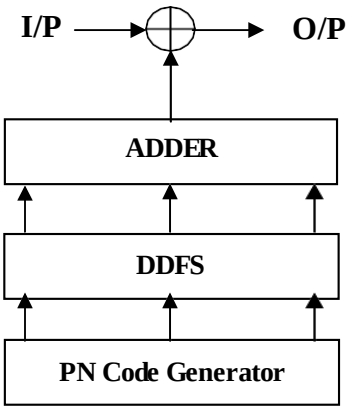

Figure (4.26) Block Diagram of HJ

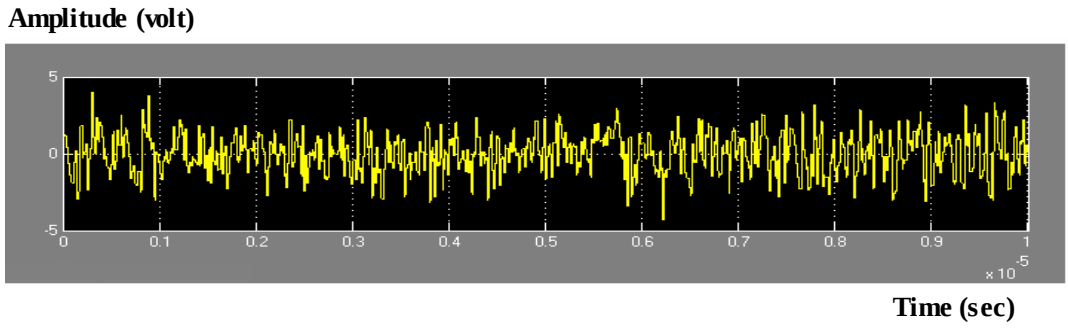

Figure (4.27): Waveform of transmitted ASK FFH/SS signals under HJ using contiguous technique

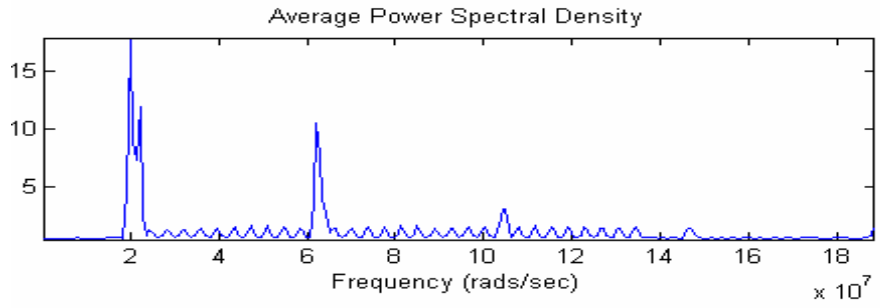

Figure (4.28): Spectrum of transmitted ASK FFH/SS signals under HJ using contiguous technique

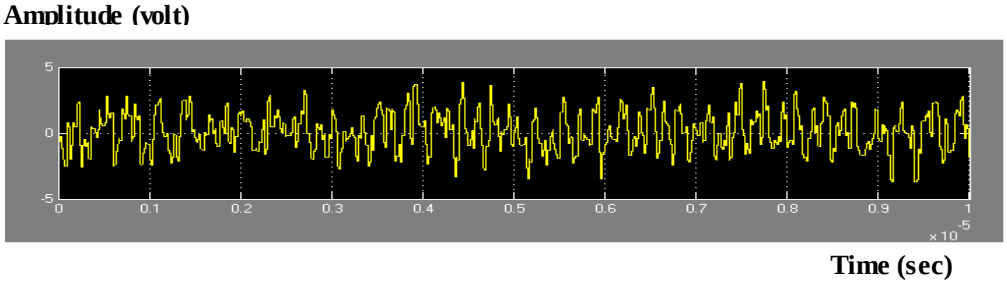

Figure (4.29): Waveform of transmitted ASK FFH/SS signals under HJ using noncontiguous technique

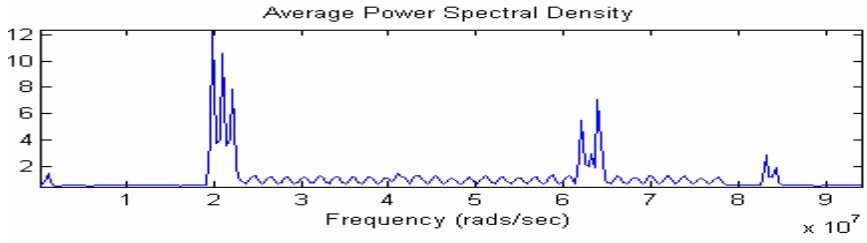

Figure (4.30): Spectrum of transmitted ASK FFH/SS signals under HJ using noncontiguous technique

4.4 The Receiver

Figure (4.1) shows the block diagram of the receiver which contains, bank of parallel digital BPFs, spread code generator, serial/parallel converter, DDFS, mixer (de-spreading), ASK demodulator, error rate calculation. Digital HPF is the same as that of the transmitter section (4.2.1.6) it is used to reject the unwanted signal before de-spreading.

4.4.1 Bank of Parallel Digital BPF

The implementing of it is shown in Figure (3.9) which contains 31 parallel digital, second order BPFs. The center frequency of each filter which is shown in Table (3.2) and (3.4) for contiguous and noncontiguous technique is the same that in DDFS. All the BPFs are controlled through the spread code generator. Figures (4.31),(4.32),(4.33) and (4.34) show the waveform and spectrum of the transmitted ASK FFH/SS signals with AWGN (SNR = -5dB), Figures (4.35),(4.36),(4.37) and (4.38) show the waveform and spectrum of the transmitted ASK FFH/SS signals under MTJ (f_j=3.16 MHz,3.32 MHz,3.48 MHz and SJR=2.181134486 dB), Figures (4.39),(4.40),(4.41) and (4.42) show

the waveform and spectrum of the transmitted ASK FFH/SS signal under HJ (f_j=3.16 MHz,3.32 MHz,3.48 MHz and SJR=2.181134486 dB) after passing through the contiguous and noncontiguous parallel digital BPF banks respectively.

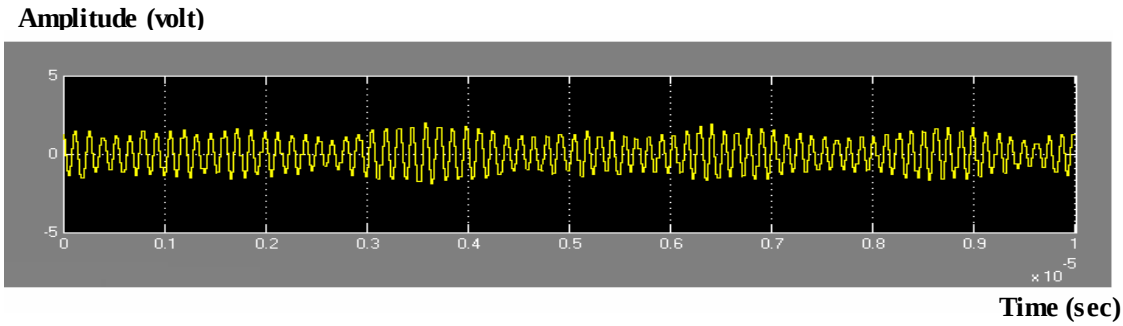

Figure (4.31): Spreading ASK FFH/SS signals under AWGN (SNR=-5dB) using contiguous technique

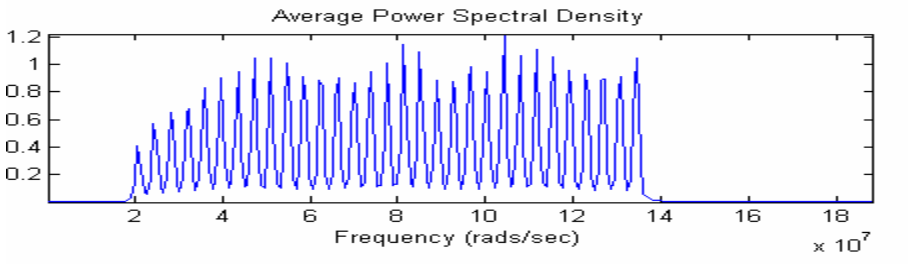

Figure (4.32): Spreading spectrum ASK FFH/SS signals under AWGN (SNR= -5dB) using contiguous technique

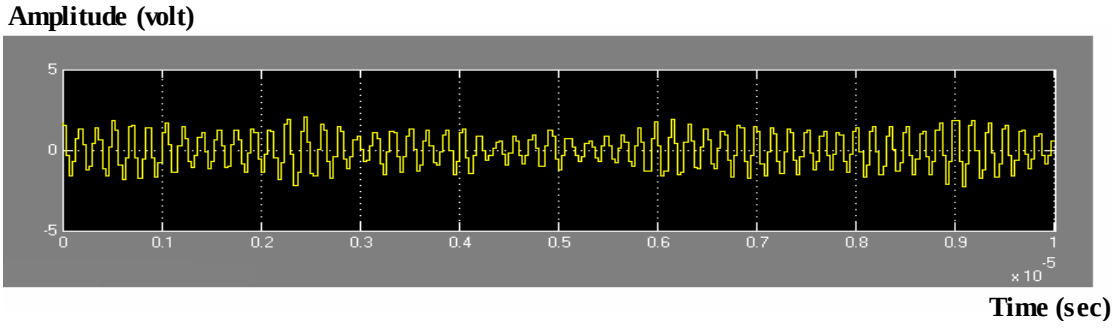

Figure (4.33): Spreading ASK FFH signals under AWGN (SNR=-5dB) using noncontiguous technique

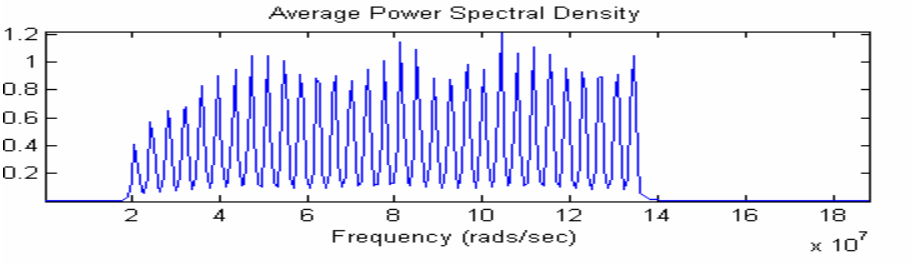

Figure (4.34): Spreading spectrum ASK FFH/SS signals under AWGN (SNR= - 5dB) using noncontiguous technique

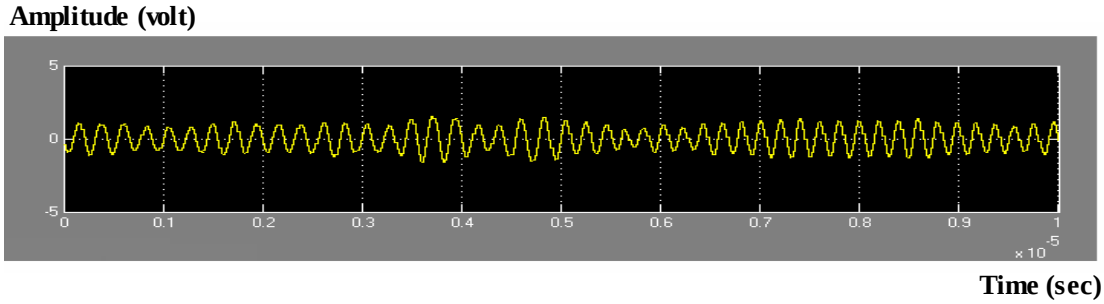

Figure (4.35): Spreading ASK FFH/SS signals under MTJ using contiguous technique

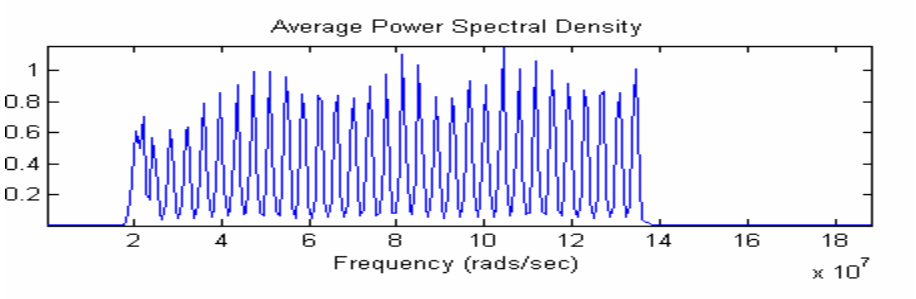

Figure (4.36): Spreading spectrum of ASK FFH/SS signals under MTJ using contiguous technique

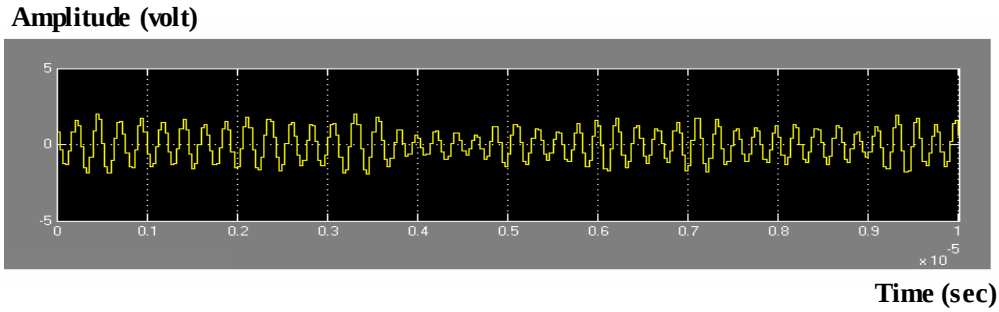

Figure (4.37): Spreading ASK FFH/SS signals under MTJ using noncontiguous technique

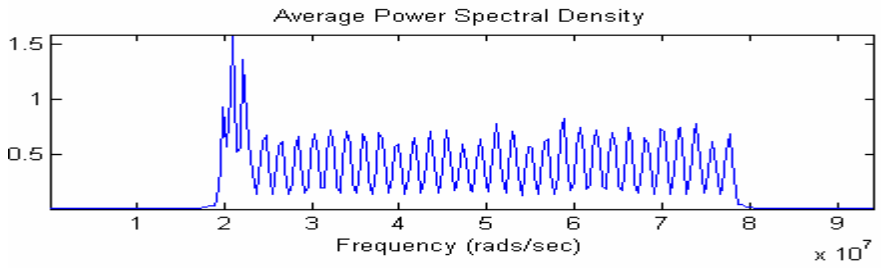

Figure (4.38): Spreading spectrum ASK FFH/SS signals MTJ using noncontiguous technique

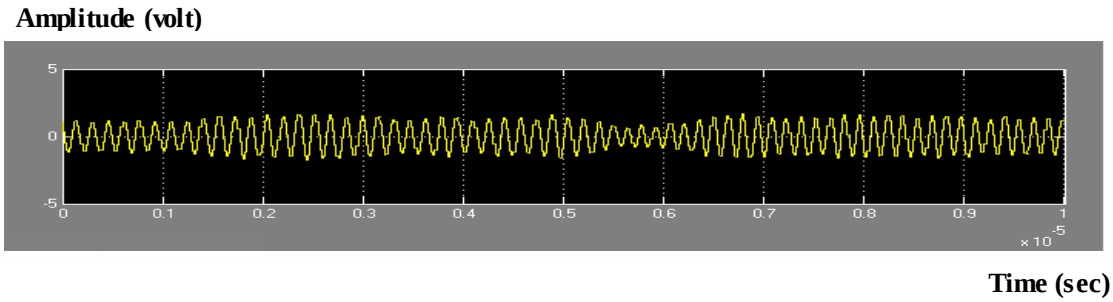

Figure (4.39): Spreading ASK FFH/SS signals under HJ for ASK FFH/SSS using contiguous technique

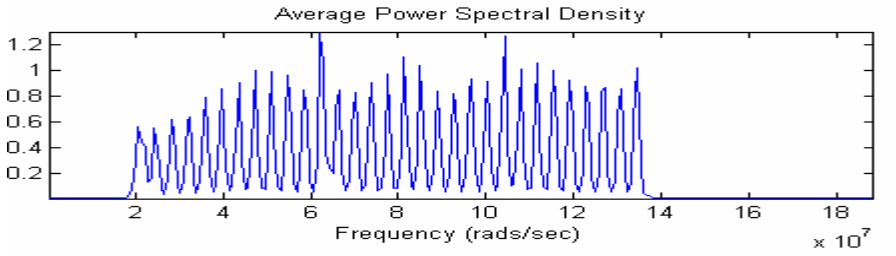

Figure (4.40): Spreading spectrum of ASK FFH/SS signals under HJ using contiguous technique

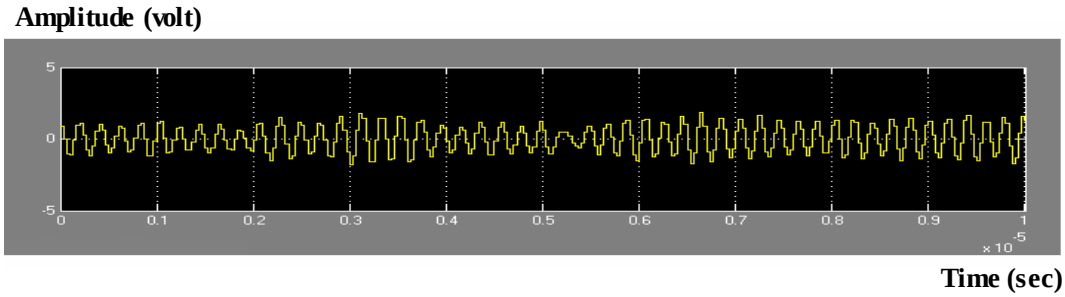

Figure (4.41): Spreading ASK FFH/SS signals under HJ using noncontiguous technique

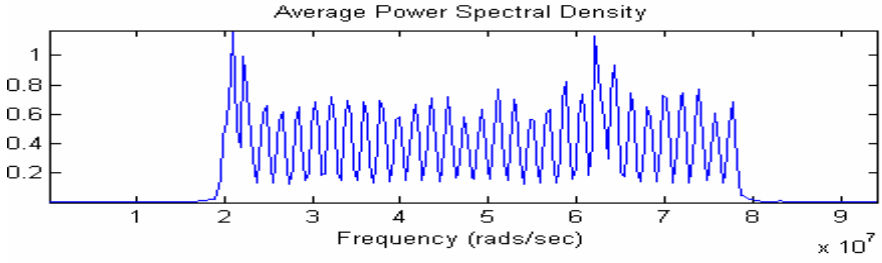

Figure (4.42): Spreading spectrum ASK FFH/SS signals under HJ using noncontiguous technique

4.4.2 Spread Code Generator.

It is the same as that of the transmitter section (4.2.1.2)

4.4.3 Serial / parallel Converter.

It is the same as that of the transmitter section (4.2.1.3) except that it is used to controlling of BPFs and DDFS signals of frequency synthesizer at the same time for the sake of keeping the synchronization between transmitter and receiver.

4.4.4 DDFS

It is the same as that of the transmitter section (4.2.1.4), its function is to make down conversion (de-spreading).

4.4.5 Data De-spreading for ASK FFH/SSS.

The data de-spreading is used at the receiver to obtain the transmitted data from the band received signals. This technique is stated in detail in section (4.2.1.5). Figures (4.43), (4.44) and (4.45) show the received waveform under, AWGN (SNR =-5 dB, BER=0.0102), MTJ and HJ each one specified (f_j=3.16 MHz, 3.32 MHz, 3.48 MHz, and SJR= 2.181134486 dB, BER=0.0001), respectively. Each figure state the following: (a) received spreading ASK FFH/SS signals after passed through contiguous digital PBF banks. (b) DDFS signals**.** (c)de-spreading signals. Figures (4.46), (4.47), (4.48) and (4.49) show waveform and spectrum of the de-spreading transmitted ASK FFH/SS signals with AWGN (SNR= -5dB). Figures (4.50),(4.51),(4.52) and (4.53) show the waveform and spectrum of the de-spreading transmitted ASK FFH/SS signal under MTJ (f_j=3.16 MHz,3.32 MHz,3.48 MHz and SJR=2.181134486 dB), Figures (4.54), (4.55),(4.56) and (4.57) show the waveform and spectrum of the de-spreading transmitted ASK FFH/SS signals under HJ (f_j=3.16 MHz,3.32MHz,3.48 MHz and SJR=2.181134486 dB) after passing through noncontiguous the bank of digital BPF banks respectively.

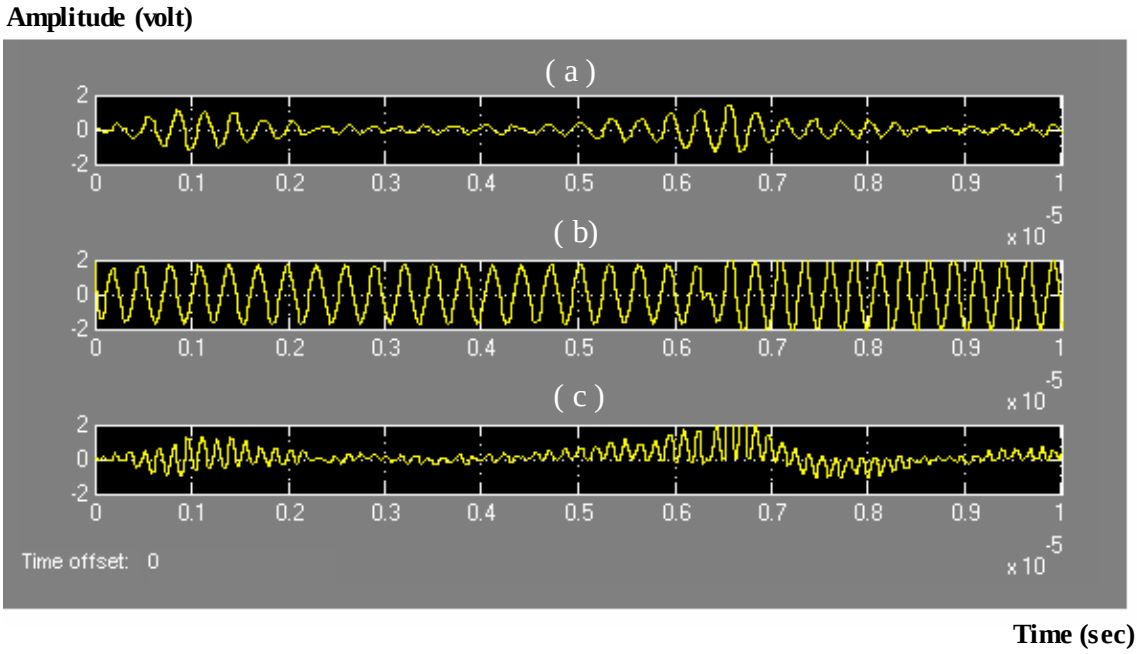

Figure (4.43): Received ASK FFH/SS signals using contiguous technique under AWGN (SNR = -5 dB, BER=0.0102)
(a) sreading signals
(b) DDFS signals.
(c) despreading signals.

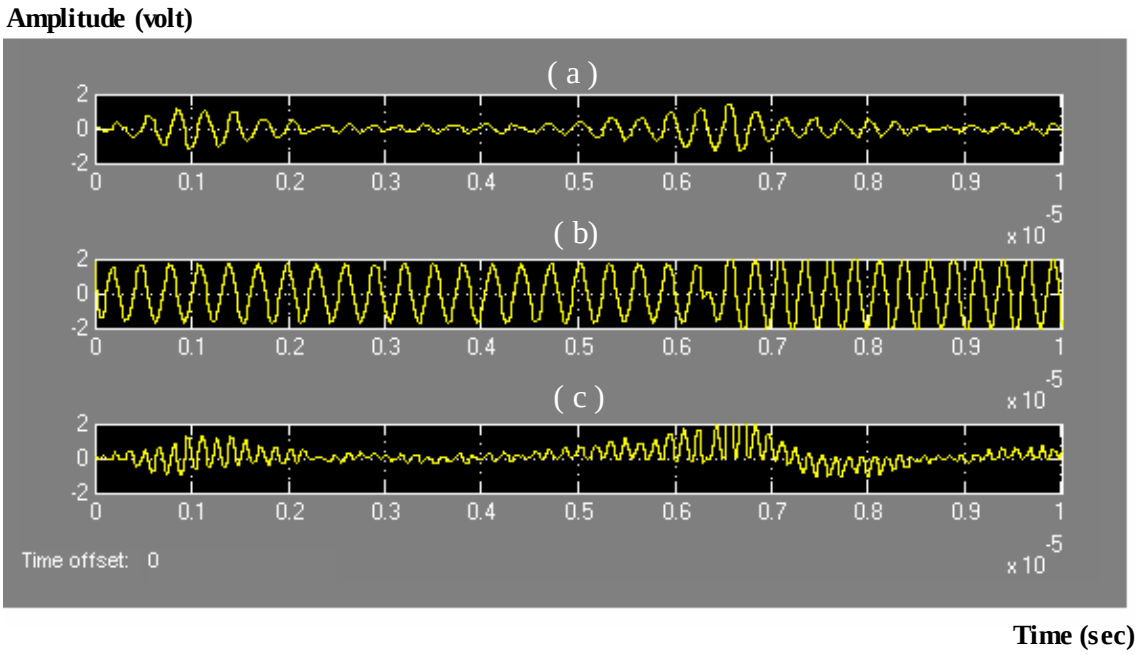

Figure (4.44): Received ASK FFH/SS signals using contiguous technique under MTJ (SJR= 2.181134486 dB, BER=0.0001)
(a) spreading signals
(b) DDFS signals.
(c) despreading signals.

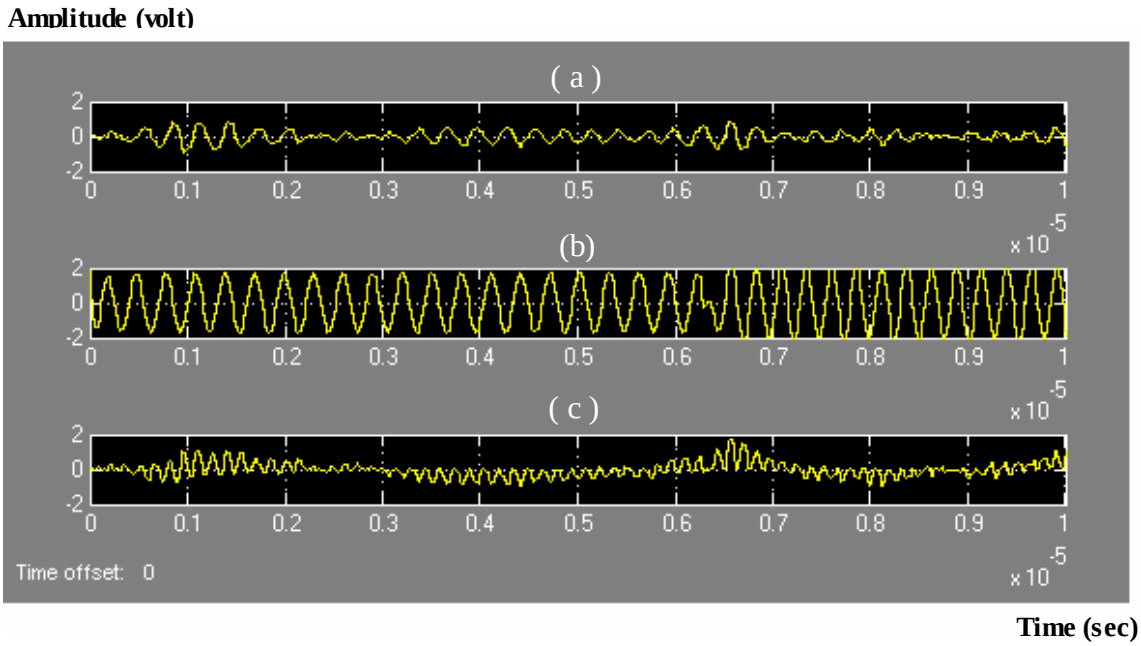

Figure (4.45): Received ASK FFH/SS signals using contiguous technique under HJ (SJR= 2.181134486 dB, BER=0.0001)
(a) spreading signals.
(b) DDFS signals.
(c) despreading signals.

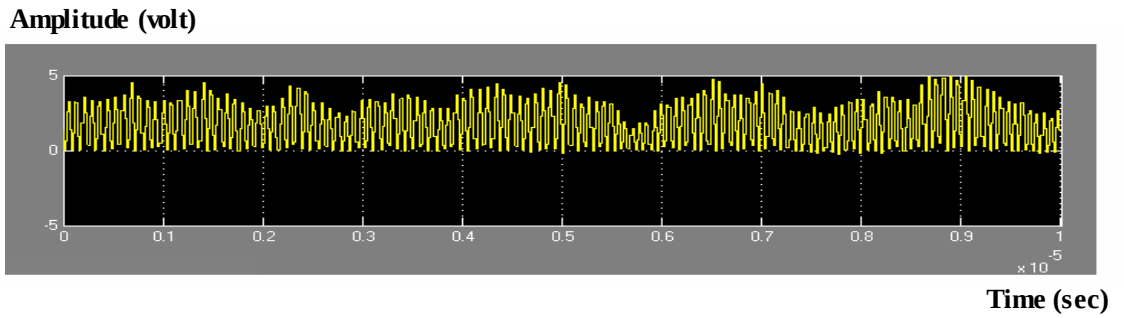

Figure (4.46): Despreading ASK FFH/SS signals under AWGN (SNR=-5dB) using contiguous technique

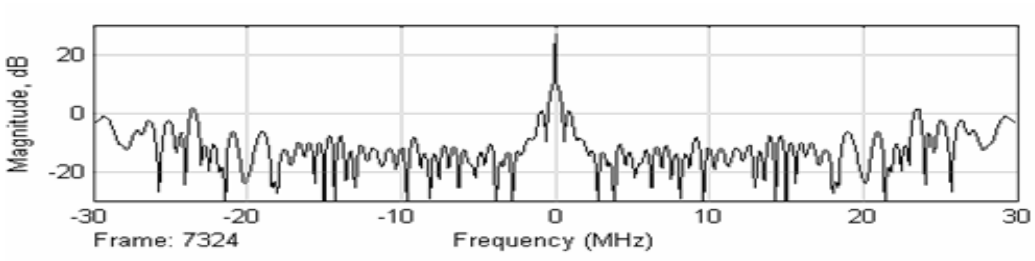

Figure (4.47): Despreading spectrum ASK FFH/SS signals under AWGN (SNR=-5dB) using contiguous technique

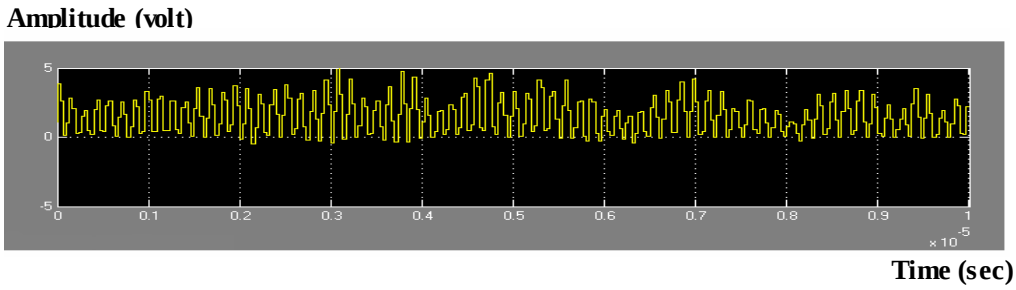

Figure (4.48): Despreading ASK FFH/SS signals under AWGN (SNR=-5dB) using noncontiguous technique

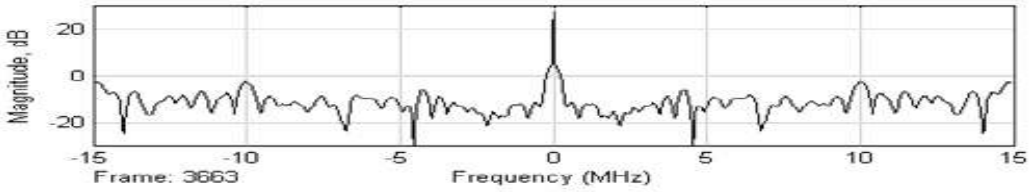

Figure (4.49): Despreading spectrum ASK FFH/SS signals under AWGN (SNR=-5dB) using noncontiguous technique

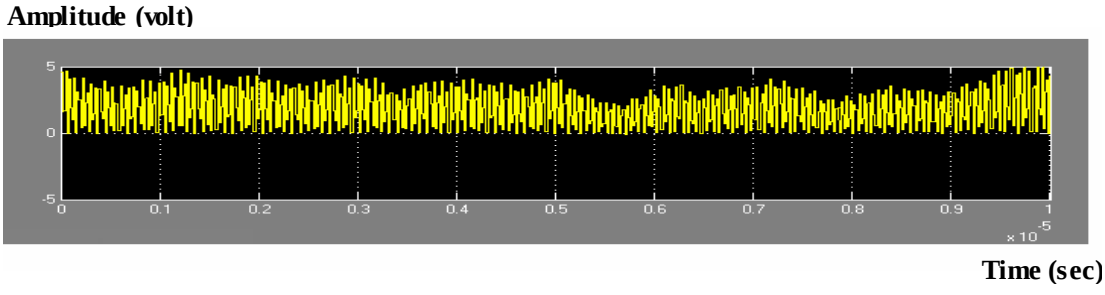

Figure (4.50): Despreading ASK FFH/SS signals under MTJ using contiguous technique

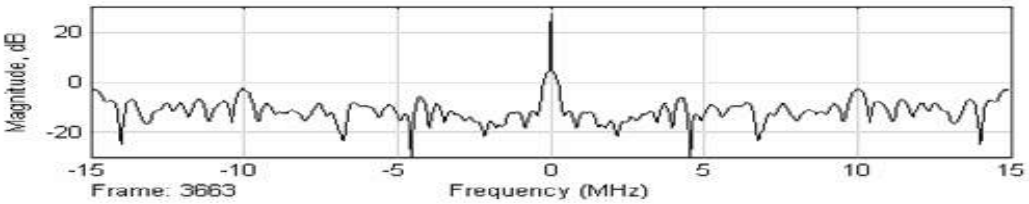

Figure (4.51): Despreading spectrum ASK FFH/SS signals under MTJ using contiguous technique

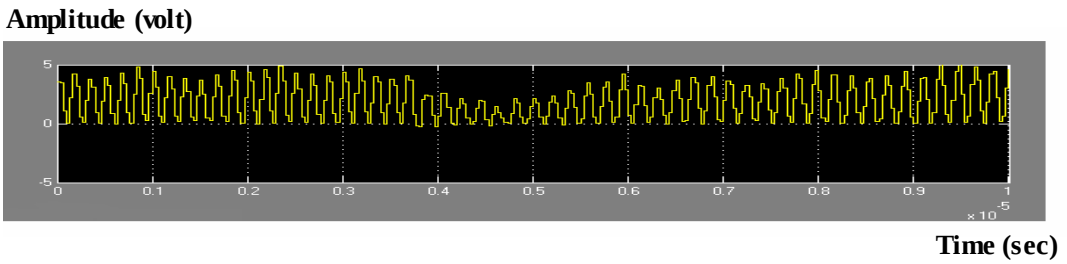

Figure (4.52): Despreading ASK FFH/SS signals under MTJ using noncontiguous technique

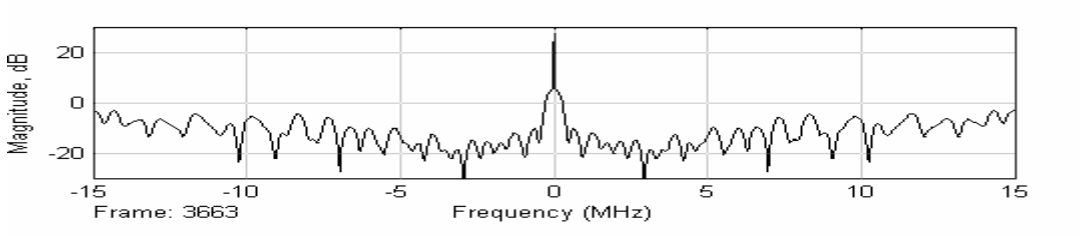

Figure (4.53): Despreading spectrum ASK FFH/SS signals under MTJ using noncontiguous technique

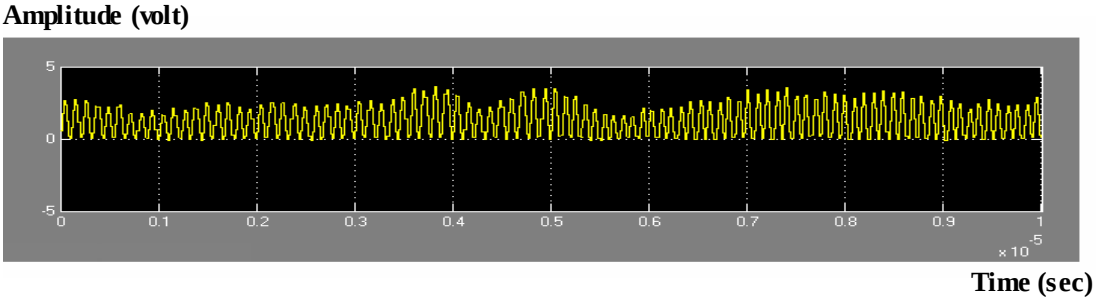

Figure (4.54): Despreading ASK FFH/SS signals under HJ using contiguous technique

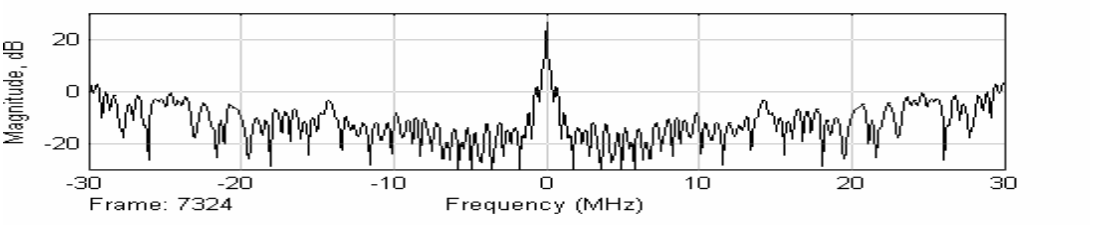

Figure (4.55): Despreading spectrum ASK FFH/SS signals under HJ using contiguous technique

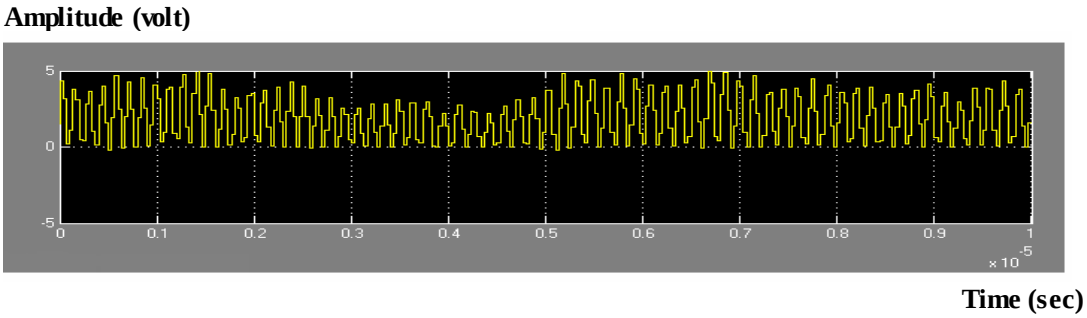

Figure (4.56): Despreading ASK FFH/SS signals under HJ using noncontiguous technique

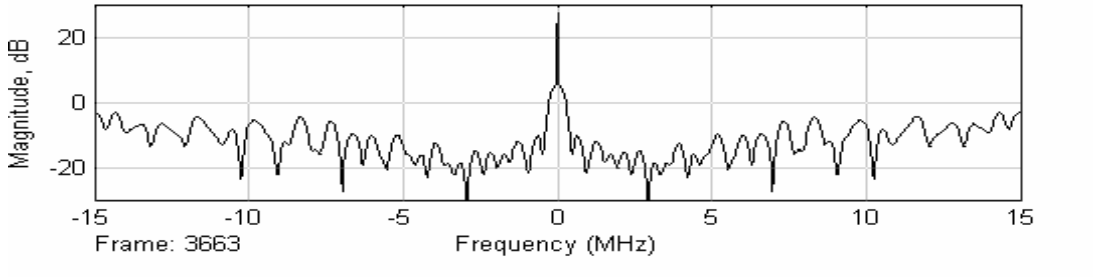

Figure (4.57): Despreading spectrum ASK FFH/SS signals under HJ using noncontiguous technique

4.4.6 ASK Demodulator

The implementation of the design using Simulink is shown in Figure (4.58), which show: IIR second order LPF, zero-order hold, and unipolar to bipolar conversion, and threshold (limiter, constant, relational operator, data type conversion), the output from the threshold is the received message. Figures (4.59), (4.60) and (4.61) show the de-spreading received detected waveform, of ASK FFH/SSS under AWGN (SNR = -5 dB, BER=0.0102), MTJ and HJ each one specified (f_j = 3.16MHz, 3.32 MHz,3.48 MHz and SJR= 2.181134486 dB, BER= 0.0001), respectively. Each figure state the detected despreading ASK FFH/SS received signals as fallow: (a) before LPF, (b) after LPF, (c) after limiter, (d) data after threshold. Figure (4.62) Shows the detected of despreading ASK FFH/SS received signals before threshold under: (a) AWGN (SNR = -5 dB) and transmitted data.(b) MTJ(f_j = 3.16 MHz , 3.32 MHz,3.48 MHz and SJR =2.181134486 dB, BER =0.0013) and transmitted data. (c) HJ(f_j = 3.16 MHz , 3.32 MHz,3.48 MHz and SJR= 2.181134486dB,BER=0.0078) and transmitted

data. Figures (4.63) , (4.64) , (4.65) , (4.66) , (4.67) , (4.68) , (4.69) , (4.70) , (4.71) , (4.72) , (4.73) and (4.74) show the detected waveform and spectrum of de-spreading ASK FFH signals after threshold under, AWGN (SNR= -5 dB) MTJ and HJ each one specified (f_j = 3.16 MHz , 3.32 MHz,3.48 MHz and SJR = 2.181134486 dB), for contiguous and noncontiguous technique respectively.

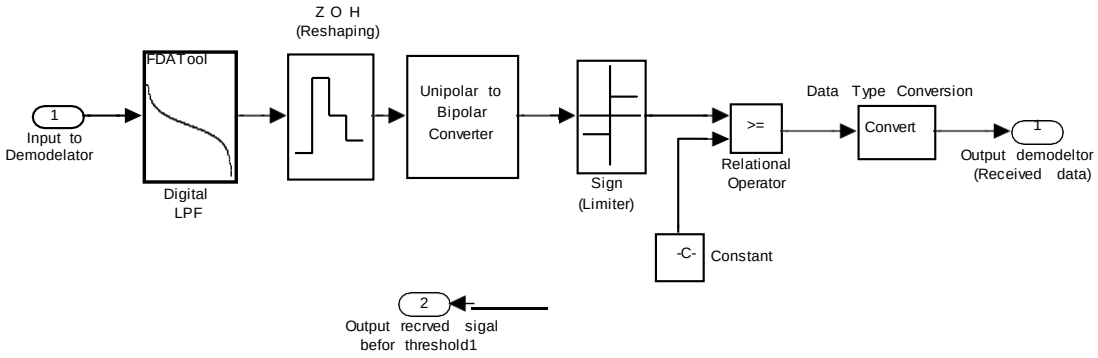

Figure (4.58): Design and simulation ASK demodulator

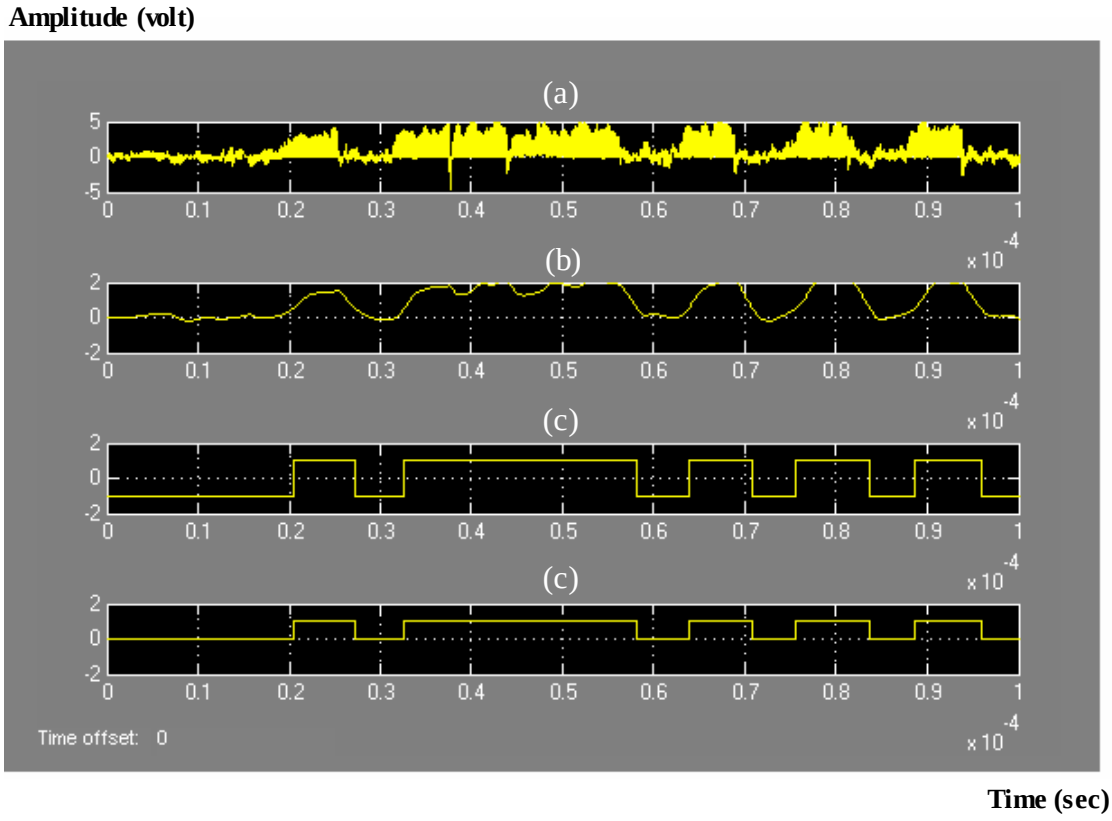

Figure (4.59): Detected of despreading received ASK FFH/SS signals under AWGN (SNR=- 5dB, BER=0.0102).
(a) signal before LPF. (b) signal after LPF.
(c) signal after limiting. (d) data after threshold

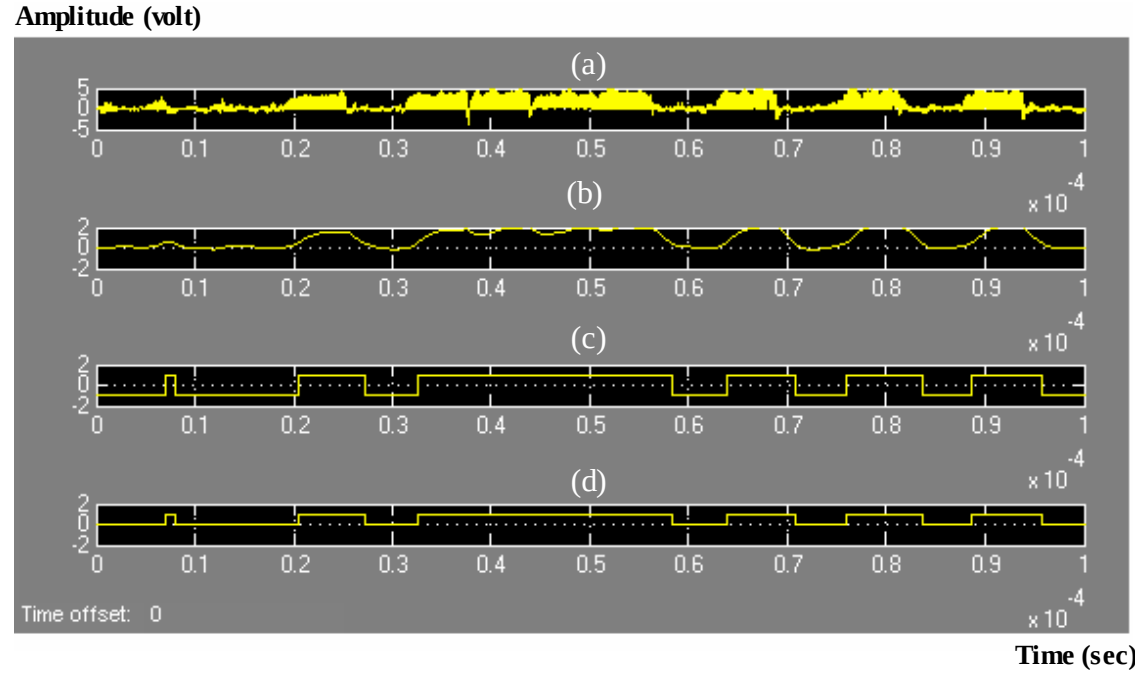

Figure (4.60): Detected of despreading received ASK FFH/SS signals under MTJ :
(a) signal before LPF. (b) signal after LPF.
(c) signal after limiting. (d) data after threshold.

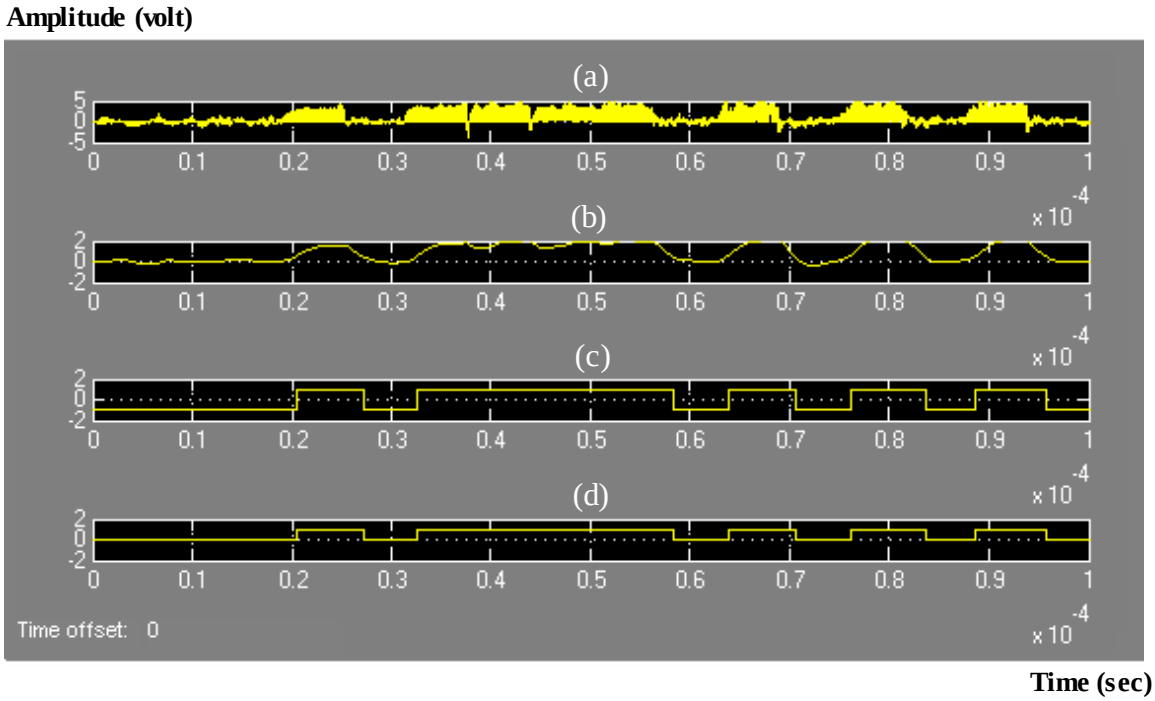

Figure (4.61): Detected of despreading received ASK FFH/SS signals under HJ:
(a) signal before LPF. (b) signal after LPF.
(c) signal after limiting. (d) data after threshold.

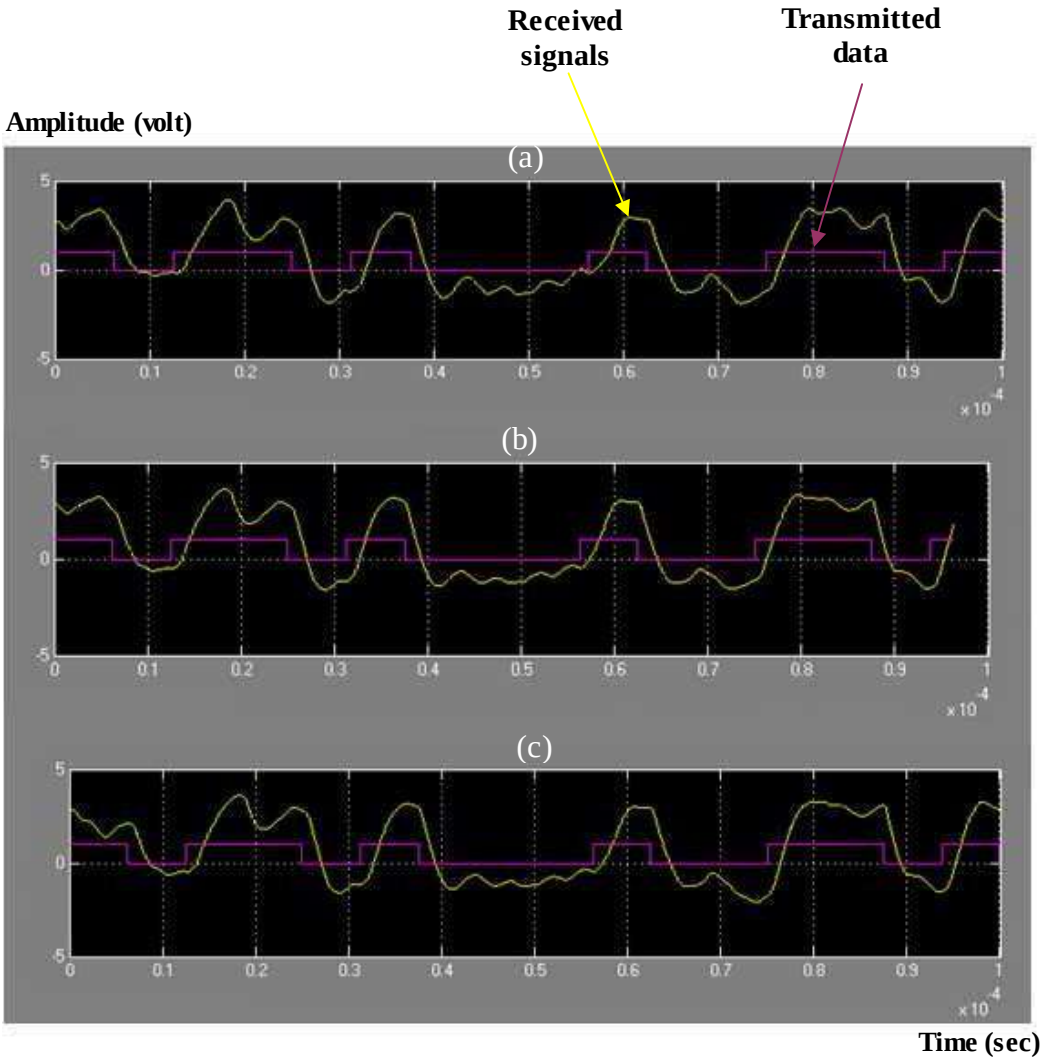

Figure (4.62): Detected of despreading received FFH/SS signals before threshold under
(a) AWGN (SNR=-5dB) and transmitted data.
(b) MTJ (f_j=3.16 MHz,3.32 MHz,3.48 MHz, SJR=2.181134486 dB, BER=0.0013) and transmitted data.
(c) HJ (f_j=3.16 MHz,3.32 MHz,3.48 MHz, SJR=2.181134486 dB, BER=0.0078) and transmitted data.

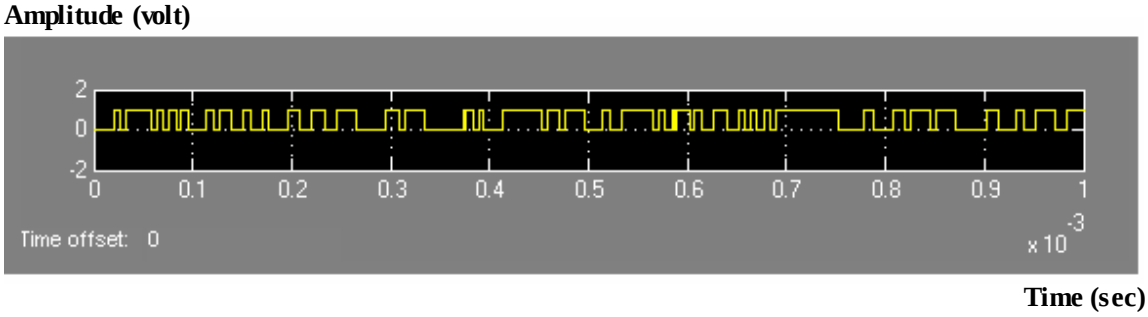

Figure (4.63): Detected despreading ASK FFH/SS signals under AWGN (SNR = -5dB) after threshold using contiguous technique

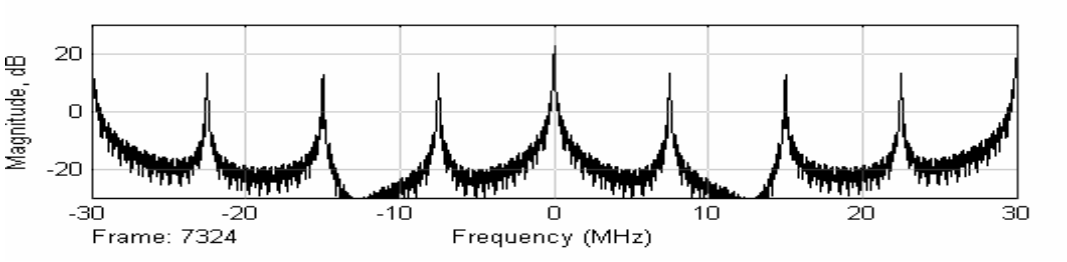

Figure (4.64): Detected despreading Spectrum ASK FFH/SS signals under AWGN (SNR=-5dB), after threshold using contiguous technique

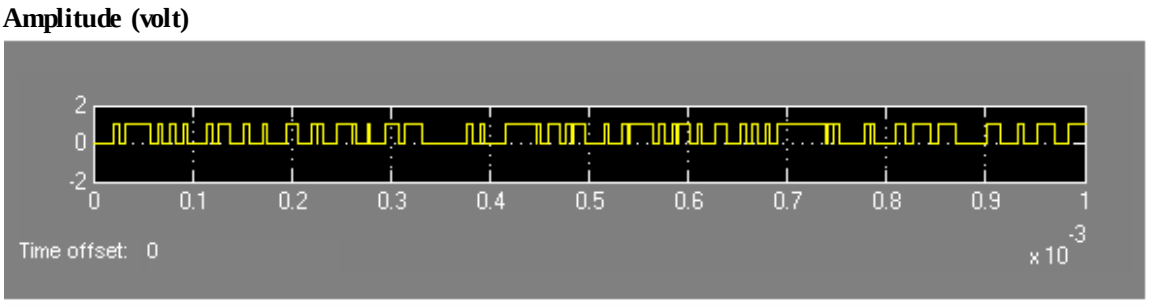

Figure (4.65): Detected despreading ASK FFH/SS signals under AWGN (SNR=-5dB), after threshold using noncontiguous technique

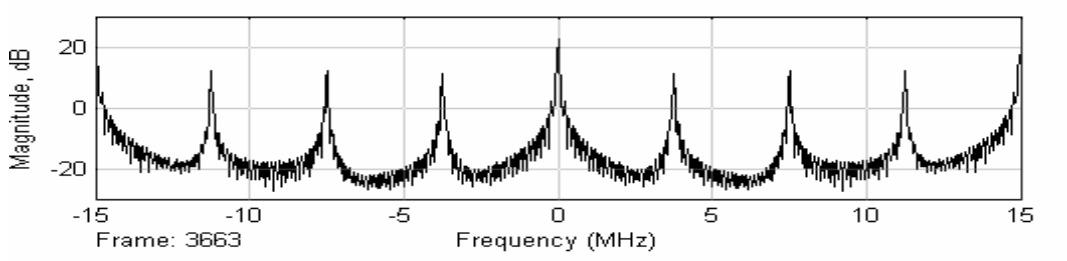

Figure (4.66): Detected despreading spectrum ASK FFH/SS signals under AWGN (SNR=-5 dB), after threshold using noncontiguous technique

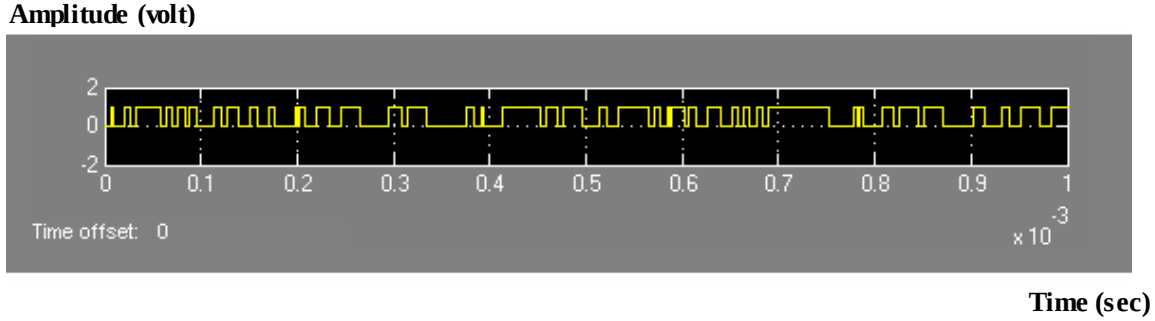

Figure (4.67): Detected despreading ASK FFH/SS signals under MTJ, after threshold using contiguous technique

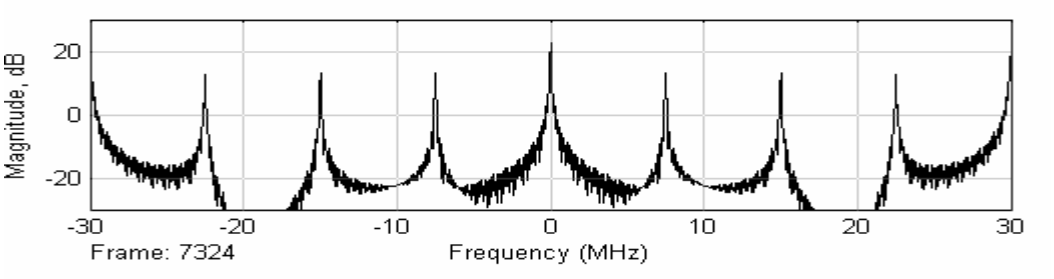

Figure (4.68): Detected despreading spectrum ASK FFH/SS signals under MTJ after threshold using contiguous technique

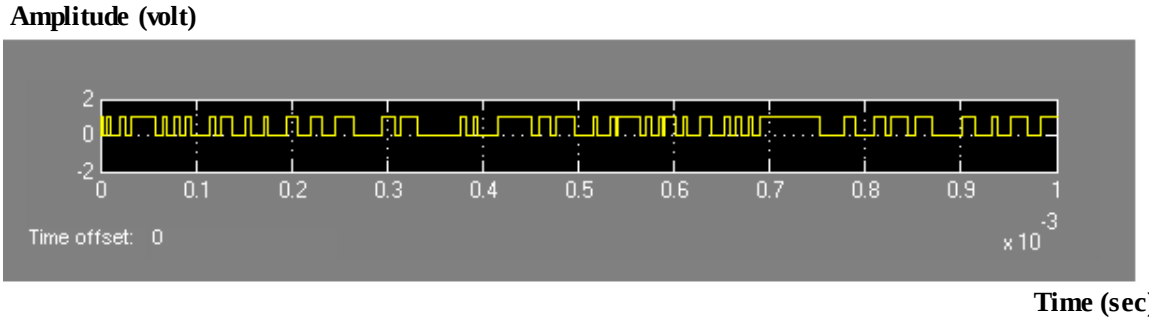

Figure (4.69): Detected despreading ASK FFH/SS signals under MTJ after threshold using noncontiguous technique

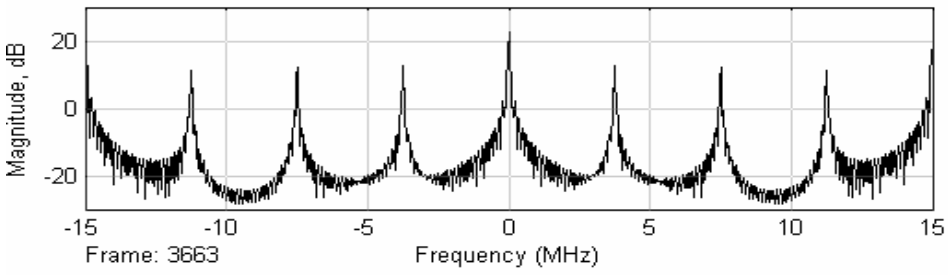

Figure (4.70): Detected despreading spectrum ASK FFH/SS signals after threshold using noncontiguous technique

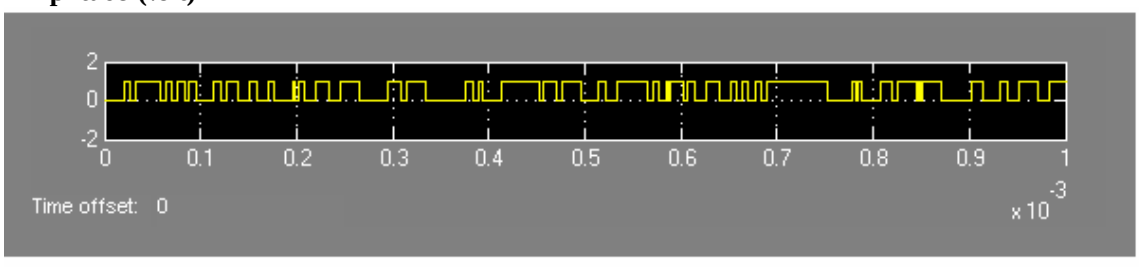

Figure (4.71): Detected despreading ASK FFH/SS signals under HJ after threshold using contiguous technique

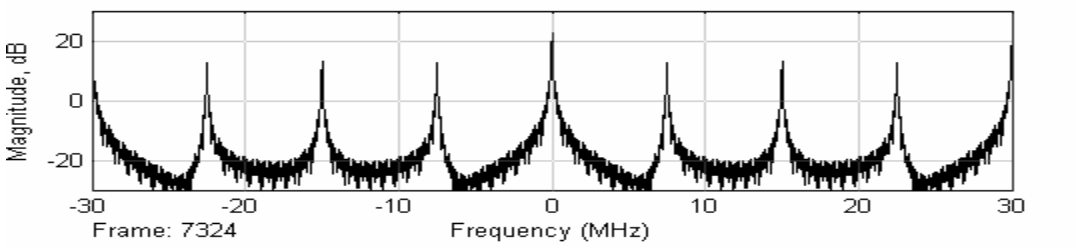

Figure (4.72): Detected despreading Spectrum ASK FFH/SS signals under HJ after threshold using contiguous technique

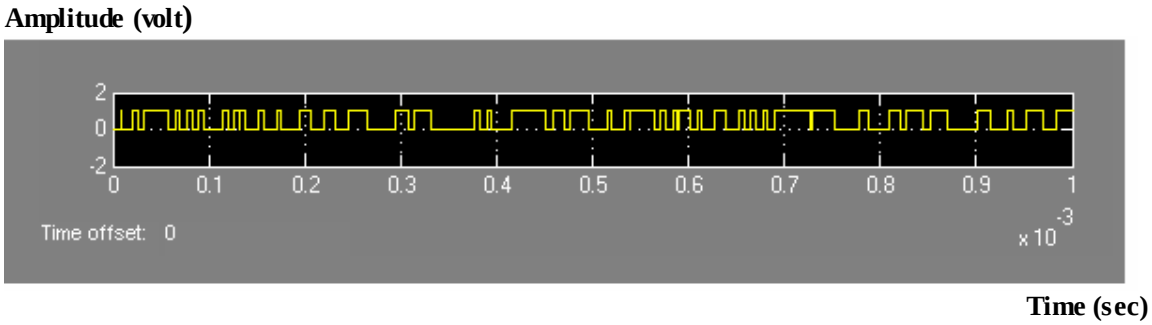

Figure (4.73): Detected despreading ASK FFH/SS signals under HJ after threshold using noncontiguous technique

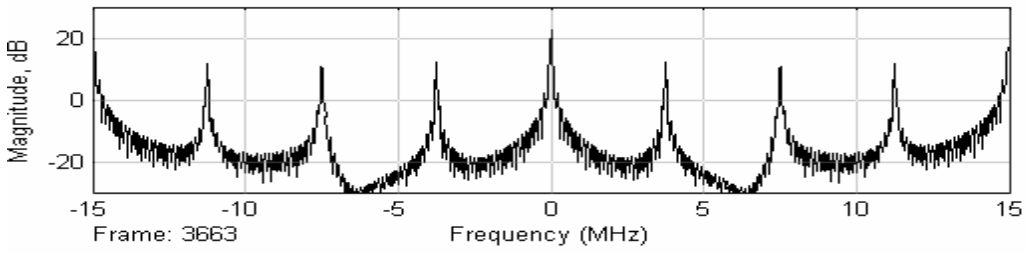

Figure (4.74): Detected despreading spectrum ASK FFH/SS signals under HJ after threshold using noncontiguous technique

4.4.7 Error Rate Calculation

The block diagram of it is shown in Figure (4.75). The block error rate calculation is gotten from Simulink DSP, and its function is to calculate BER. It has two inputs: one is the message from the demodulator (Rx) and the other from the data generator (Tx) at the transmitter after adding the measured delay between transmitter and received message (6.25μ sec). Figures (4.76),(4.77) and (4.78) show detected data and transmitted data with delay (6.25 μ sec). In

general, an error in a digital transmission facility occurs when existing pulses are lost or transmitted 1's are detected by the receiver as 0's. The bit error rate is the average rate at which the errors occur and can be expressed as [64]:

$$BER = \frac{Ne}{NT} \tag{4.1}$$

where :

Ne , NT : number of error bits and transmitted bits during simulation time

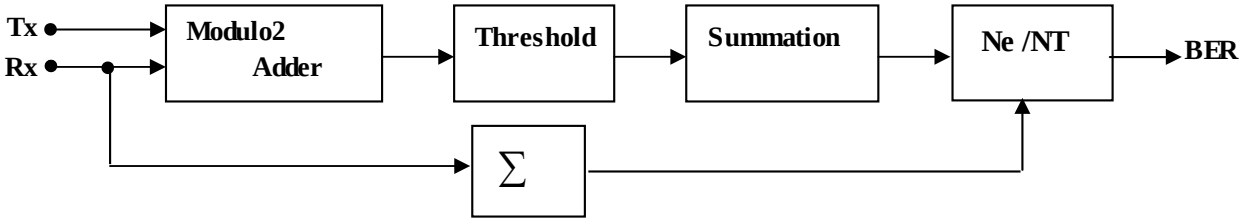

Figure (4.75): Block diagram of error rate calculation

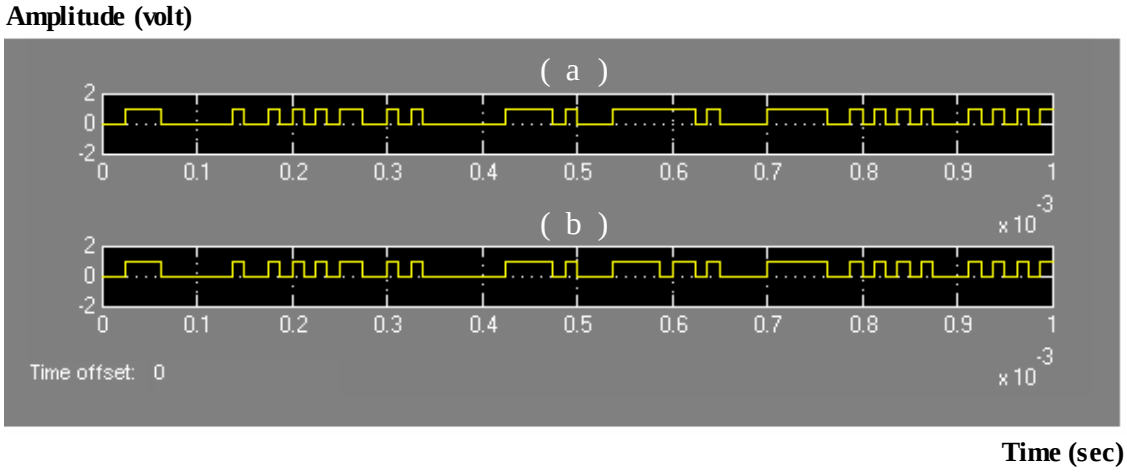

Figure (4.76): Final received data waveform under AWGN (SNR = -5 dB)
(a) Transmitted data after delay (6.25) μ sec.
(b) Received data.

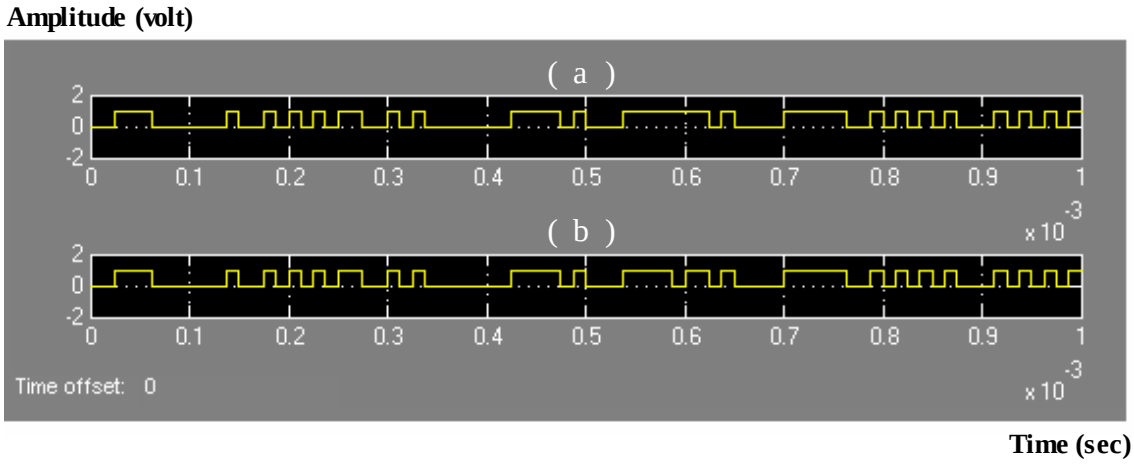

Figure (4.77) Final received data waveform under MTJ:
(a) transmitted data after delay (6.25) µ sec.
(b) received data .

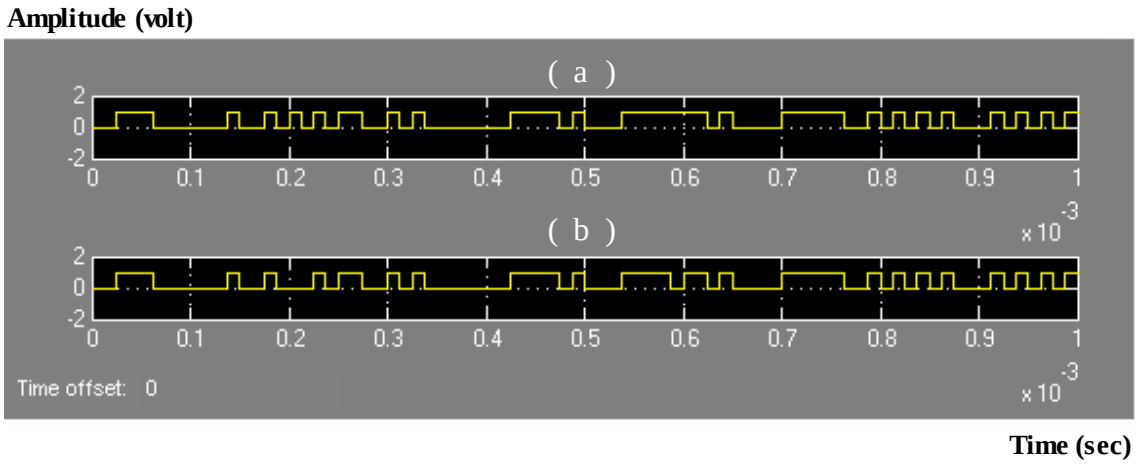

Figure (4.78): Final received data waveform under HJ:
(a) transmitted data after delay (6.25) µ sec.
(b) received data .

4.5 Simulation Results

The performance of any digital system is the measuring of BER for received data. Therefore in this proposed system we study the effect of the noise (AWGN) and jamming (MTJ, HJ) to the ASK FFH/SSS using contiguous and noncontiguous technique.

4.5.1 Effect AWGN

During simulation process and after 0.62 ms simulation time the number of bits is 10000 bits, if we take different values of SNR in dB from AWGN block for each run and calculate BER by using error rate calculation from communication block set, the results of these calculation are shown in Figure (4.79) for ASK FFH/SSS using contiguous and noncontiguous technique respectively. To calculate the G_P in dB, from equation (2.4) which state that

$$G_P = \frac{B_m \times 2^n - 1}{B_m} = 2^n - 1 \quad , \quad G_P\ (dB) = 10 \log \left(2^n - 1\right) = 10 \log 31 = 14.9\ dB_m \ , \ for \quad n = 5$$

It is clear that from Figure (4.79), the BER performance for ASK FFH/SSS using contiguous technique is better than that using noncontiguous technique for 5 dB ≥ SNR ≥ 13 dB and the reverse is correct for (5 dB < SNR > 13 dB).

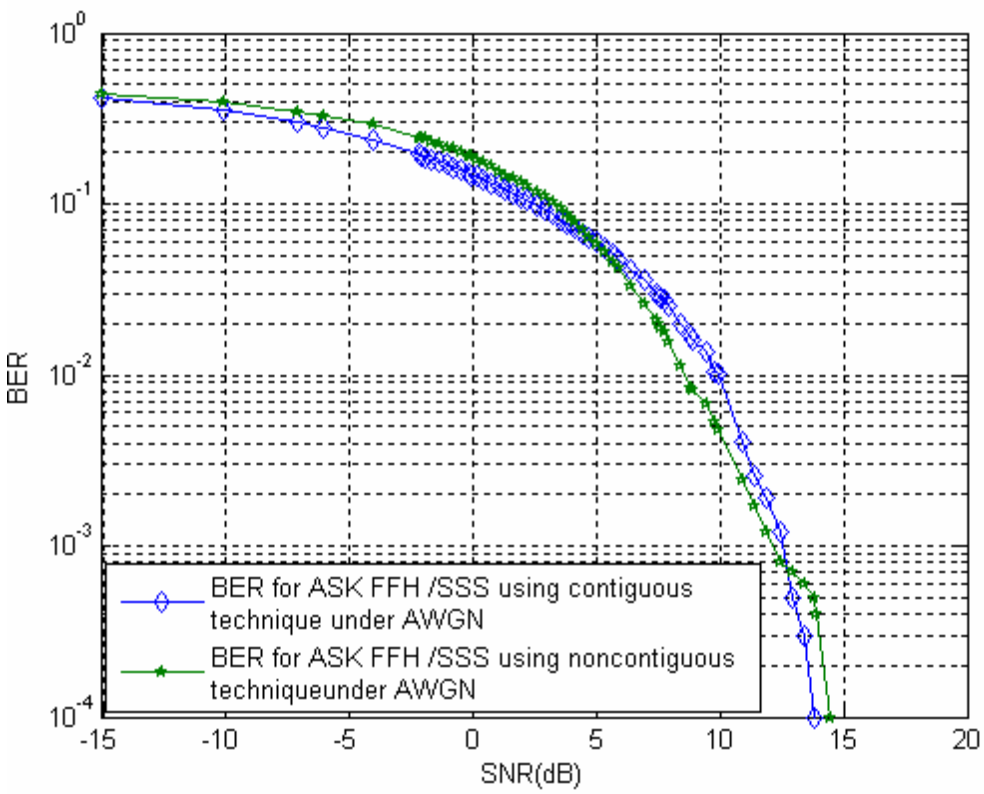

Figure (4.79): BER versus SNR (dB) for ASK FH/SSS under AWGN using contiguous and noncontiguous

4.5.2 Effect of Jamming.

The two system are tested under the following types of jamming:

A- Effect of Multitone Jamming (MTJ).

As stated in section (2.4.2)and section (4.3.2), Figure (4.26) shows the block diagram of MTJ (f_j =3.16 MHz , 3.32MHz , 3.48 MHz)**,** different values of signals are taken of MTJ to obtain many values of SJR in dB and reading the corresponding BER by using error rate calculation block from communication block set, during the simulation process after 0.62 ms simulation time, the number of bits is 10000 bits for each run. The results of these calculations are shown in Figure (4.80) which shows the relationship between BER and SJR (dB) FFH/SSS under MTJ using contiguous and noncontiguous technique respectively. It is clear that ASK FFH/SSS using contiguous technique has better BER performance than that using noncontiguous technique (gained SJR 13 dB, for BER 1 x 10^{-4}).

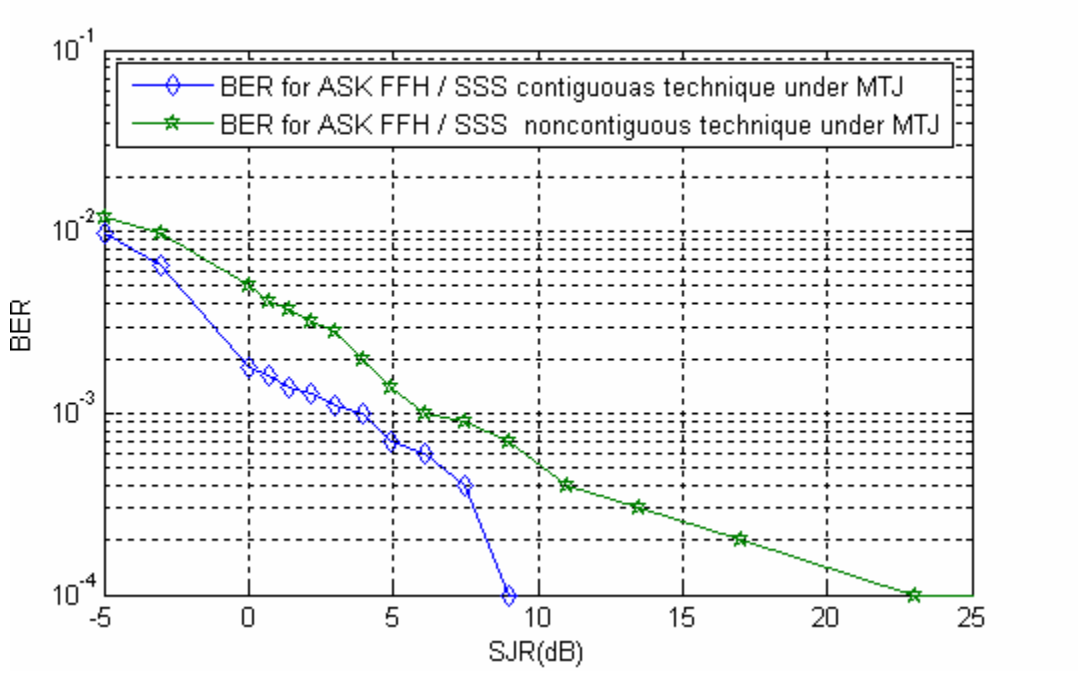

Figure (4.80): BER versus SJR (dB) for ASK FH/SSS under MTJ using contiguous and noncontiguous technique

B. Effect of Hopper Jamming (HJ)

It is explained in section (2.4.3) and (4.3.3) Figure (4.31) shows the block diagram of HJ (f_j = 3.16 MHz, 3.32MHz, 3.48 MHz) which it has severed effect than that of MTJ. Also the calculating the effect of this type is done by run the system with simulation time 0.62 ms to get 10000 bit for each run and calculated the BER. The results of these calculations are shown in Figure (4.81) which shows the relationship between BER and SJR (dB) FFH SSS under HJ using contiguous and noncontiguous technique respectively.

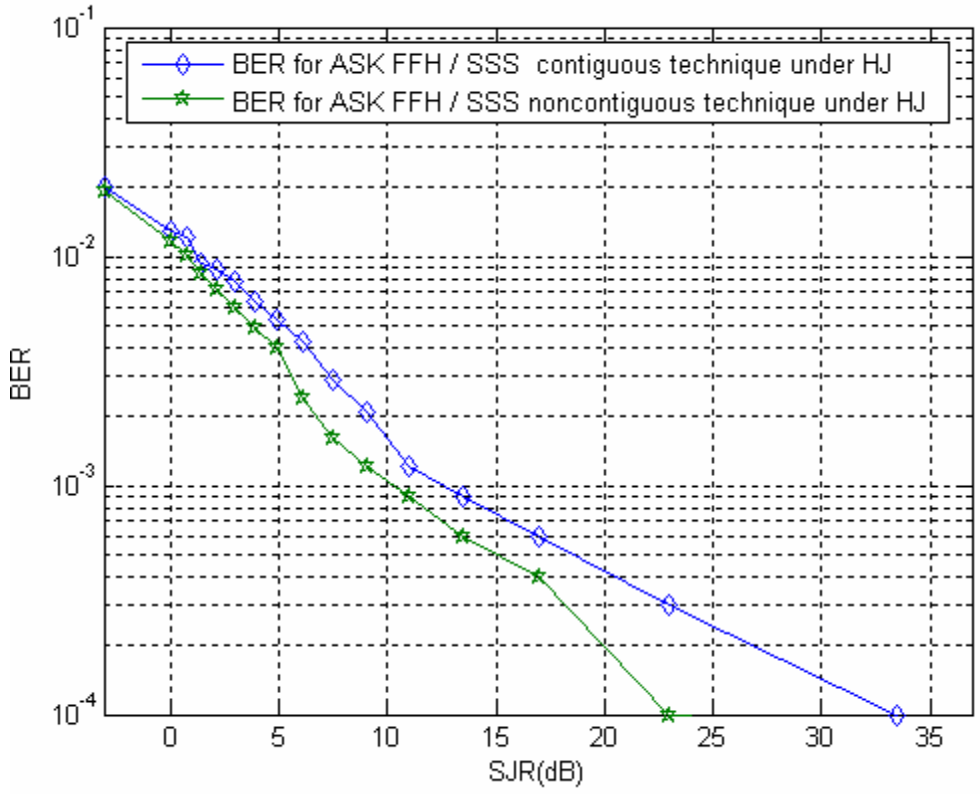

Figure (4.81): BER versus SJR (dB) for ASK FFH / SSS under HJ using contiguous and noncontiguous technique

It is clear that ASK FFH/SSS using noncontiguous technique has better BER performance than that of contiguous technique, (gained SJR 11 dB for BER 1 x 10^{-4})

Chapter Five

Design and Simulation of FSK FFH/SS Transceiver

5.1 Introduction

In this chapter FSK FFH/SS transceiver for hopping rate of 160 k hop/sec and 160 k bit/sec data rate using contiguous and noncontiguous IIR second order Butterworth BPF banks are designed successfully in real time using MATLAB-Simulink tool. These two systems are tested under AWGN and two types of jamming.

5. 2 The Proposed System

The block diagram of proposed system for FSK /FFH transceiver using contiguous and noncontiguous technique, is shown in Figure (5.1a) and it is implemented using MATLAB-Simulink version 7, as shown in Figure (5.1b). This contains, the transmitter, transmission channel, contiguous and noncontiguous digital BPF banks and receiver.

5.2.1 The Transmitter

The transmitter contains: data generator, BFSK modulator, spread code generator, serial/parallel converter, DDFS, mixer (spreading of FSK signals) and digital HPF. The mixer and data generator are taken from communication block set (MATLAB-Simulink).

5.2.1.1 Data Generator

The binary data generator (Bernoulli Binary Generator) from Simulink communication block is set, and adjusted with probability of zero, 50% and 50% one's. It is transmitted within data rate 160 k bit/sec. The waveform and spectrum of data are shown in Figures (5.2) and (5.3).

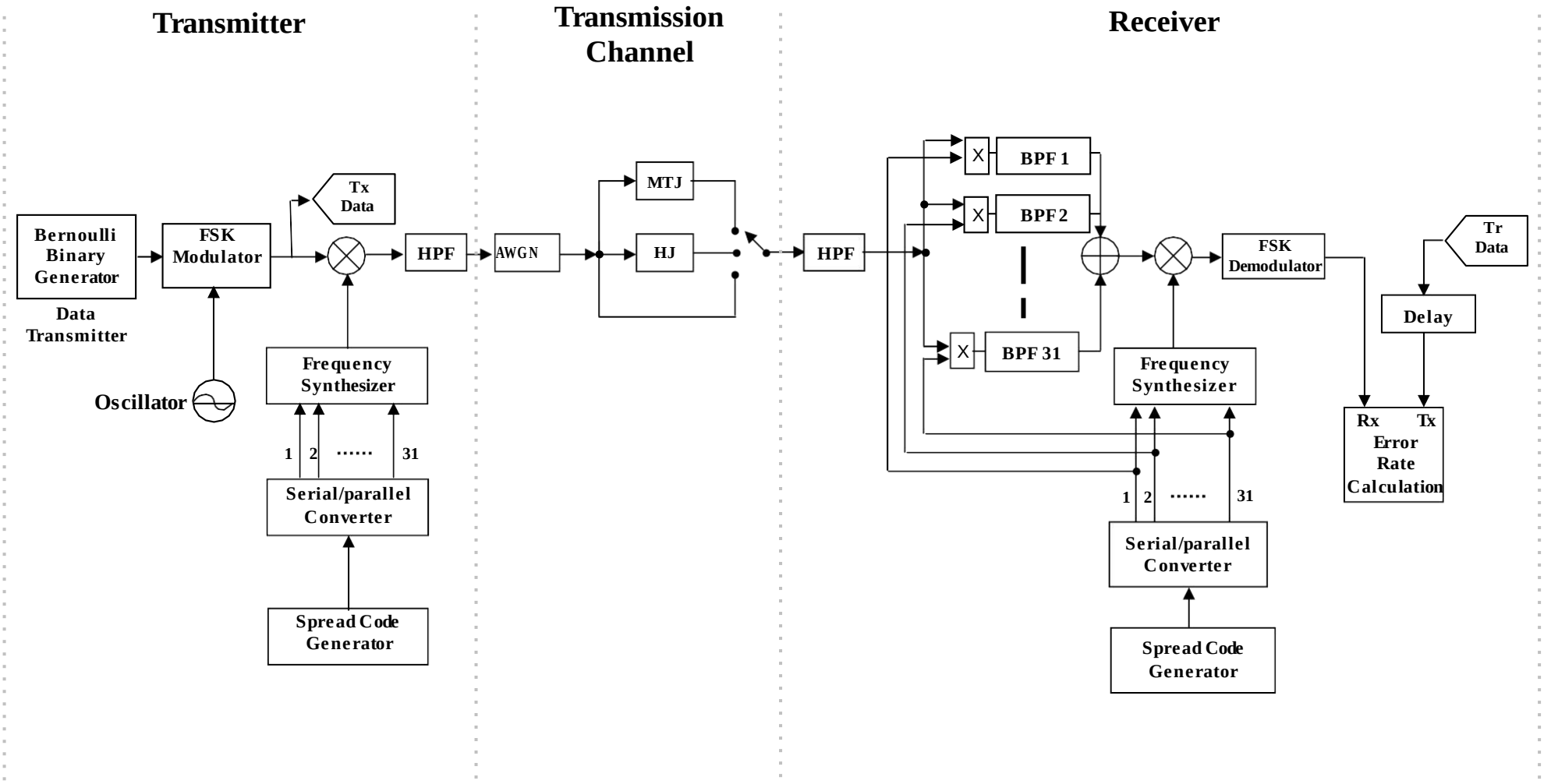

Figure (5.1a) Transceiver block diagram of FSK FFH /SS system.

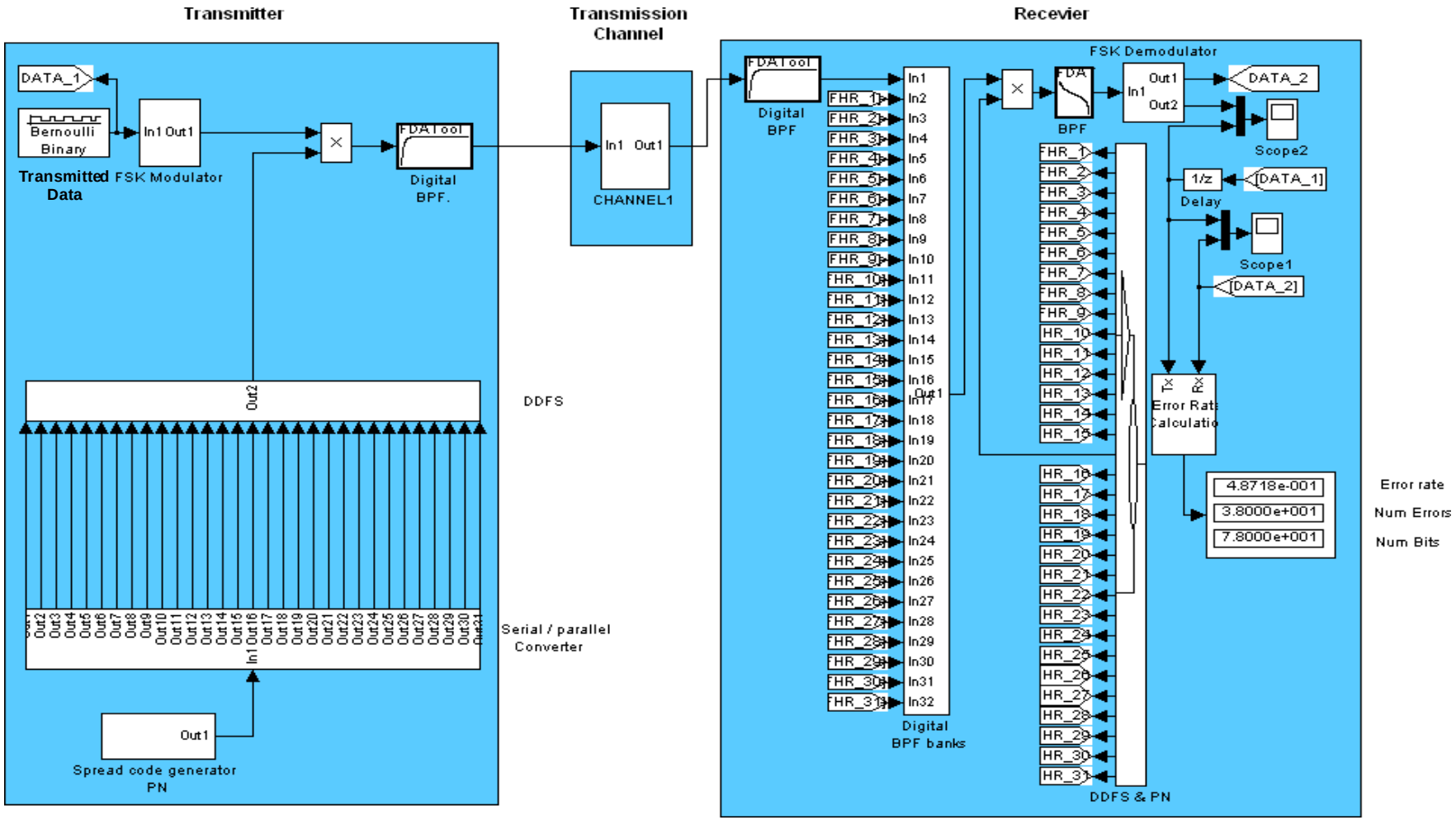

Figure (5.1b): Design and simulation of FSK FFH /SS transceiver system.

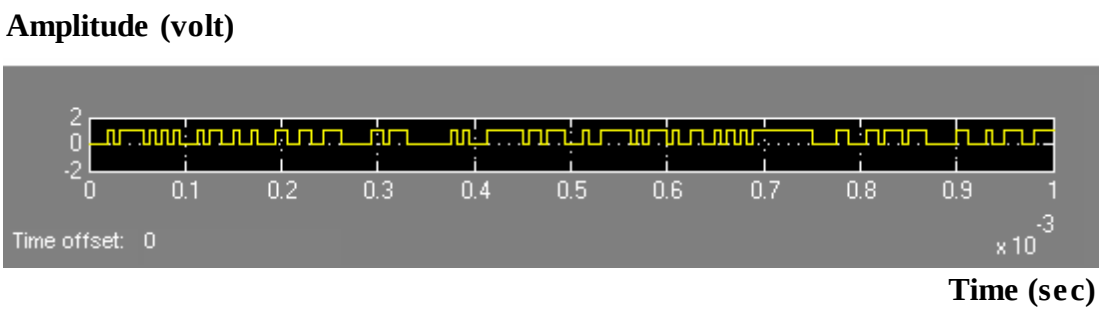

Figure (5.2) : Waveform of data 160 k bit/sec

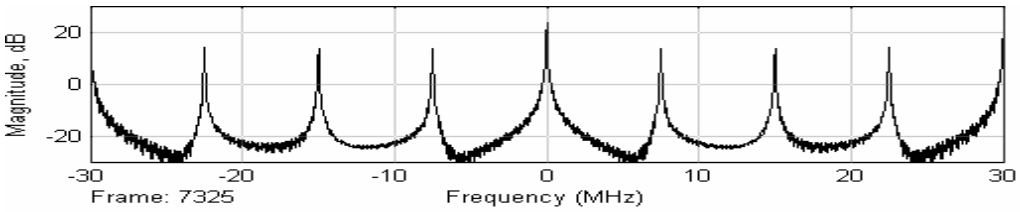

Figure (5.3): Spectrum of data 160 k bit/sec

5.2.1.2 BFSK Modulator.

The BFSK modulator design and its implementation using Simulink is shown in Figure (5.4). It was implemented choosing f_{m1} = 400 kHz, f_{m2} = 800 KHz in order to get the separation between two adjacent frequency 400 KHz ($f_{m1}= 1/T_h$, $f_{m2} = 2/T_h$) for operating this proposed system with transmit data rate 160 k bit/sec and out of distortion. Figures (5.5) ,(5.6) and (5.7) show the generation of BFSK waveform of f_{m1} , f_{m2} cosine waves. Figure (5.8) shows the spectrum of f_{m1} , f_{m2} of BFSK.

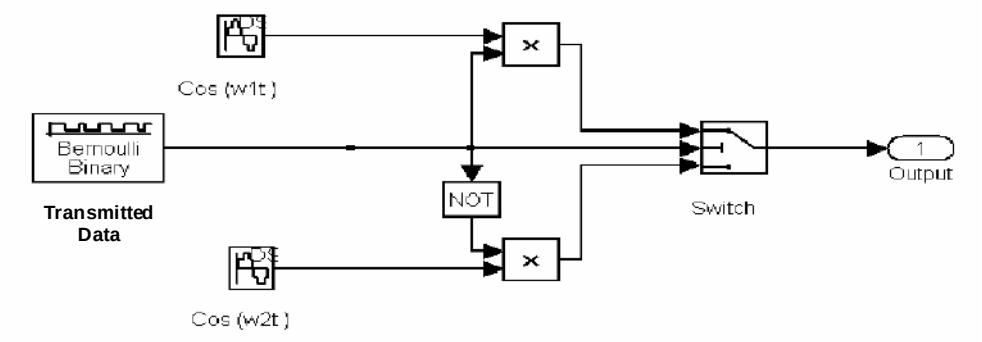

Figure (5. 4): Design and simulation of BFSK modulator [w_1 = (2 f_1 t), w_2= (2 f_2 t)] , [f_1 (f_{m1}) = 400KHz, f_2 (f_{m2}) = 800 KHz]

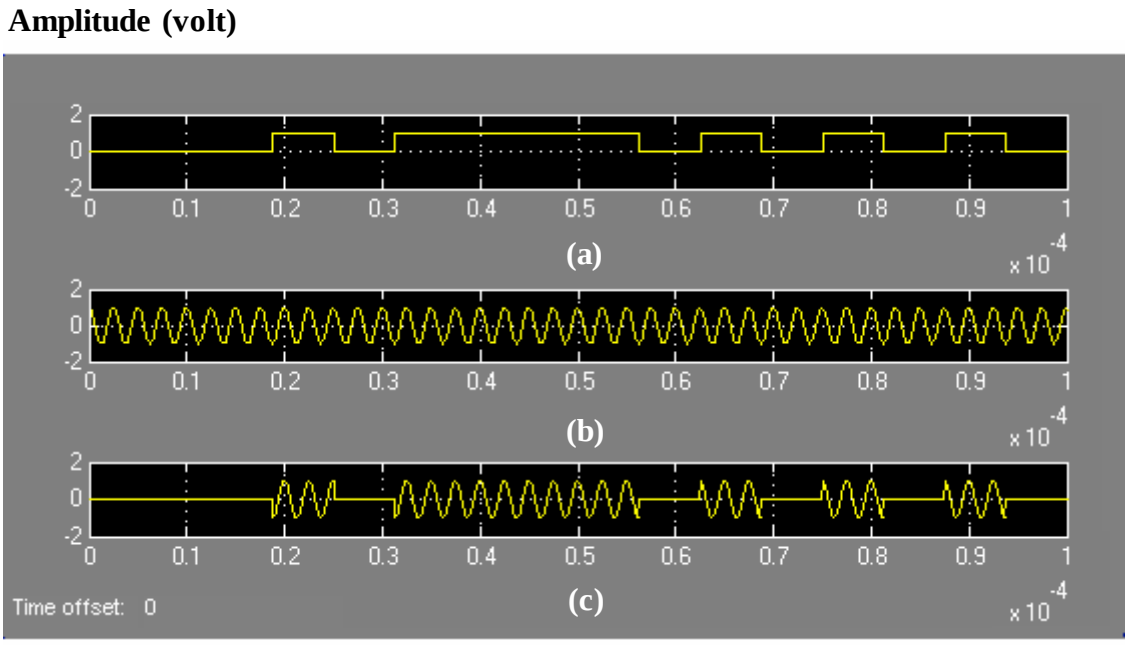

Figure (5.5): Waveform of :
(a) transmitted binary data of rate 160 k bit/sec.
(b) waveform of cos (2 f_{m1}). (c) ASK of cos (2 f_{m1}).

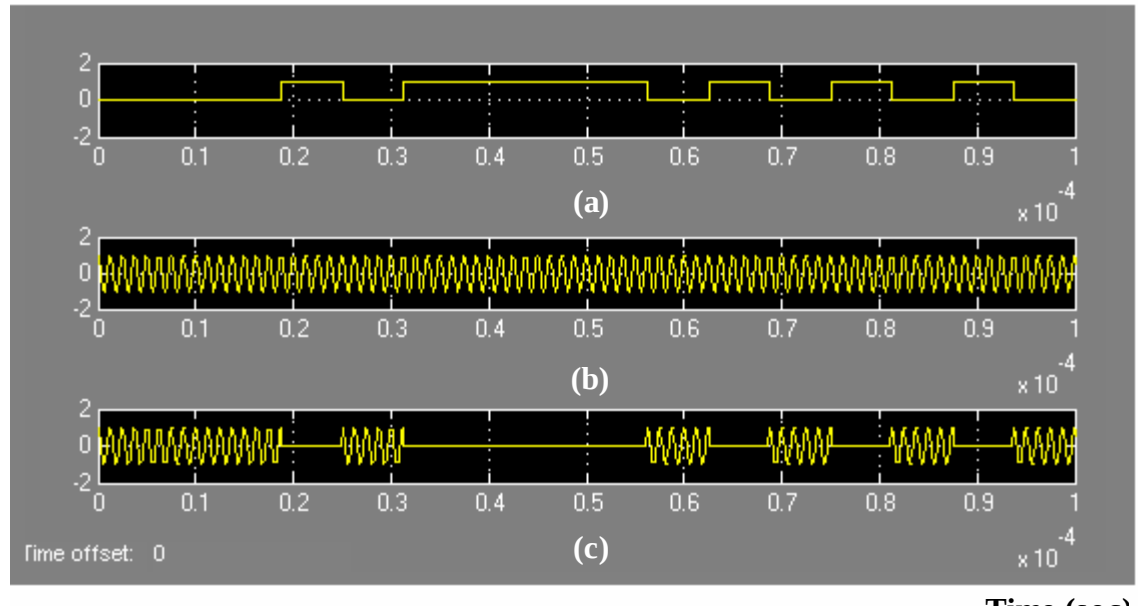

Figure (5.6): Waveform of :
(a) transmitted binary data of rate 160 k bit/sec.
(b) waveform of cos (2 f $_{m2}$) (c) ASK of cos (2 f_{m2})

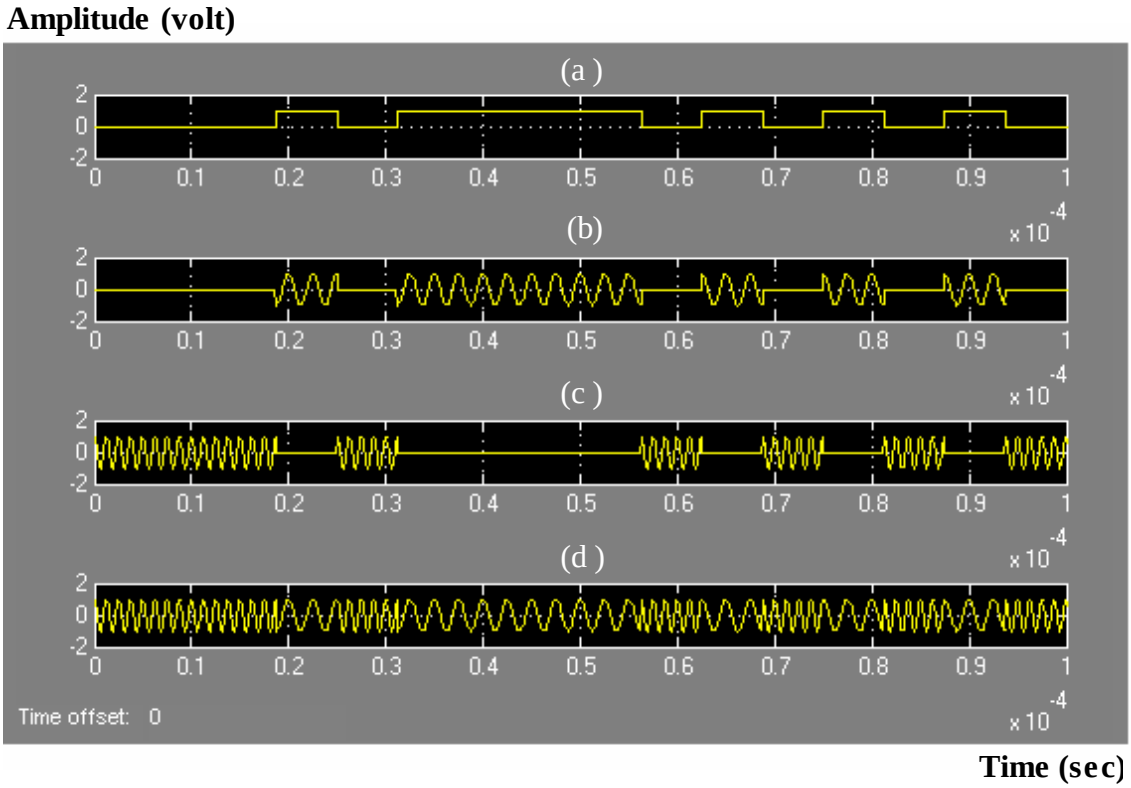

Figure (5.7): Waveform of :
(a) transmitted binary data of rate 160 k bit/sec
(b) ASK of cos (2 f_{m1}).
(c) ASK of cos (2 f_{m2}). (d) waveform of BFSK.

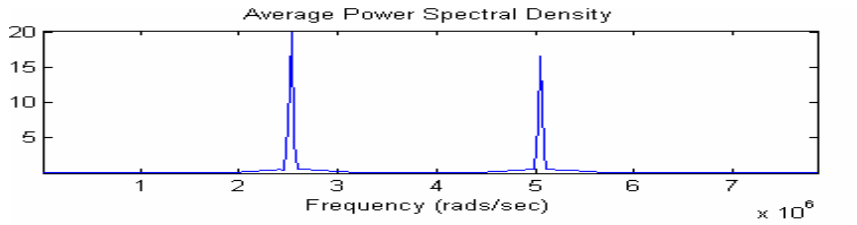

Figure (5.8): Spectrum of BFSK

5.2.1.3 Spread Code Generator

It is the same as that stated in chapter four (section 4.2.1.2), except that the difference in spectrums of 31 bit maximal linear code of PN sequence generated which are shown in Figures (5.9) and (5.10), for the proposed FSK FFH/SSS using contiguous and noncontiguous technique respectively.

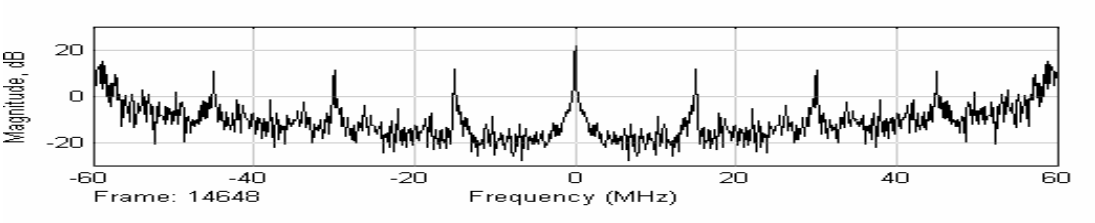

Figure (5.9): Spectrum of 31 bit maximal linear code using contiguous technique

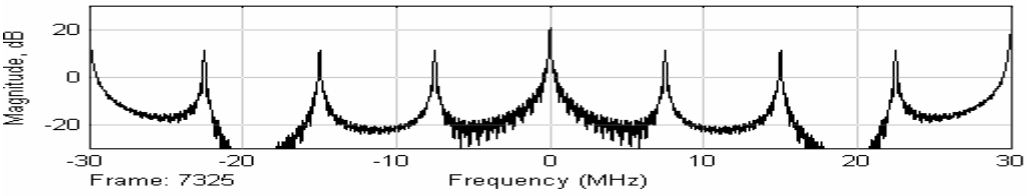

Figure (5.10): Spectrum of 31bit maximal linear code using noncontiguous technique

5.2.1.4 Serial / Parallel Converters

It is the same as that stated in chapter four section (4.2.1.3).

5.2.1.5 DDFS

It is the same as that stated in chapter four section (4.2.1.4), except that the DDFS signals spectrum outputs are shown in Figure (5.11) for the proposed system FSK FH/SSS.

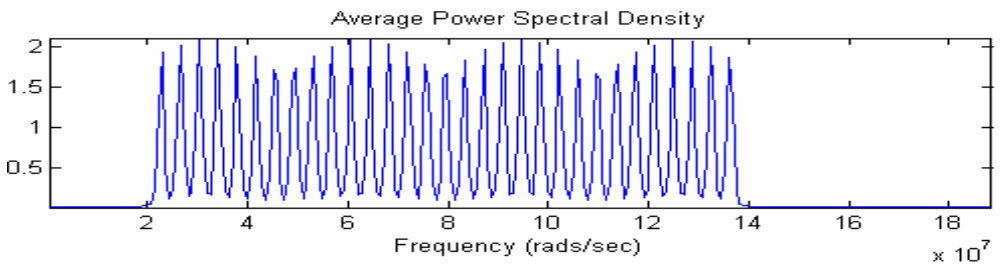

Figure (5.11): Spectrum of 31 signals of DDFS

5.2.1.6 Data Spreading for FSK FFH/SSS

The basic idea of FH, and all type of spread spectrum is spreading the data over a wide bandwidth, before transmitted. This technique is stated in detail in chapter four (section 4.2.1.5). Figure (5.12) shows the waveforms of transmitted data and signal that produces the spreading of transmitted data using FSK FFH/SS which is done in this proposed system. Figures (5.13) and (5.14) show the waveform and spectrum of spreading of transmitted of data using BFSK FFH/SS which is done in this proposed system BFSK FH/SSS using contiguous technique before transmitted.

5.2.1.7 Digital HPF

It is the same as that stated in chapter four sections (4.2.1.6) except that it is used to reject one side band of the BFSK modulator besides the rejection of unwanted signals.

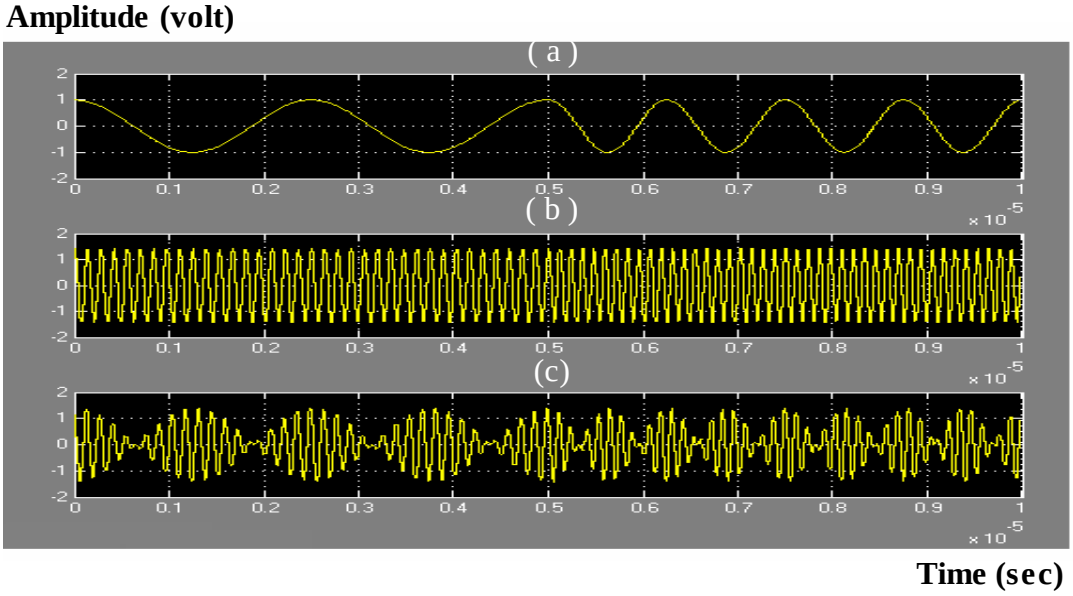

Figure (5.12): Waveforms of FSK FFH/SS:
(a) waveforms of BFSK.
(b) DDFS signals.
(c) spreading data (FSK) after HPF

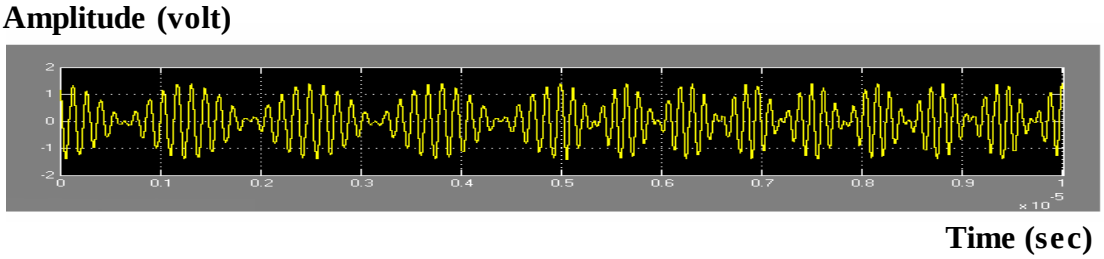

Figure (5.13): Waveform of spreading FSK FFH/SS signals using contiguous technique

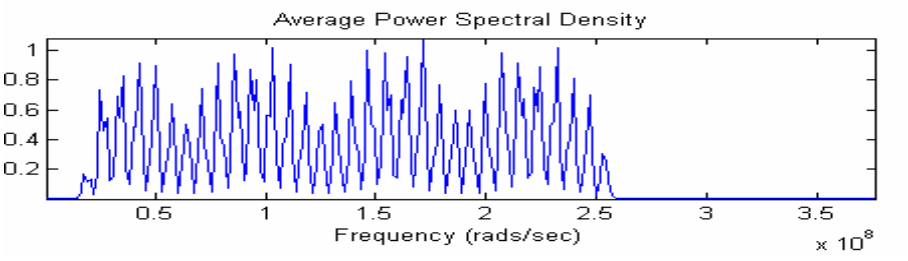

Figure (5.14): Spectrum of spreading data of FSK FFH/SS before transmitted using contiguous technique

5.3 The Channel.

The FH/SSS which is shown in Figure (5.1) has been used to transmit data through transmission channel which is the same as that stated in chapter four, section (4.3).

5.3.1 AWGN.

It is the same as that stated in chapter four (section 4.3.1), except that the waveform and spectrum of the transmitted signal under AWGN (SNR = -10 dB) are shown in Figures (5.15), (5.16), (5.17) and (5, 18) using contiguous and noncontiguous technique.

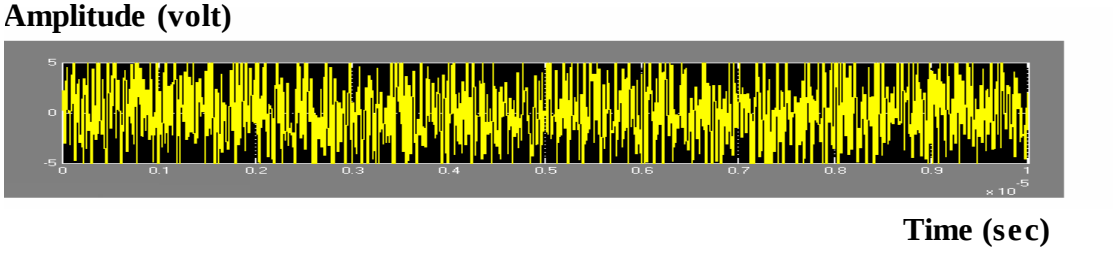

Figure (5.15): Waveform of transmitted FSK/SS signals under AWGN (SNR = -10dB) using contiguous technique

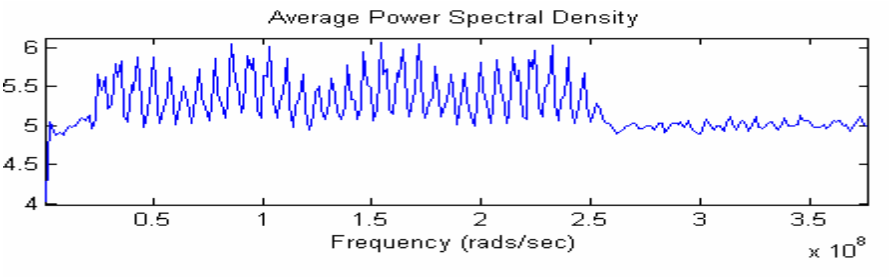

Figure (5.16): Spectrum of transmitted FSK FFH/SS signals under (SNR=-10 dB) transmitted using contiguous technique

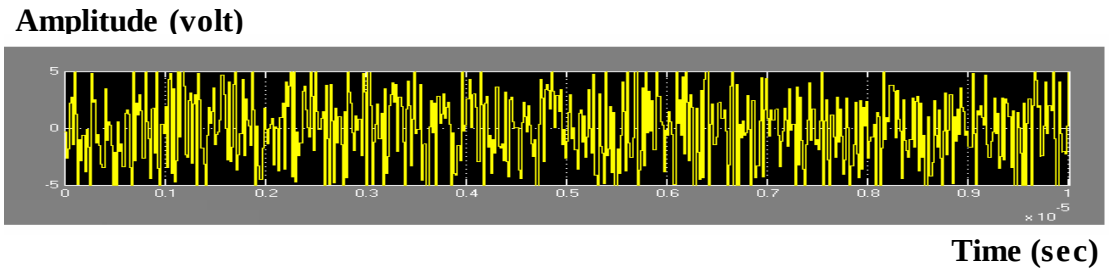

Figure (5.17): Waveform of transmitted FSK FFH/SS signals under AWGN (SNR = -10dB) using noncontiguous technique

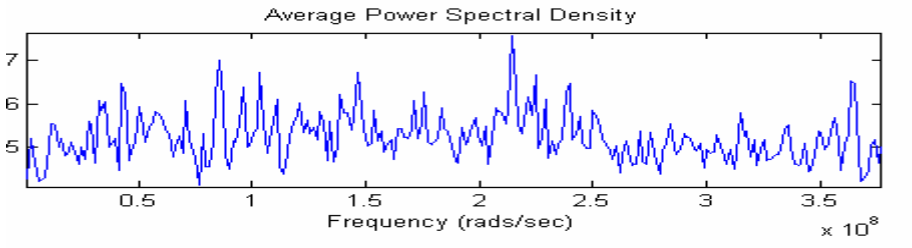

Figure (5.18): Spectrum of transmitted FSK FFH/SS signals under (SNR=-10 dB) using noncontiguous technique

5.3.2 Multitune Jamming(MTJ)

It is the same as that stated in chapter four section (4.3.2) .The waveform and spectrum of transmitted signals under MTJ and AWGN are shown in Figures (5.19), (5.20),(5.21) and (5.22) before contiguous and noncontiguous BPF banks respectively.

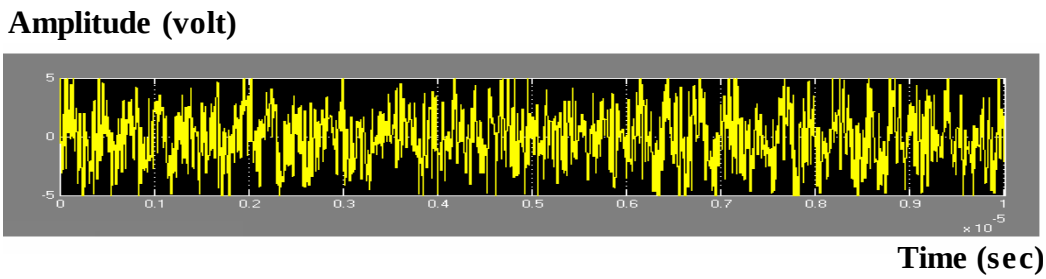

Figure (5.19): Waveform of transmitted FSK FFH/SS signals under MTJ using contiguous technique

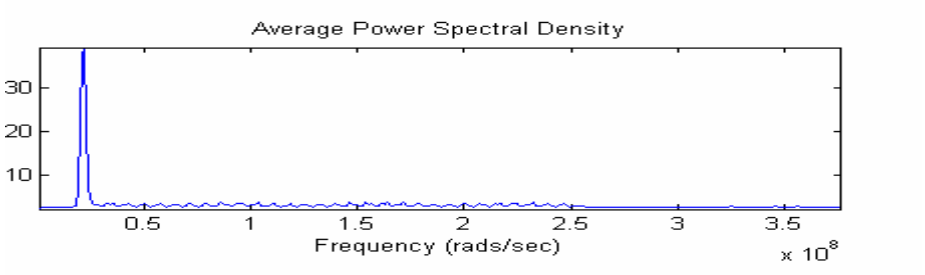

Figure (5.20): Spectrum of transmitted FSK FFH/SS signals under MTJ using contiguous technique

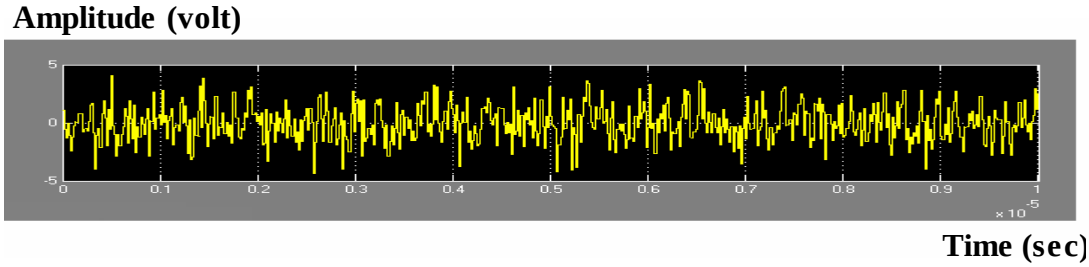

Figure (5.21): Waveform of transmitted FSK FFH/SS signals under MTJ using noncontiguous technique

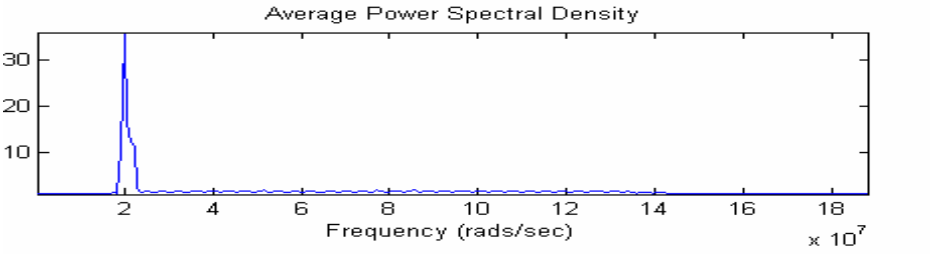

Figure (5.22): Spectrum of transmitted FSK FFH/SS signals under MTJ using noncontiguous technique

5.3.3 Hopper Jamming (HJ).

It is the same as that stated in chapter four section (4.3.3).The waveforms of BFSK FFH/SS transmitted signals under HJ and AWGN are shown in Figures (5.23), (5.24), (5.25) and (5.26) for contiguous and non-contiguous technique respectively.

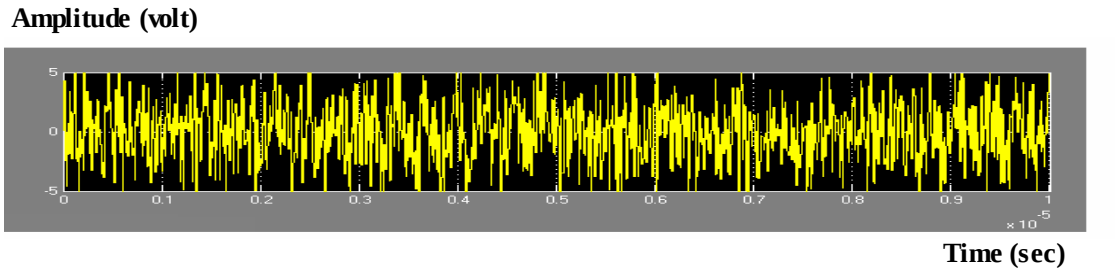

Figure (5.23): Waveform of transmitted FSK FFH/SS signals under HJ using contiguous technique

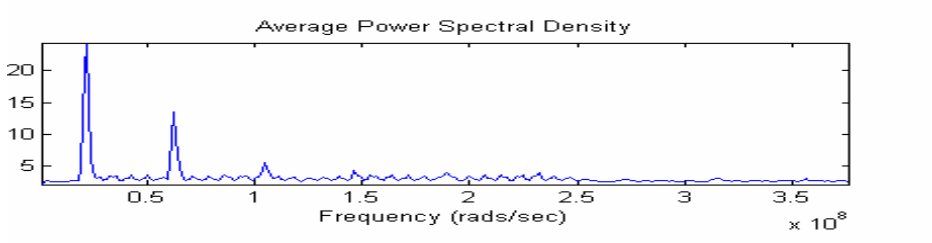

Figure (5.24): Spectrum of transmitted FSK FFH/SS signals under HJ using contiguous technique

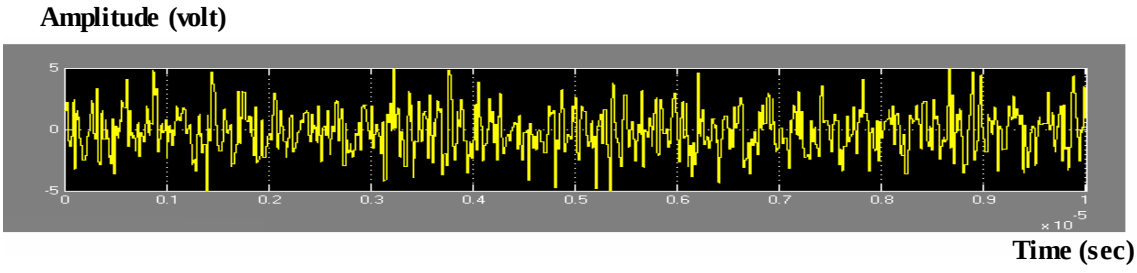

Figure (5.25): Waveform of transmitted FSK FFH/SS signals under HJ using contiguous technique

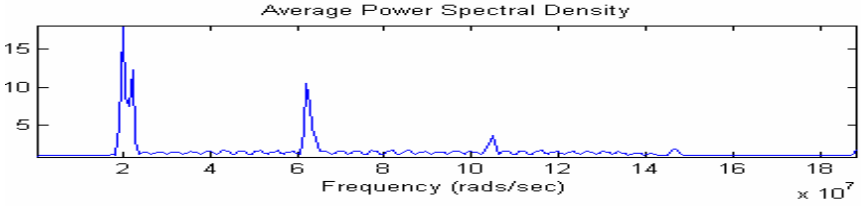

Figure (5.26): Spectrum of transmitted FSK FFH/SS signals under HJ using noncontiguous technique

5.4 The Receiver.

Figure (5.1), shows the block diagram of the receiver which contains Digital HPF which is the same as that stated in chapter four section (4.2.1.6), bank of parallel digital BPFs, spread code generator, serial/parallel converter, DDFS, mixer (dispreading of BFSK signals), FSK demodulator, error rate calculation.

5.4.1 Bank of Parallel Digital BPF

Figure (3.9) shows the block diagram of it which contains 31 parallel digital, second order band pass filters. The center frequency of each filter which is shown in table (3.5), (3.7), for contiguous and noncontiguous technique is the same as that in DDFS. All the BPFs are controlled through the spread code generator. Figures (5.27),(5.28),(5.29) and (5.30) show the waveform and spectrum of the transmitted FSK FFH/SS signals with AWGN (SNR=-10dB) Figures (5.31),(5.32),(5.33) and (5.34) show the waveform and spectrum of the transmitted FSK FFH/SS signals under MTJ (f_j=3.16 MHz,3.32 MHz,3.48 MHz and SJR=2.181134486 dB). Figures (5.35), (5.36),(5.37) and (5.38) show the waveform and spectrum of the transmitted FSK FFH/SS signals under HJ (f_j=3.16 MHz,3.32 MHz,3.48 MHz and SJR=2.181134486 dB) after passing through contiguous and noncontiguous digital BPF banks before dispreading respectively.

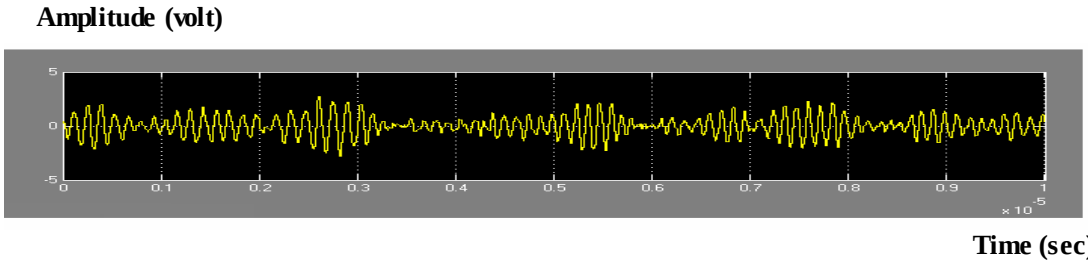

Figure (5.27): Spreading FSK FFH/SS signals under AWGN (SNR= 10dB) using contiguous technique

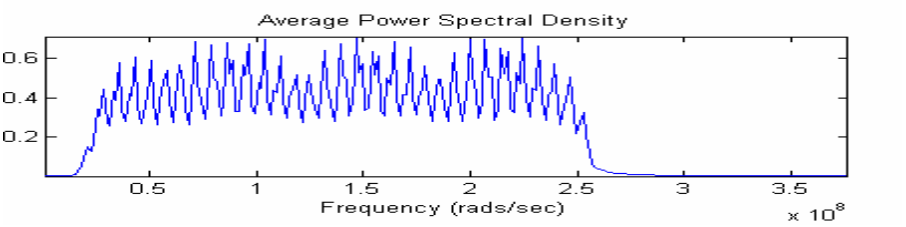

Figure (5.28): Spreading spectrum FSK FFH/SS signals under AWGN (SNR=-10dB) using noncontiguous technique

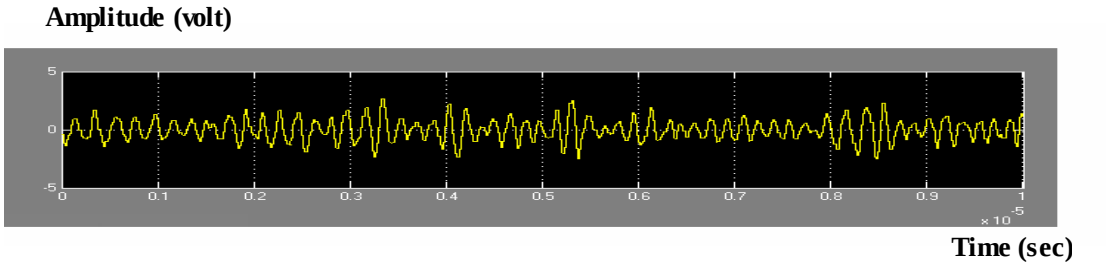

Figure (5.29): Spreading FSK FFH/SS signals under AWGN (SNR=-10dB) using noncontiguous technique

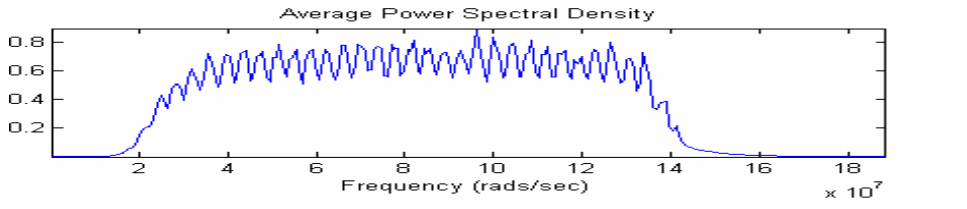

Figure (5.30): Spreading Spectrum FSK FFH/SS signals under AWGN (SNR=-10dB) using noncontiguous technique

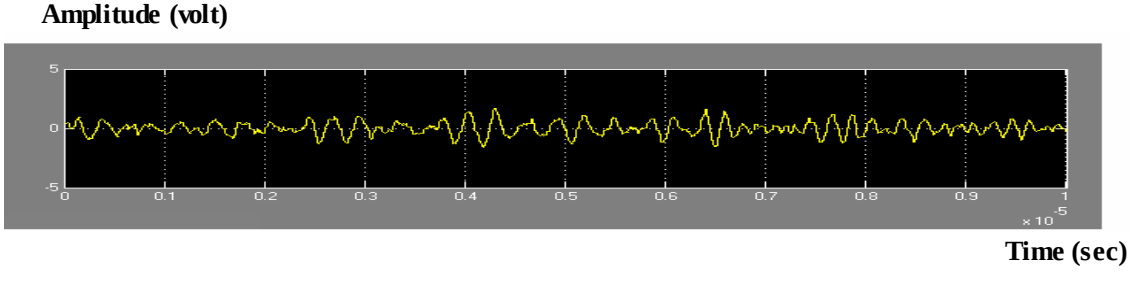

Figure (5.31) Spreading FSK FFH/SS signals under MTJ using contiguous technique

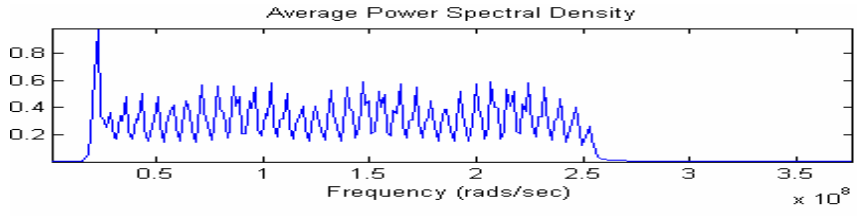

Figure (5.32): Spreading Spectrum FSK FFH/SS signals under MTJ (SJR=2.181134486 dB) using contiguous technique

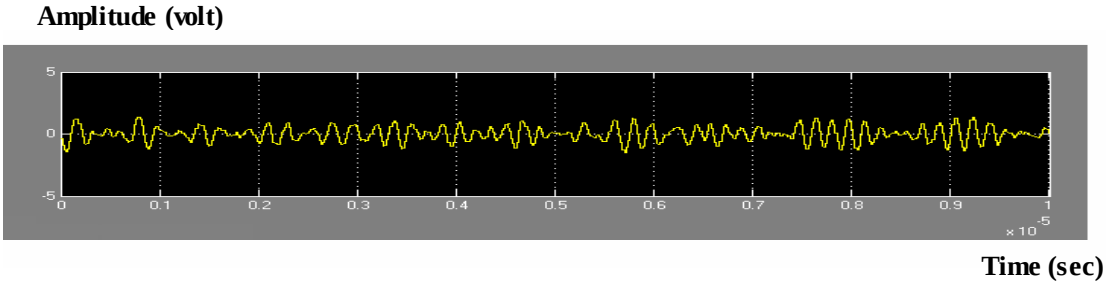

Figure (5.33): Spreading FSK FFH/SS signals under MTJ using noncontiguous technique

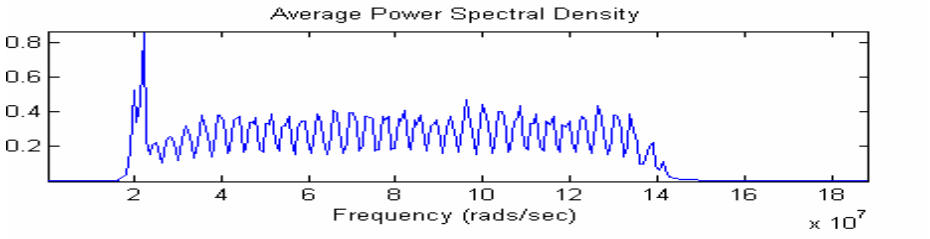

Figure (5.34): Spreading spectrum FSK FFH/SS signals under MTJ using noncontiguous technique

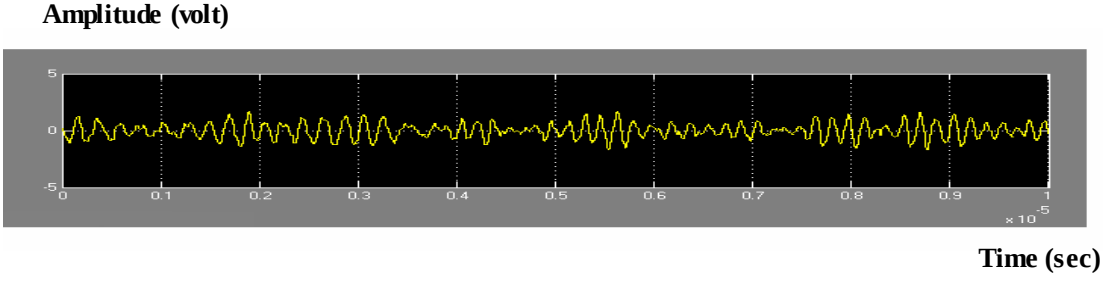

Figure (5.35): Waveform FSK FFH/SS signals under HJ using contiguous technique

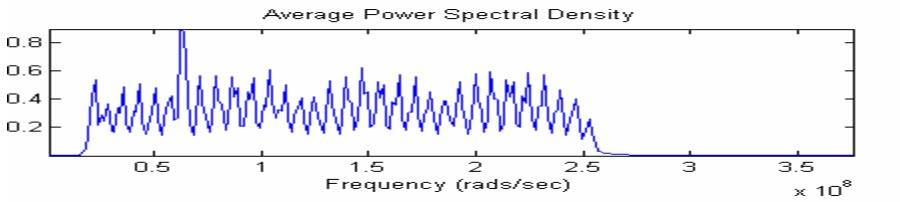

Figure (5.36): Spreadin spectrum FSK FFH/SS signals under HJ using contiguous technique

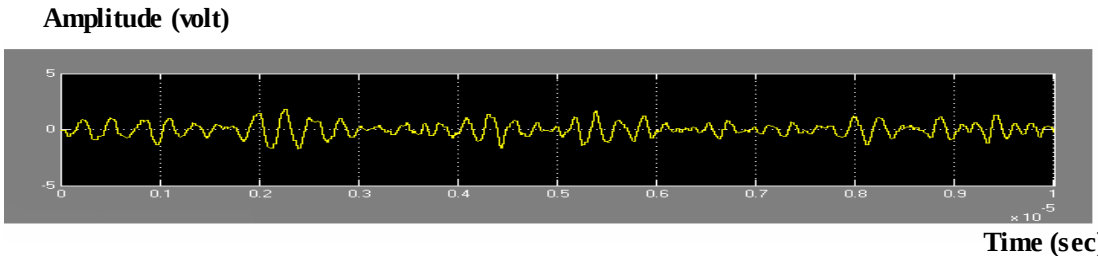

Figure (5.37): Spreading FSK FFH/SS signals under HJ (SJR=2.181134486 dB) using noncontiguous technique

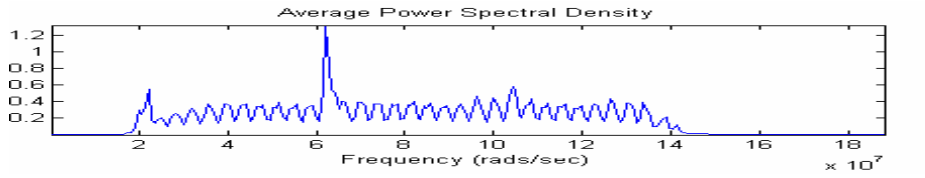

Figure (5.38): Spreading spectrum FSK FFH/SS signals under HJ using noncontiguous technique

5.4.2 Spread Code Generator.

It is the same as that of the transmitter section (5.2.1.3)

5.4.3 Serial / parallel Converter

It is same as that stated in chapter four section (4.2.1.3).

5.4.4 DDFS

It is the same as that of the transmitter section (5.2.1.5), its function is to make down conversion (de-spreading).

5.4.5 Data Despreading for FSK FFH/SSS

This technique is used at the receiver to obtain the transmitted data from a wide bandwidth received signal. It is stated in chapter four section (4.2.1.5). Figures (5.39), (5.40) and (5.41) show the received waveform under, AWGN (SNR =-10 dB), MTJ and HJ each one specified (f_j=3.16 MHz,3.32 MHz,3.48 MHz and SJR= 2.181134486 dB, BER=0.0001) respectively. Each figure state the following:

(a) received spreading of FSK FFH/SS signals after passed through contiguous digital BPF banks. (b) DDFS signals**.** (c) despreading signals. Figures (5.42), (5.43), (5.44), (5.45), (5.46), (5.47), (5.48), (5.49), (5.50), (5.51), (5.52) and (5.53) show waveform and spectrum of the despreading transmitted FSK FFH/SS signals under, AWGN (SNR=-10dB),MTJ and HJ each one specified (f_j = 3.16 MHz ,3.32 MHz ,3.48 MHz and SJR=2.181134486 dB) of the proposed system after contiguous and noncontiguous digital BPF banks respectively.

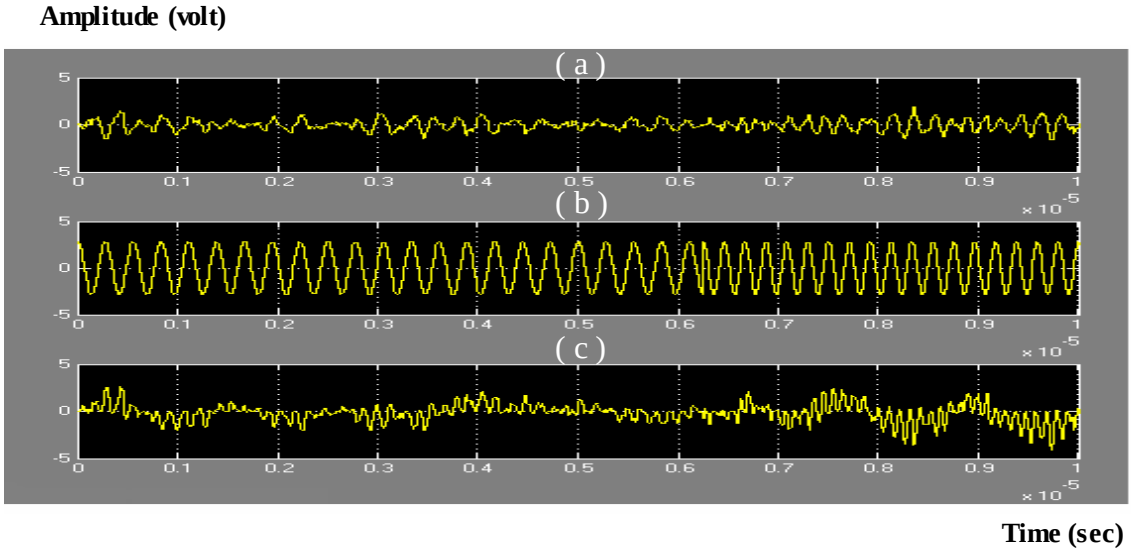

Figure (5.39): Received FSK FFH/SS signals using contiguous technique under AWGN (-10 dB):
(a) spreading signal .
(b) DDFS signals.
(c) despreading signals.

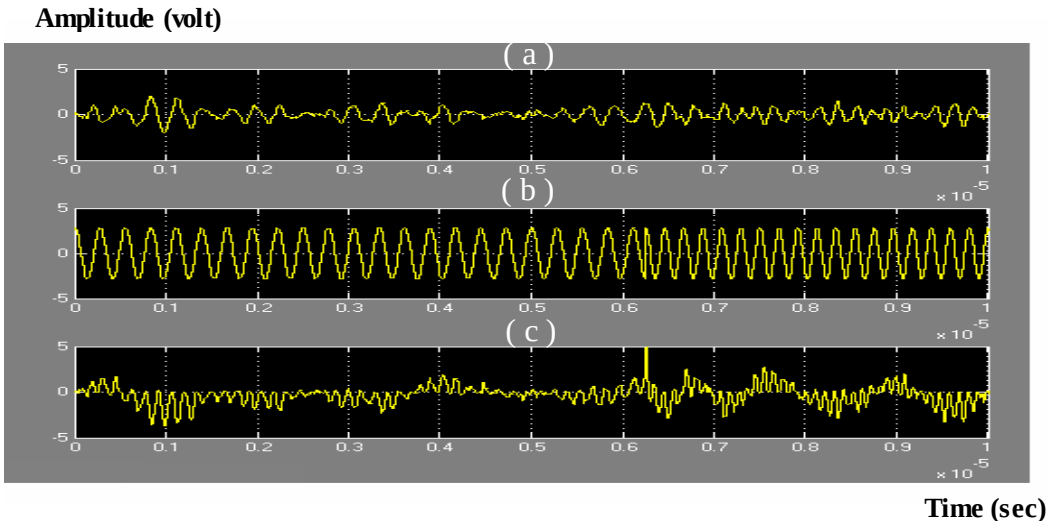

Figure (5.40): Received FSK FFH/SS signals using contiguous technique under MTJ:
(a) spreading signal .
(b) DDFS signals.
(c) despreading signals.

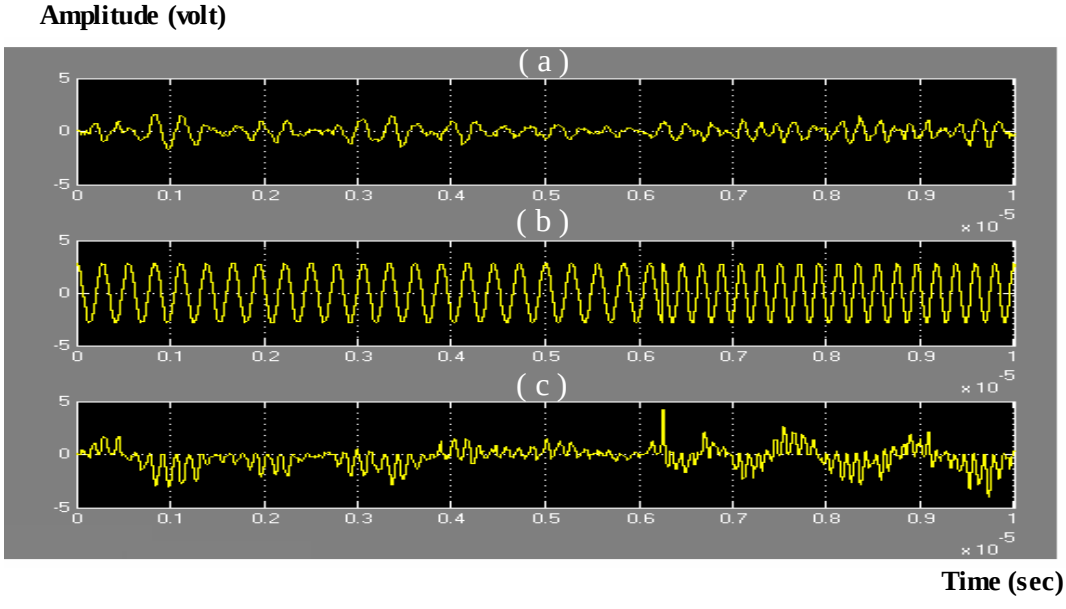

Figure (5.44): Received FSK FFH/SS signals using contiguous technique under HJ:
(a) spreading signal.
(b) DDFS signals.
(c) despreading signals.

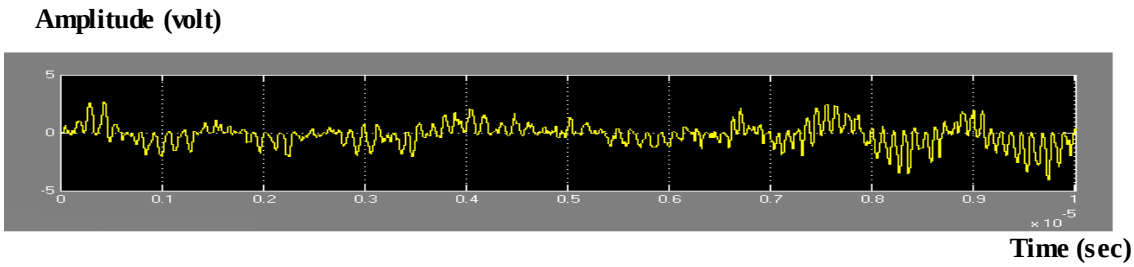

Figure (5.42): Despreading FSK FFH/SS signals using contiguous technique under AWGN (SNR=-10dB)

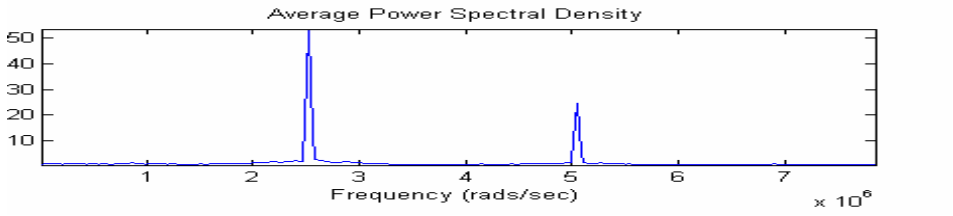

Figure (5.43): Despreding spectrum FSK FFH/SS signal using contiguous technique under AWGN (SNR = - 10dB)

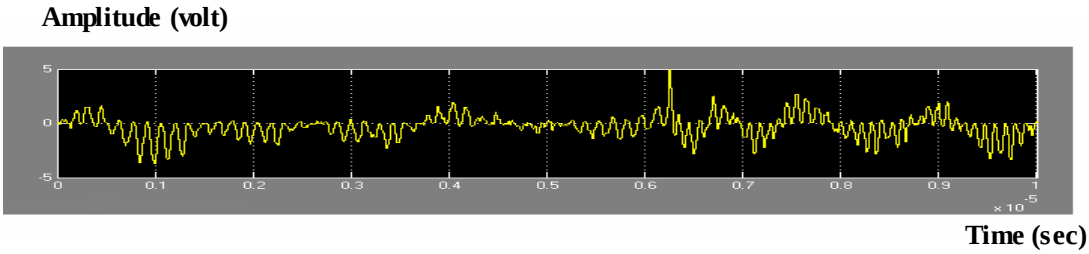

Figure (5.44): Despreading FSK FFH/SS signals using noncontiguous technique under AWGN (SNR=-10dB, BER=0.0601)

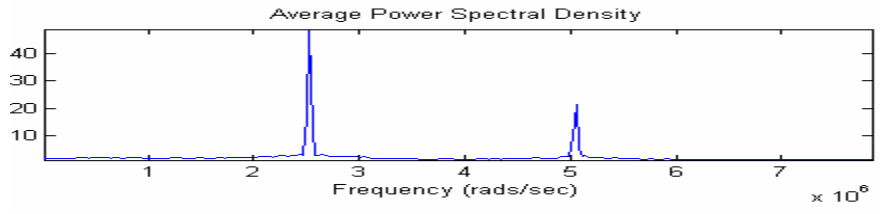

Figure (5.45): Dispreading spectrum FSK FFH/SS signals using noncontiguous technique under AWGN (SNR=- 10dB)

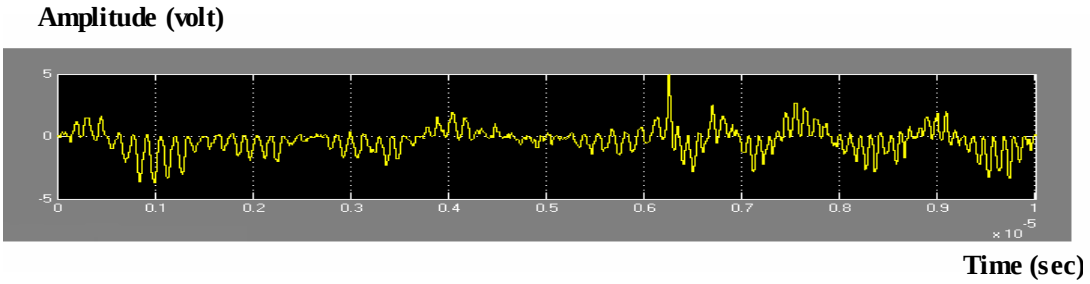

Figure (5.46): Despreading FSK FFH/SS signals using contiguous technique under MTJ.

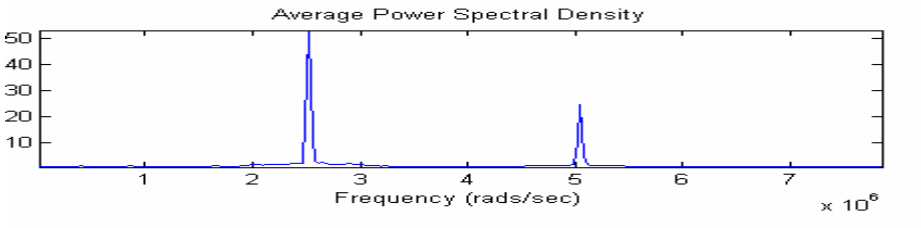

Figure (5.47): Despreading spectrum FSK FFH/SS signals using contiguous technique under MTJ.

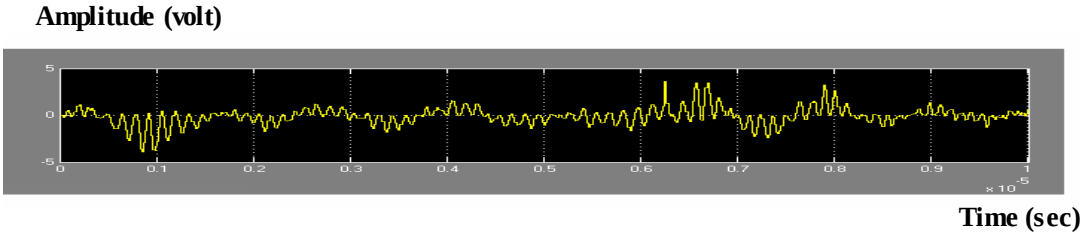

Figure (5.48): Despreading FSK FFH/SS signals using noncontiguous technique under MTJ.

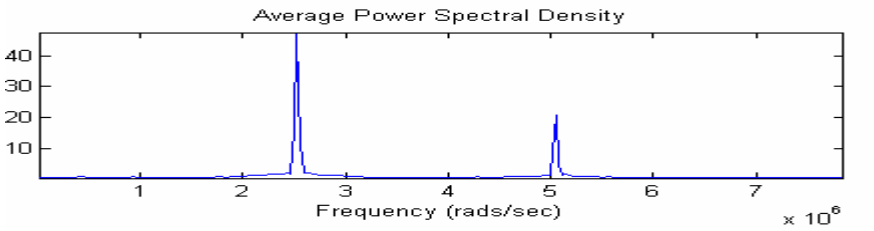

Figure (5.49): Despreading spectrum FSK FFH/SS signals using noncontiguous technique under MTJ.

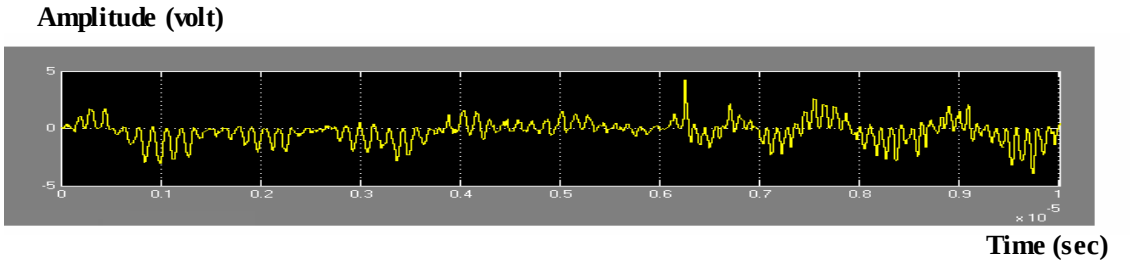

Figure (5.50): Despreading FSK FFH/SS signals using contiguous technique under HJ.

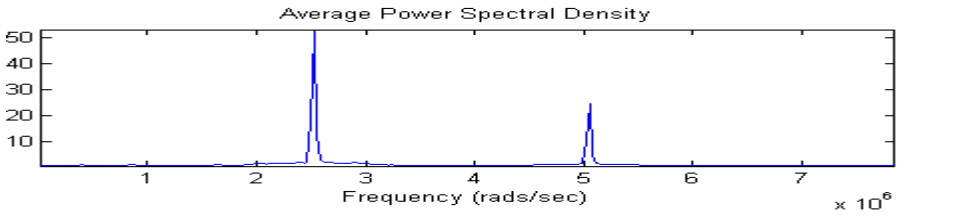

Figure (5.51): Despreading spectrum FSK FFH/SS signals using contiguous technique under HJ

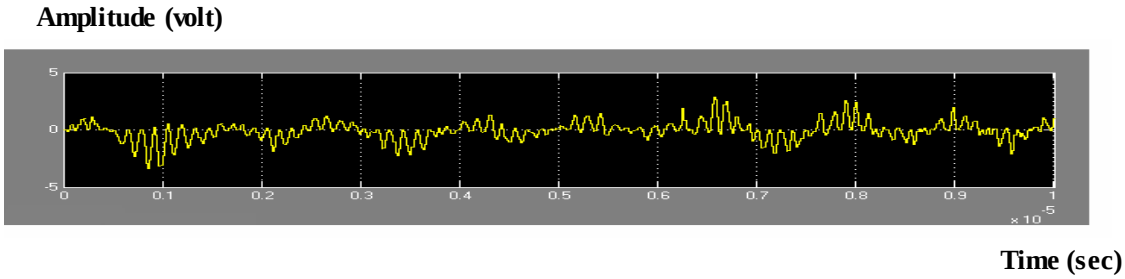

Figure (5.52): Despreading FSK FFH/SS signals using noncontiguous technique under HJ

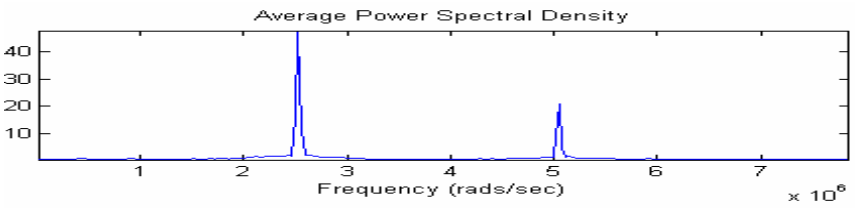

Figure (5.53): Despreading spectrum FSK FFH/SS signals using contiguous technique under HJ

5.4.6 FSK Demodulator

In the receiver of BFSK FFH/SSS noncoherent detection is used due to Doppler effect. Figure (5.54) shows, the implantation design of BFSK noncoherent demodulator using Simulink, which contains a pair of matched filters followed by envelope detectors. The filter in the upper path is matched to the FSK signal of frequency (f_{m1} = 400 kHz), and the filter in the lower path is matched to the signal of frequency (f_{m2}=800KHz). These matched filters function as BPFs centered at f_{m1} and $f_{m2,}$ respectively. The upper digital band pass filter allows the received signal of frequency (f_{m1}) 400 KHz, and the lower digital BPF allows the received signal of frequency (f_{m2}) 800 KHz to pass respectively of the BFSK FFH/SS received signals. Figures (5.55), (5.56) and (5.57) show the waveform of the noncoherent BFSK detected signals passed through upper BPF, envelope detector and LPF (f_{ct} = 160 KHz) filter under AWGN (SNR = -10 dB), MTJ and HJ each one specified (f_j = 3.16MHz,3.32 MHz ,3.48 MHz and SJR = 2.181134486 dB), respectively. Figures (5.58), (5.59) and (5.60) show the waveform of the noncoherent BFSK detected signals passing through lower BPF, envelope detector and LPF (f_{ct} = 160 KHz) filter under AWGN (SNR = -10dB), MTJ and HJ each one specified (f_j=3.16 MHz,3.32 MHz,3.48 MHz and SJR =2.181134486 dB), respectively. Figures (5.61), (5.62) and (5.63) show the detected of spreading BFSK FFH/SS received signals after passing through subtractions, zero order hold (ZOH), and limiting (Sign) respectively. Figures (5,64), (5,65) and (5,66) show the detected of spreading BFSK FFH/SS received signals before limiting , after limiting and after threshold respectively. Fig.(5.67) shows the transmitted data and detected of spreading BFSK FFH/SS received signals under AWGN (SNR = -10dB), MTJ and HJ each one specified (f_j = 3.16MHz,3.32 MHz ,3.48 MHz and SJR = 2.181134486 dB).

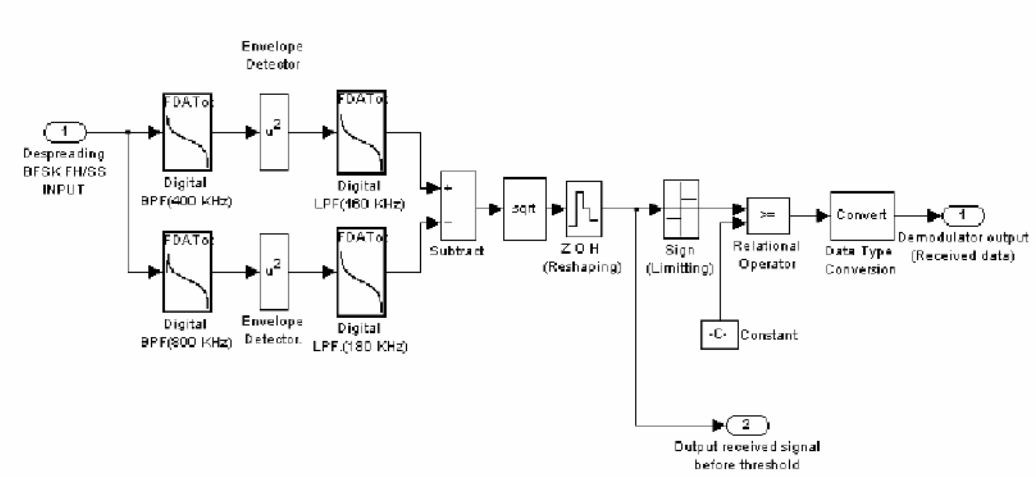

Figure (5.54): Design and simulation of noncoherent BFSK demodulator for FFH /SS receiver using Simulink

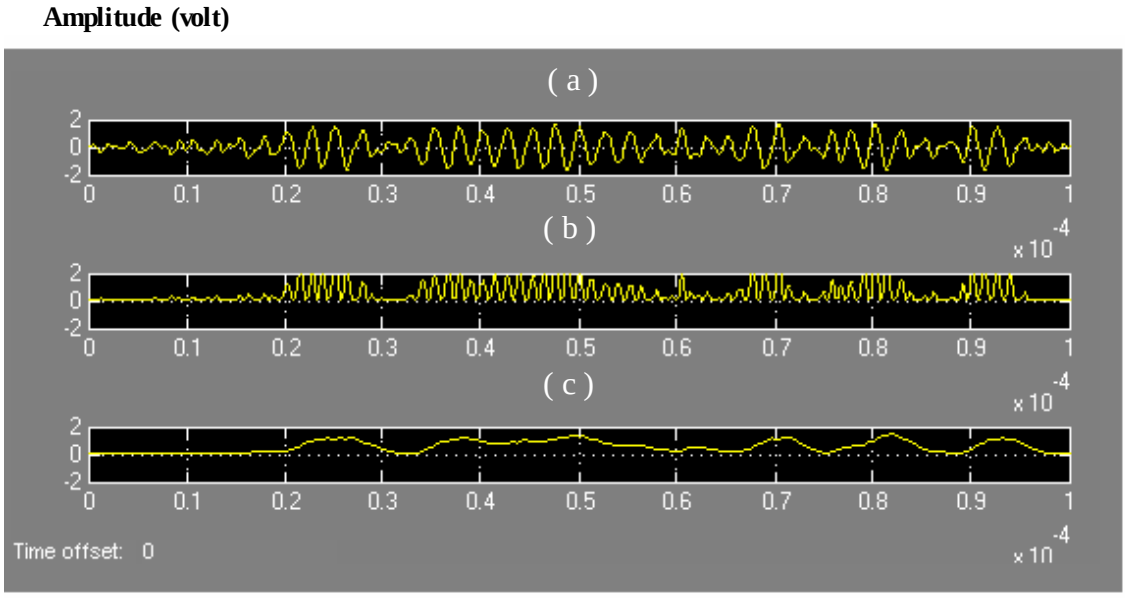

Figure (5.55): Detected of despreading received BFSK FFH/SS signals under AWGN (SNR=- 10dB):
(a) after upper BPF (f_{m1} = 400 KHz.
(b) after upper envelope detector (U^2)
(c) after upper LPF (f_{ct} = 160 KHz)

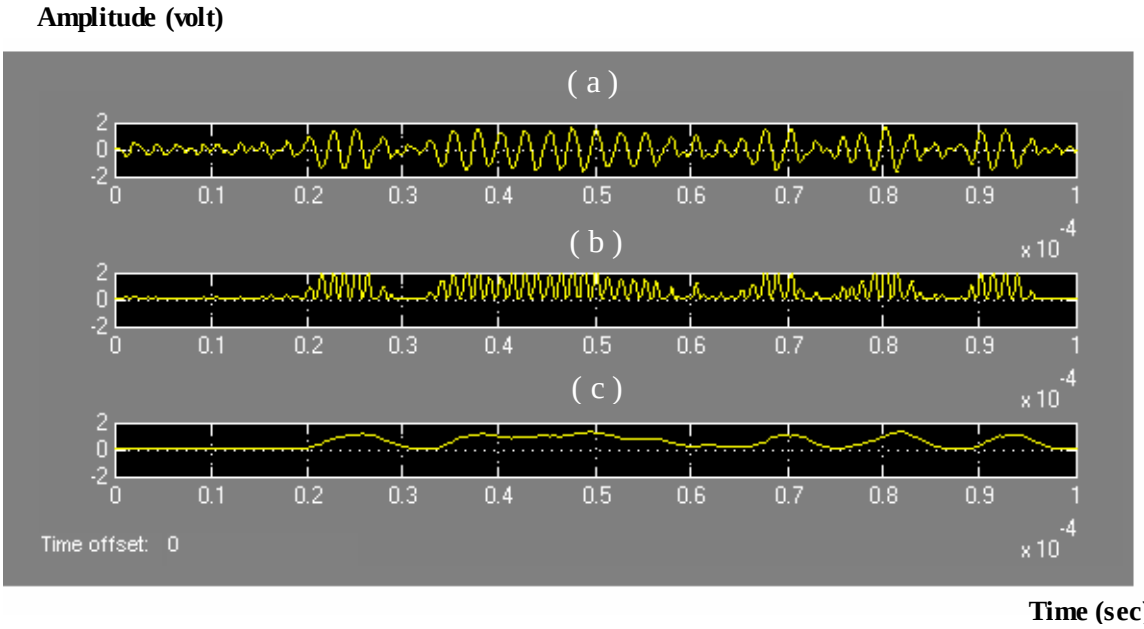

Figure (5.56): Detected of despreading received BFSK FFH/SS signals under MTJ
(a) after upper BPF (f_{m1} = 400 KHz).
(b) after upper envelope detector (U^2).
(c) after upper LPF (f_{ct} = 160 KHz).

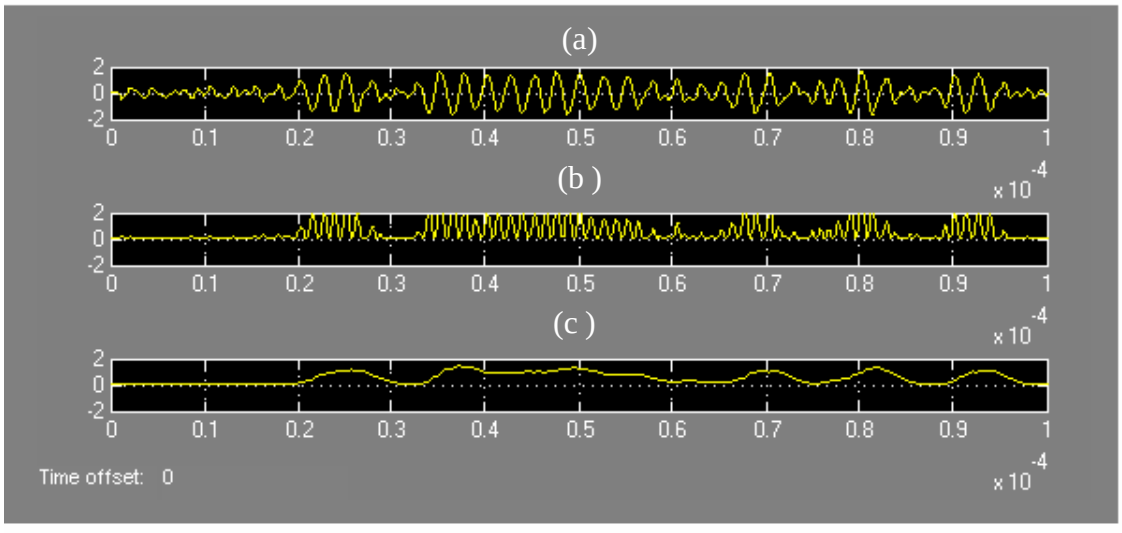

Figure (5.57): Detected of despreading received BFSK FFH/SS signals under HJ
(a) after upper BPF (f_{m1} = 400 KHz).
(b) after upper envelope detector (U^2).
(c) after upper LPF (f_{ct} = 160 KHz).

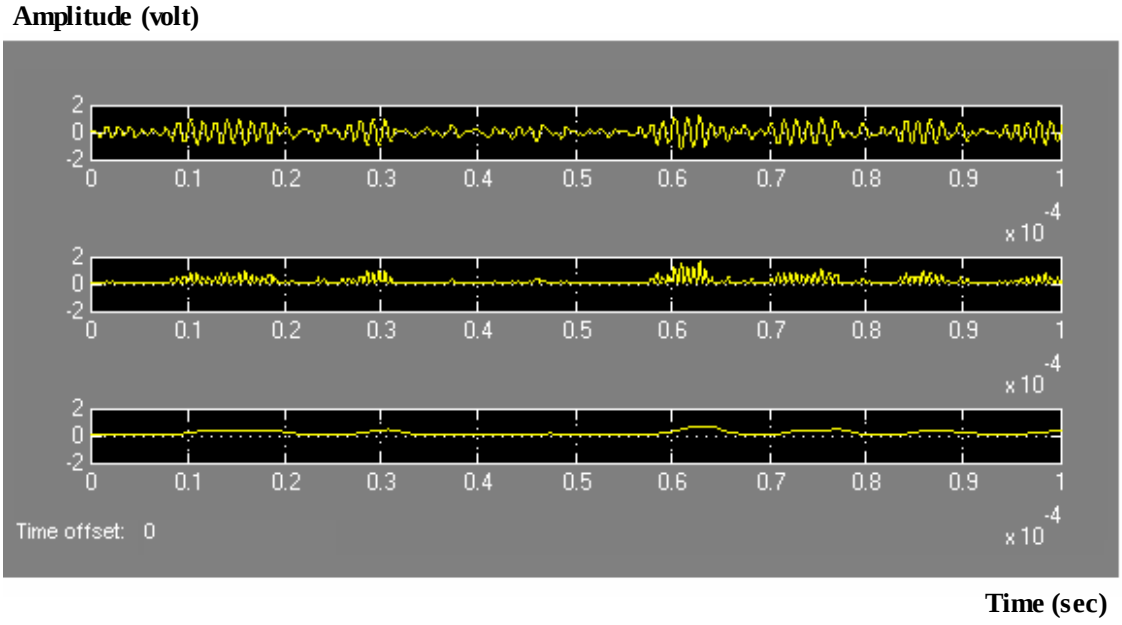

Figure (5.58): Detected of despreading received BFSK FFH/SS signals under AWGN (SNR=- 10dB):
(a) after lower BPF (f_{m2} = 800 KHz).
(b) after lower envelope detector .
(c) after lower LPF (f_{ct} = 160 KHz).

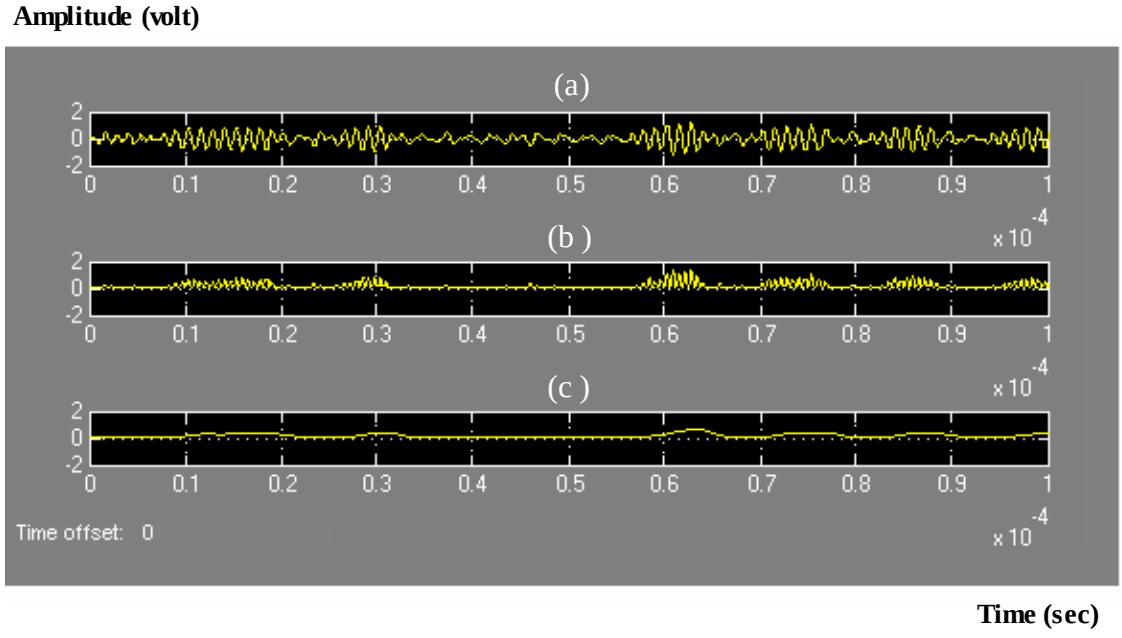

Figure (5.59): Detected of despreading received BFSK FFH/SS signals under MTJ (SJR= 2.181134486 dB):
(a) after lower BPF (f_{m2} = 800 KHz.
(b) after lower envelope detector (U^2).
(c) after lower LPF (f_{ct} = 160 KHz).

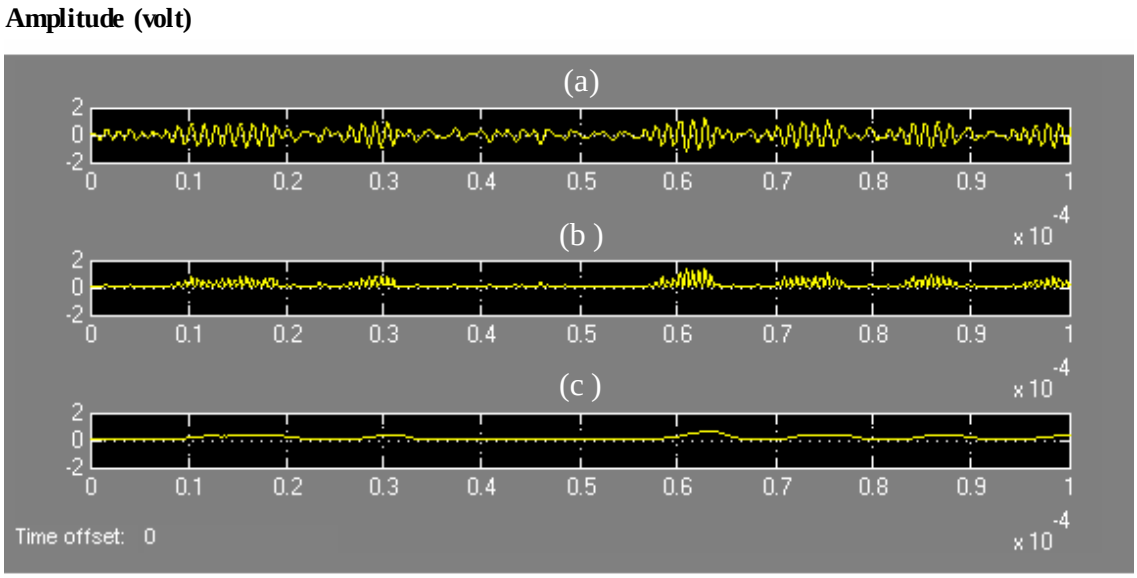

Figure (5.60): Detected of despreading received BFSK FFH/SS signals under HJ:
(a)after lower BPF (f_{m2} = 800 KHz.
(b) after lower envelope detector (U^2).
(c) after lower LPF (f_{ct} = 160 KHz).

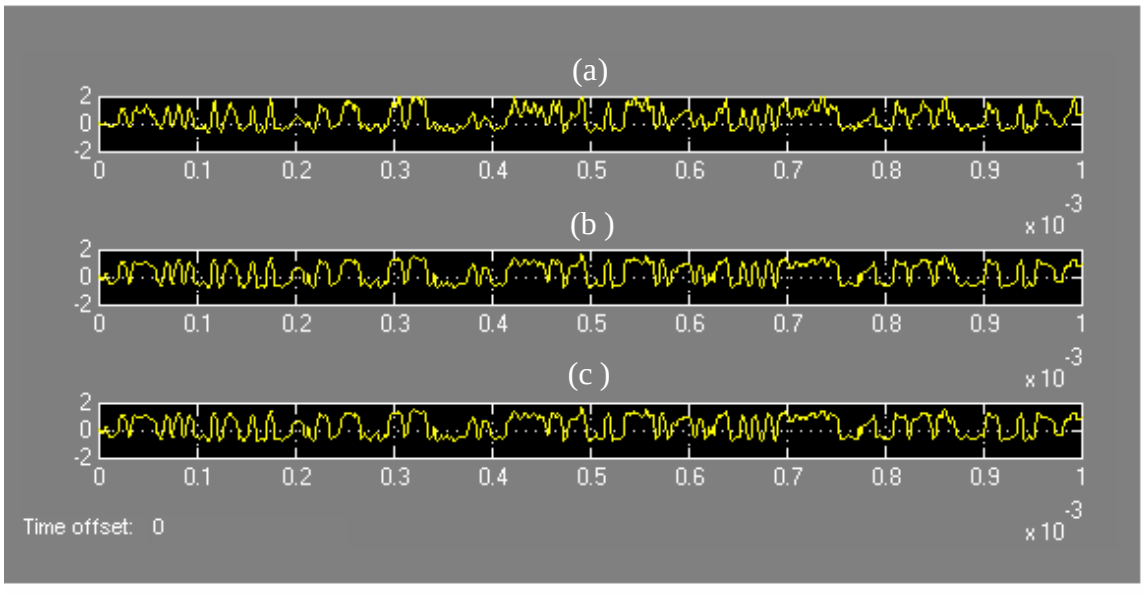

Figure (5. 61): Detected of despreading received BFSK FFH/SS signals under AWGN (SNR=- 10dB):
(a) detected signal after subtraction.
(b) detected signal after sqrt.
(c) detected data after reshaping.

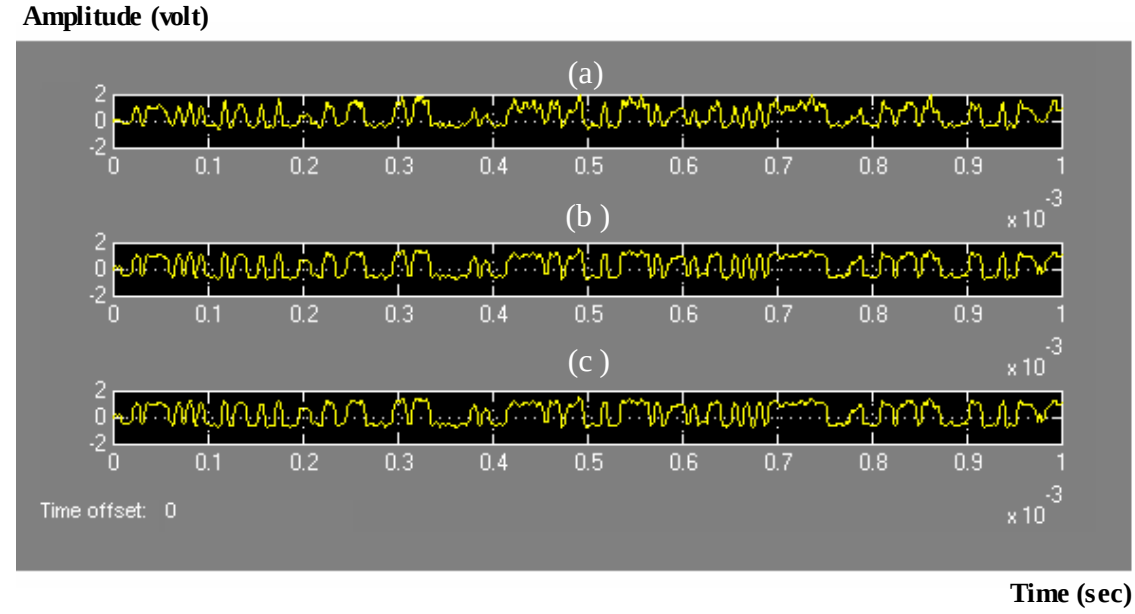

Figure (5.62): Detected of despreading received BFSK FFH/SS signals under MTJ :
(a) detected signal after subtraction.
(b) detected signal after sqrt.
(c) detected data after reshaping.

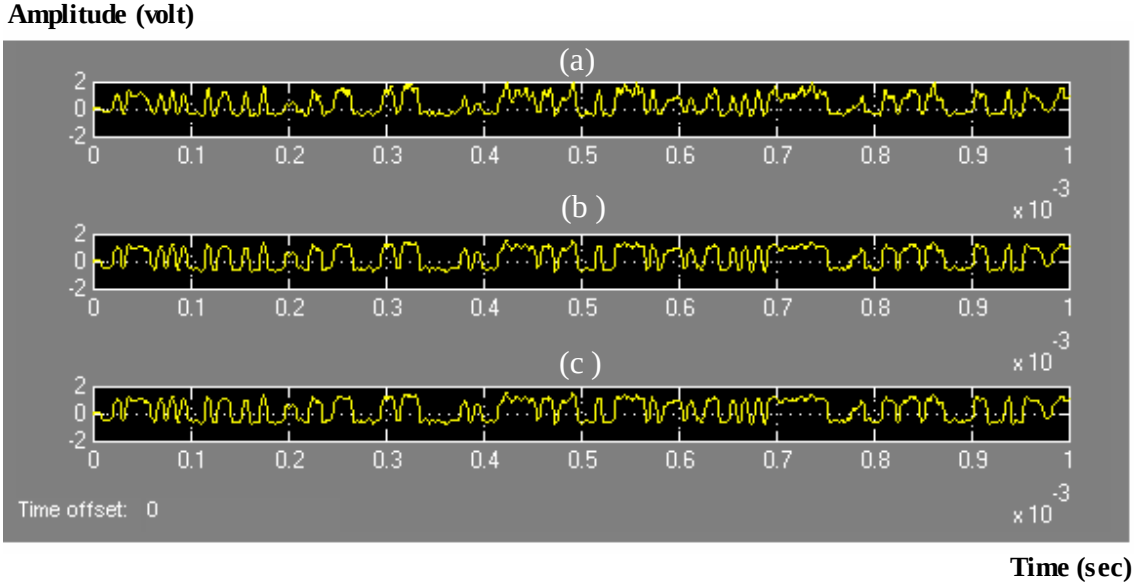

Figure (5.63): Detected of despreading received BFSK FFH/SS signals under HJ:
(a) detected signal after subtraction.
(b) detected signal after sqrt.
(c) detected data after reshaping.

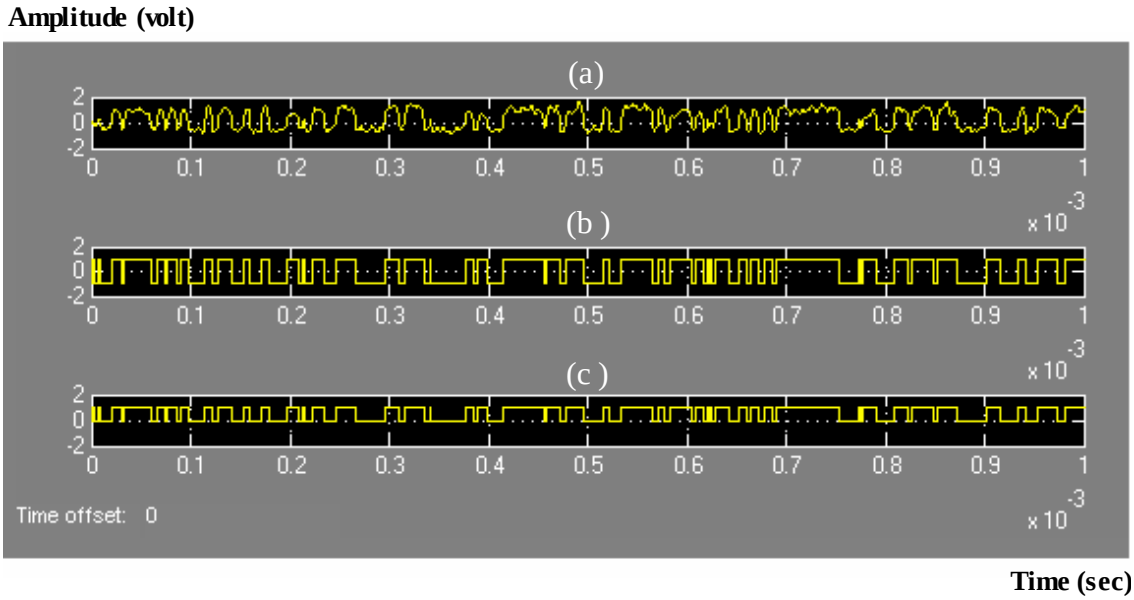

Figure (5.64): Detected of despreading received BFSK FFH/SS signals under AWGN (SNR=- 10dB)
(a) detected signal before limiting.
(b) detected signal after limiting.
(c) detected data after threshold.

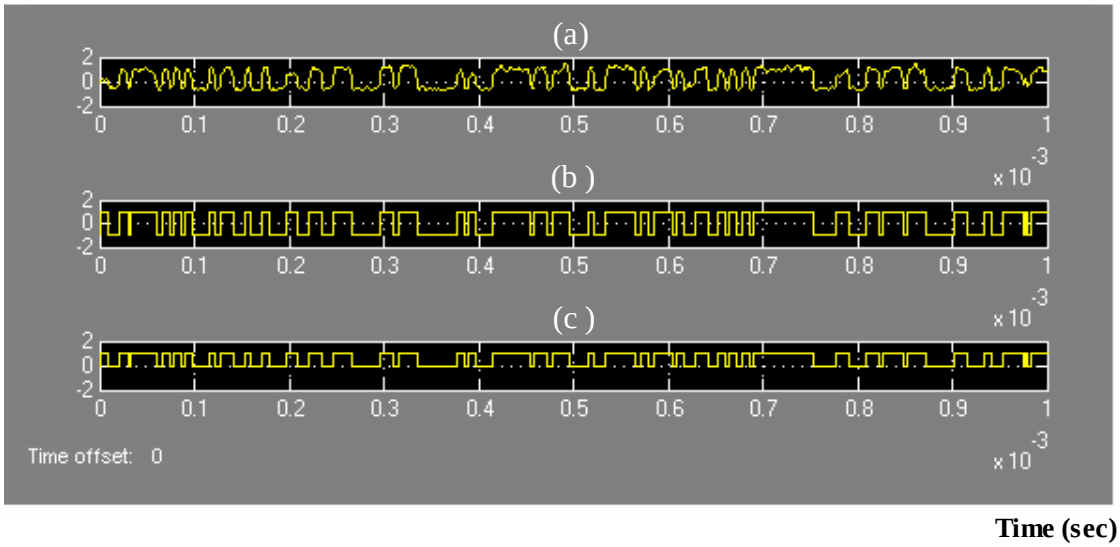

Figure (5.65): Detected of despreading received BFSK FFH/SS signals under MTJ:
(a) detected signal before limiting.
(b) detected signal after limiting.
(c) detected data after threshold.

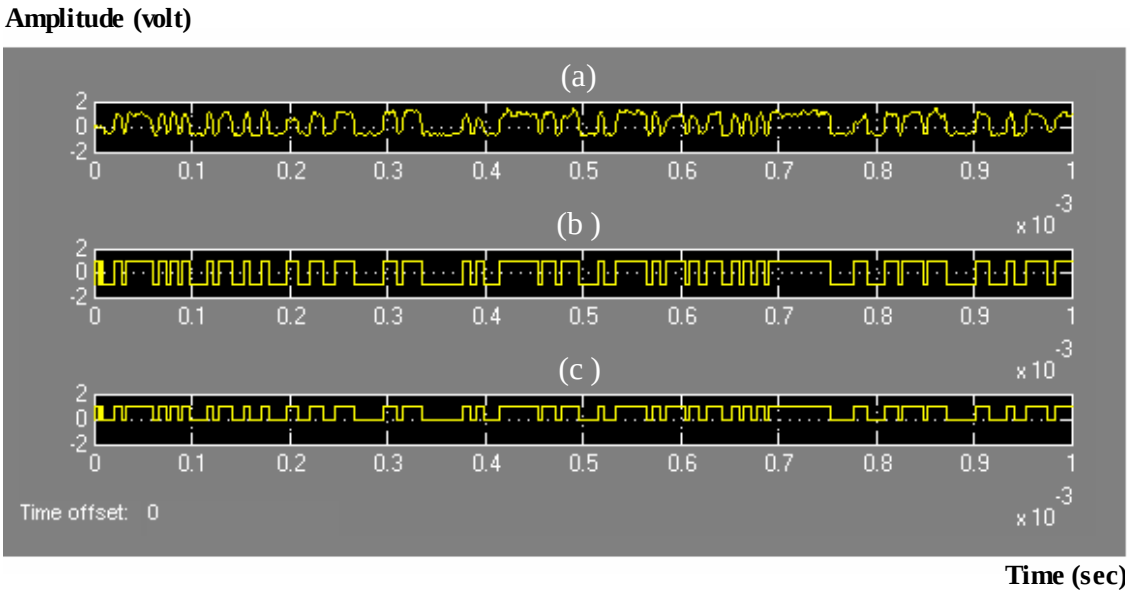

Figure (5.66): Detected of despreading received BFSK FFH/SS signals under HJ:
(a) detected signal before limiting.
(b) detected signal after limiting.
(c) detected data after threshold.

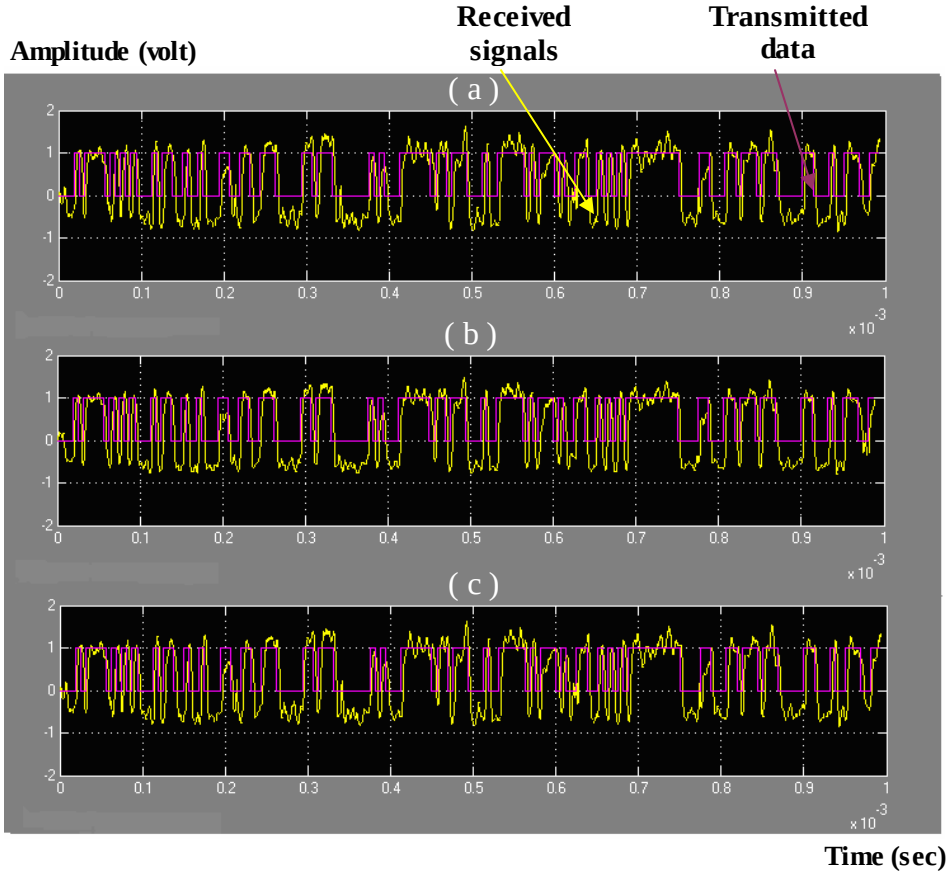

Figure (5.67): Transmitted data and detected of spreading BFSK FFH/SS signals received before threshold under:
(a) AWGN (SNR=-10dB).
(b) MTJ (f_j = 3.16MHz, 3.32 MHz, 3.48 MHz, SJR=2.181134486 dB).
(c) HJ (f_j = 3.16MHz, 3.32 MHz, 3.48 MHz, SJR=2.181134486 dB).

5.4.7 Error Rate Calculation

The block diagram of it is shown in Figure (4.75). The block of the error rate calculation is gotten from Simulink DSP, and its function is to calculate BER. It has two inputs: one is the message from the BFSK noncoherent receiver detector and the other from the data generator at the transmitter with the measured delay between transmitter and receiver message. Figures (5.68), (5.69) and (5.70) show received detected data and transmitted data with delay (6.25) μ sec respectively.

In telecommunication transmission, system performance is frequently specified in terms of the average probability of error P_e . This term is also known in various references and among test equipment vendors and systems integrators as bit error rate (BER). The bit error rate is the average rate at which the errors occur and can be expressed as stated in chapter four, section (4.4.7), and equation (4.1).

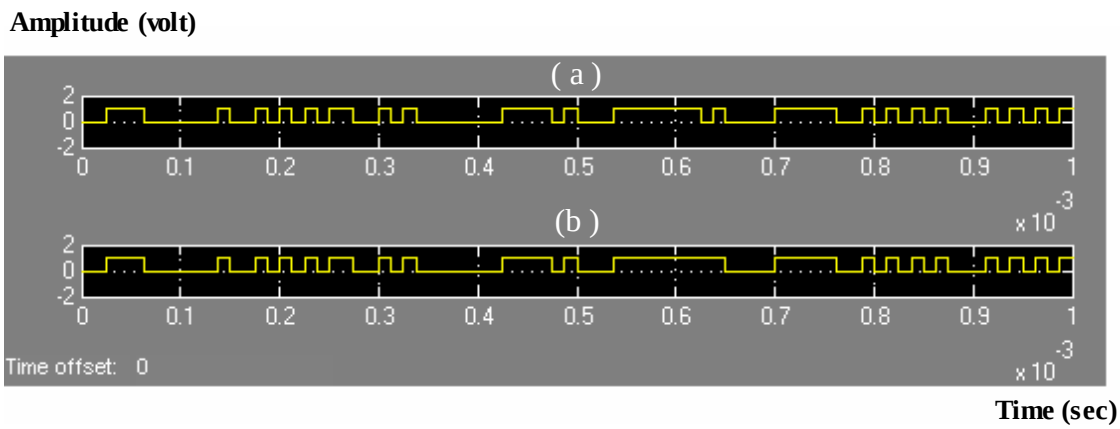

Figure (5.68): Final received data waveform under AWGN (SNR = -10 dB)
(a) transmitted data after delay (6.25) μ sec.
(b) received data .

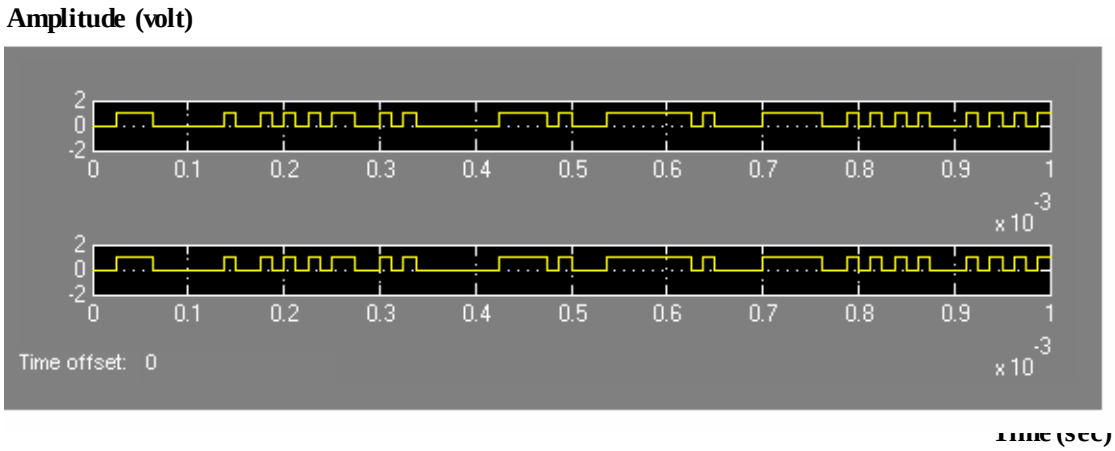

Figure (5.69): Final received data waveform under MTJ :
(a) transmitted data after delay (6.25) µ sec.
(b) received data.

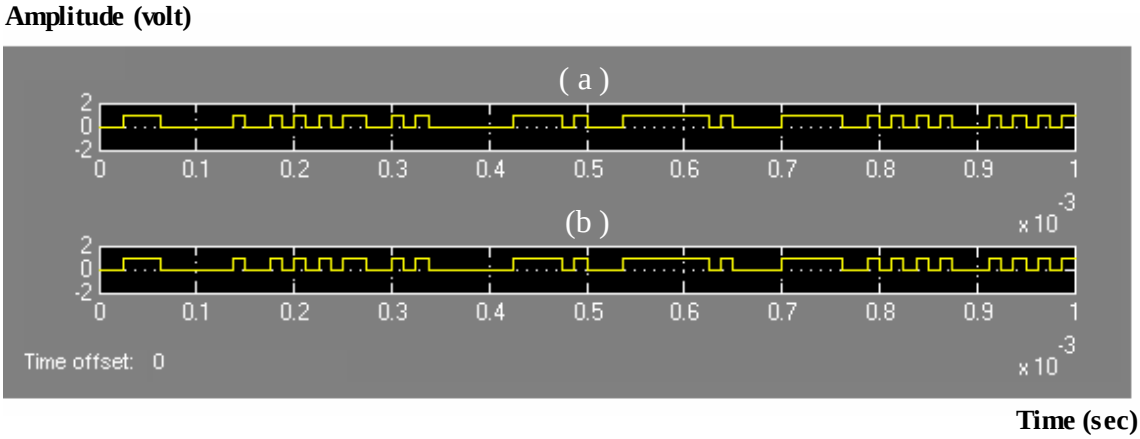

Figure (5.70): Final received data waveform under HJ:
(a) transmitted data after delay (6.25) µ sec.
(b) received data .

5.5 Simulation Results

The performance of any digital system is the measuring of the BER for received data. Therefore, in this proposed system we study the effect of the noise (AWGN) and jamming (MTJ, HJ) to the FSK FFH/SSS using contiguous and noncontiguous technique.

5.5.1 Effect of AWGN

During simulation process and after 0.62 ms simulation time the number of bits was 10000 bits, taking different values of SNR in dB from AWGN block for each run and calculate BER by using error rate calculation from calculation block set ,the results of these calculation are shown in Figure (5.71) for FSK FFH/SSS using contiguous and noncontiguous technique. The calculation of G_P is the same as that in section (4.5.1).

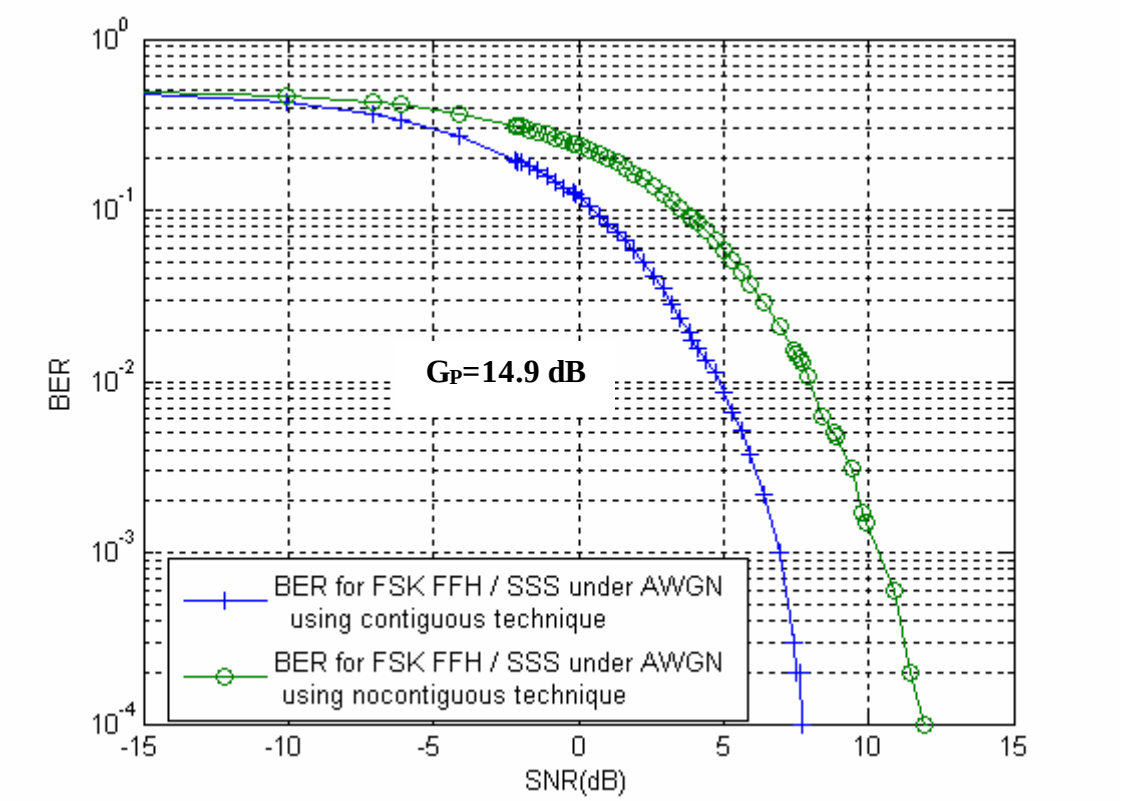

Figure (5.71): BER versus SNR (dB) for BFSK contiguous FH/SSS under AWGN using contiguous and noncontiguous technique

It is clear that from Figure (5.71) the BER performance FSK FFH/SSS using contiguous technique is better than that of using noncontiguous technique (gained SNR 5dB for BER 1×10^{-4}).

5.5.2 Effect of Jamming

The system has been tested under the following types of jamming:

Effect of MTJ, as stated in section (2.6.2) and section 4.3.2, Figure (4.26) shows the block diagram of MTJ (f_j =3.16 MHz, 3.32 MHz, 3.48 MHz). We take different values of signals of MTJ to obtain many values of SJR in dB and read the corresponding BER by using error rate calculation block from communication block set, during the simulation process after 0.62 m sec simulation time, the number of bits is 10000 bits for each run. The results are shown in Figure (5.72) which shows the relationship between BER and SJR (dB) FFH/SSS using contiguous and noncontiguous technique respectively.

It is clear that be FSK FFH/SSS using noncontiguous technique has better BER performance than that using contiguous technique (gained SJR 3dB for BER 1×10^{-4}).

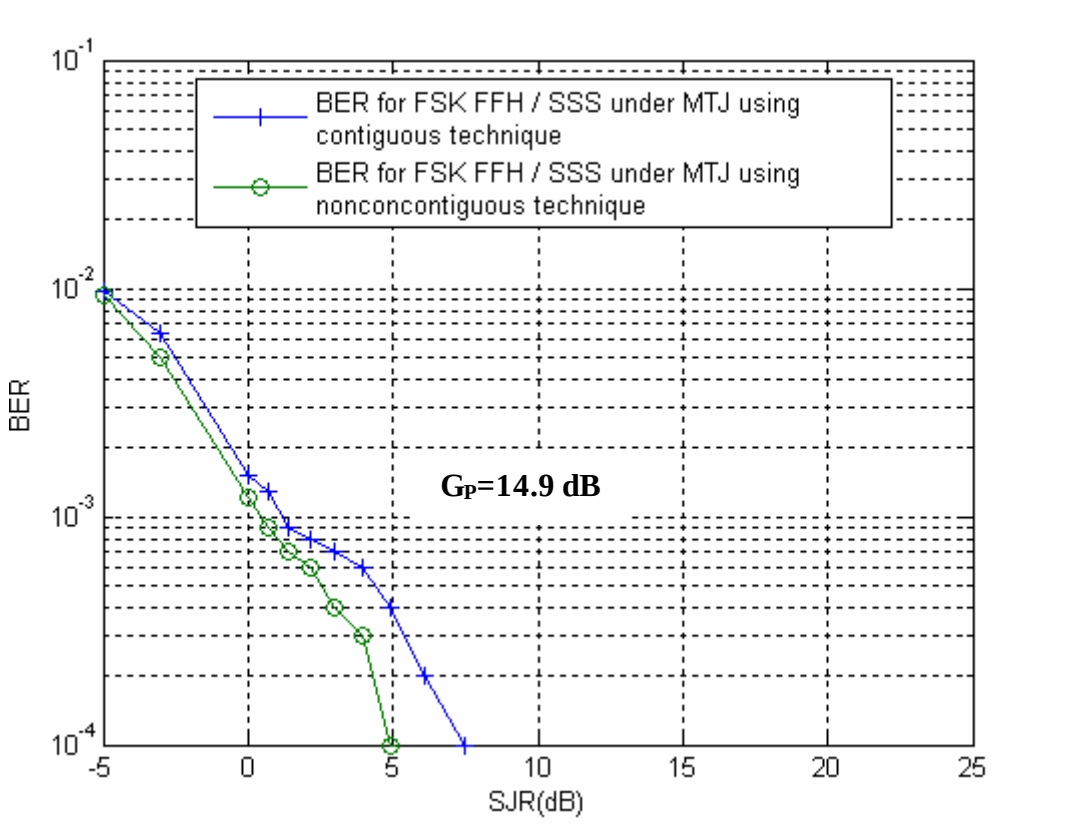

Figure (5.72): BER versus SNR (dB) for BFSK FH/SSS under MTJ using contiguous and noncontiguous technique.

B. Effect of Hopper Jamming (HJ).

It is explained in sections (2 .6.3 and 4.3.3) Figure (4.31) shows the block diagram of HJ (f_j =3.16 MHz, 3.32 MHz, 3.48 MHz) which it has severed effect than that of MTJ. Also we calculate the effect of this type by run the system with simulation time 0.62 ms to get 10000 bit for each run and calculated the BER. The results of these calculations are shown in Figure (5.73) which shows the relationship between BER and SJR (dB) FFH/SSS using contiguous and noncontiguous technique respectively. It is clear that BFSK FFH/SSS using noncontiguous technique has better BER performance than that of contiguous technique (gained SJR 5 dB for BER 1 x 10^{-4}).

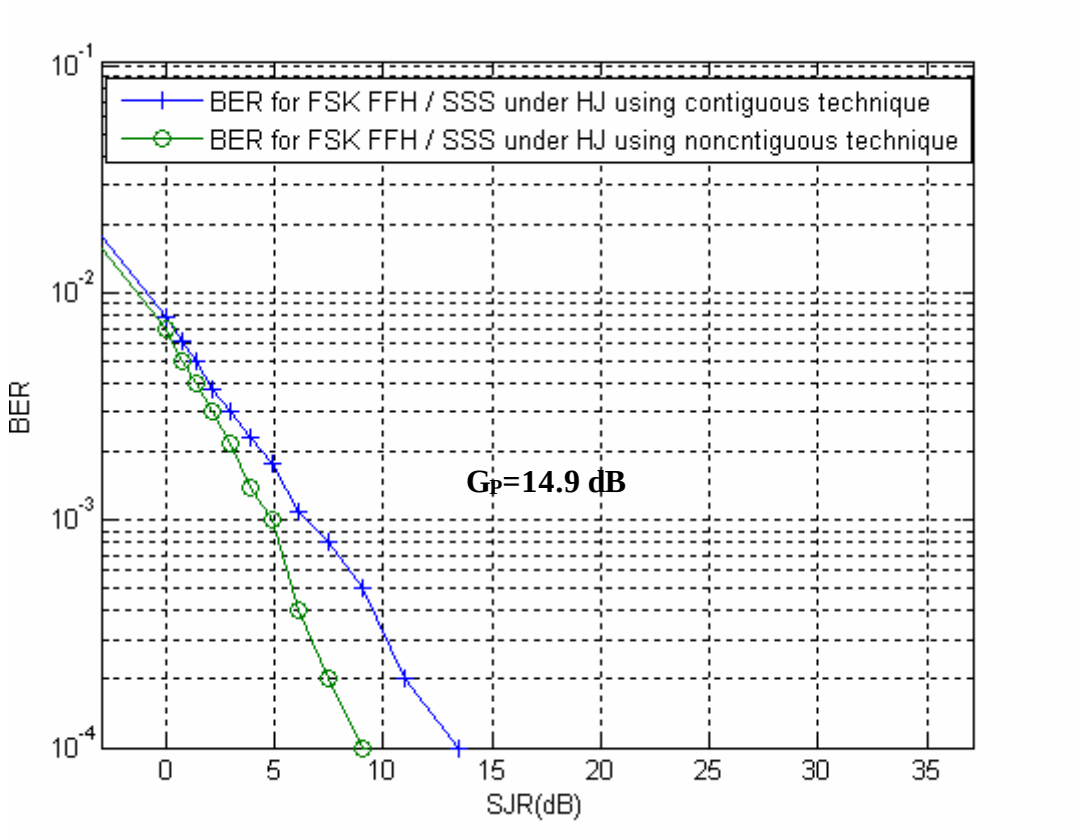

Figure (5.73): BER versus SJR (dB) for FSK FFH/SSS under HJ using contiguous and noncontiguous technique.

5.6 Results of Comparison between ASK and BFSK FFH/SSS

A comparison is made between ASK and BFSK FFH SSS using BP contiguous and noncontiguous filters. These results are calculated when these four proposed systems are tested under the effect of noise (AWGN) and jamming (MTJ and HJ) which can be stated as follows: Figures (5.74), (5.75) and (5.76) show the simulation results of these four proposed ASK and BFSK FFH/SS systems using contiguous and noncontiguous technique under the effect of AWGN, MTJ, HJ respectively. Table (5.1) shows the frequency band and bandwidth for each type of the ASK and FSK FFH/SS transceiver systems. Table (5.2) shows the summary of the comparisons between all the proposed systems.

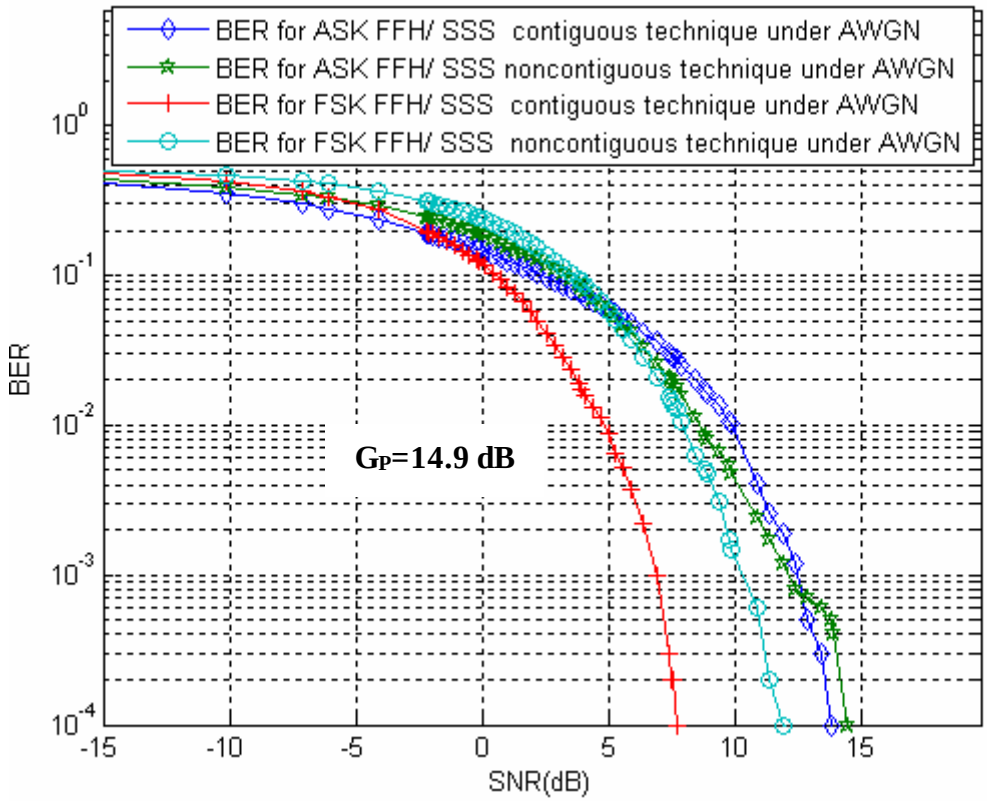

Figure (5.74): BER versus SNR (dB) for ASK and FSK FFH/SSS using contiguous and noncontiguous technique respectively under the effect of AWGN.

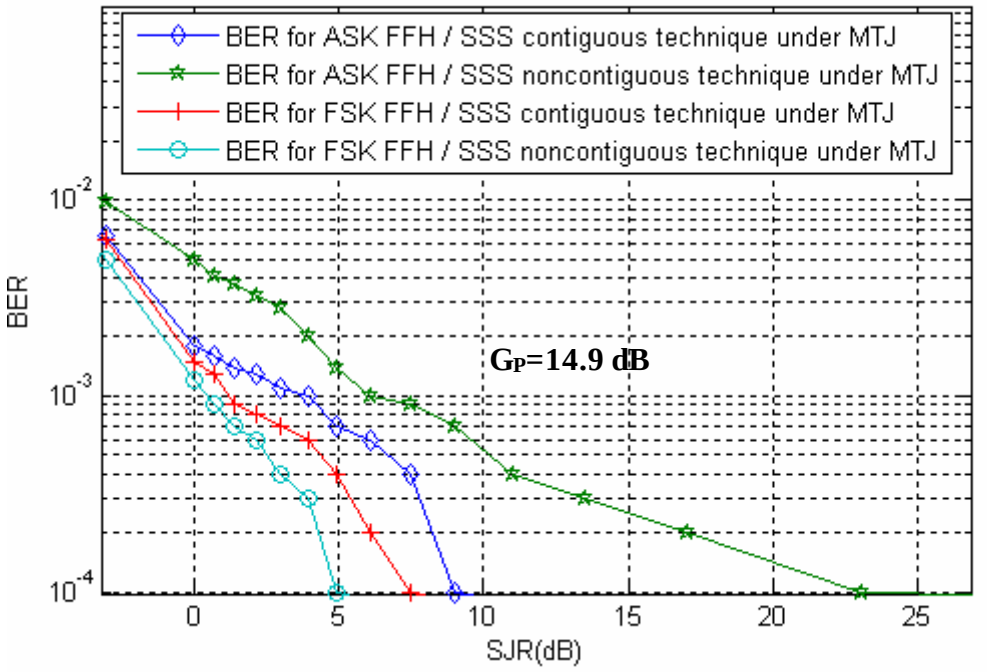

Figure (5.75): BER versus SJR(dB)for ASK and FSK FFH/SSS using contiguous and noncontiguous technique respectively under the effect of MTJ.

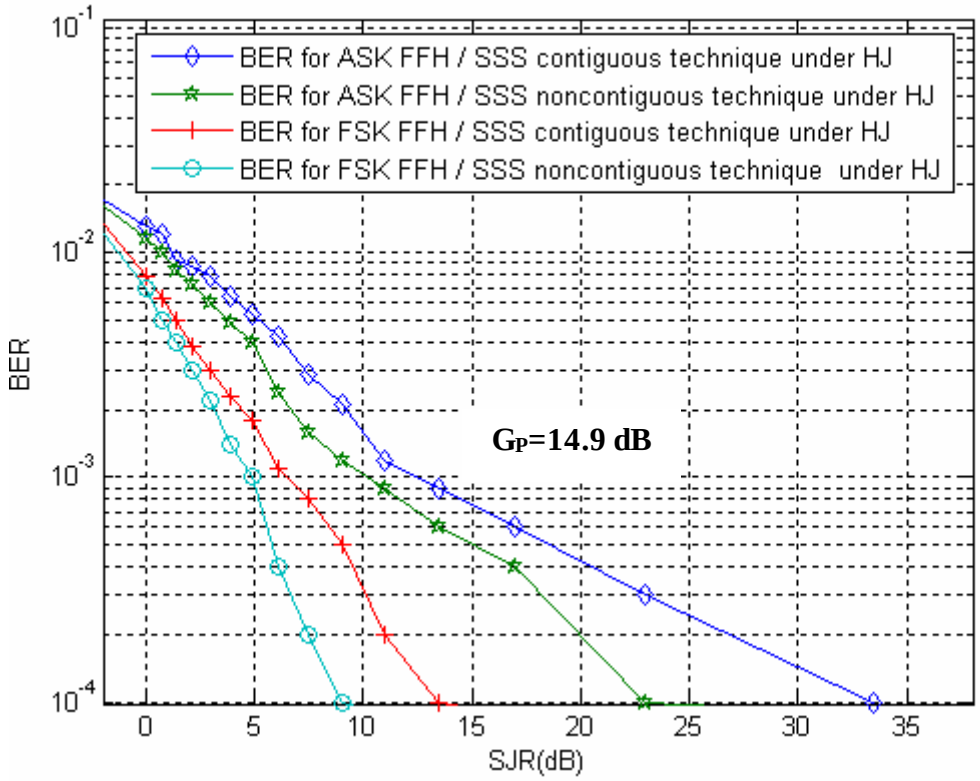

Figure (5.76): BER versus SJR(dB) for ASK and FSK FFH/SSS using contiguous and noncontiguous technique respectively under the effect of HJ.

Proposed System	*Bandwidth*	*Frequency Band*
ASK FFH/SS system using contiguous technique	**18 MHz**	**3-21 MHz**
ASK FFH/SS system using noncontiguous technique	**9.6 MHz**	**3-12.6 MHz**
FSK FFH/SS system using contiguous technique	**37. 2 MHz**	**3-40.2 MHz**
FSK FFH/SS system using noncontiguous technique	**19.2 MHz**	**3-22.2 MHz**

Table (5.1): The bandwidth and frequency band for each one of all proposed FFH/SS transceiver systems

Parameter under test	*BER performance*			
	BFSK FFH/SSS using contiguous technique	**BFSK FFH/SSS using noncontiguous technique**	**ASK FFH/SSS using contiguous technique**	**ASK FFH/SSS using noncontiguous technique**
AWGN	**Best for all other proposed System. (for BER 1x10^{-4}, SNR 7.71 dB)**	**More than the ASK FFH/SSS. (for BER 1x10^{-4},SNR 11.91 dB).**	**More than the ASK FFH/SSS. (for BER 1x10^{-4},SNR 13.81 dB)**	**Less performance for all proposed systems. (for BER 1x10^{-4},SNR 14.46 dB)**
MTJ	**More than the ASK FFH/SSS. (for BER 1x10^{-4}, SNR 7.446 dB)**	**Best for all other proposed systems. (for BER 1x10^{-4}, SNR 4.9474 dB)**	**More than the ASK FFH/SSS. (for BER 1x10^{-4}, SNR 9.03 dB)**	**Less performance for all proposed systems. (for BER 1x10^{-4},SNR 23.01 dB)**
HJ	**More than the ASK FFH/SSS. (for BER 1x10^{-4}, SNR 13.47 dB)**	**Best for all proposed systems. (for BER 1x10^{-4}, SNR 7.446 dB)**	**Less performance for all proposed systems. (for BER 1x10^{-4},SNR 33.466 dB)**	**More than the ASK FFH/SSS. (for BER 1x10^{-4},SNR 23 dB)**

Table (5.2): The BER performance for all proposed FH/SS transceiver systems

Chapter Six

Conclusions and Recommendations for Future Work

6.1 Conclusions

In responding to the demands for secure and anti-jamming communication systems, and in spite of complexity of the FH/SSS, four wireless FFH/SS transceiver systems were designed using MATLAB-Simulink and operated in real time successfully. These four types are, ASK and FSK FFH/SS transceiver systems using contiguous and noncontiguous technique respectively.

As a result, one can draw the following conclusions: -

a. The synchronization of all the four types of systems of FFH/SSS designed is achieved by using a designed contiguous and noncontiguous technique second order IIR Butterworth BPF banks in receiver side.
b. All four systems spread the data in high frequency band, with bandwidths 18 MHz (3-21 MHz),37.2MHz (3-40.2 MHz) ,9.6 MHz (3-12.6 MHz) ,19.2MHz (3-22.2 MHz), for ASK and BFSK FFH/SS transceiver systems using contiguous and noncontiguous technique respectively.
c. It is clear that BFSK FFH SSS has better BER performance for noise (AWGN) and jamming (MTJ, HJ), as shown in chapter five section (5.6).
d. The two designed ASK FFH/SSS have bandwidths less than that of BFSK FFH/SSS, but their BER performance is less than that of FSK FFH/SSS.
e. Two types of digital filters were designed using contiguous and noncontiguous technique. The bandwidths become smaller using noncontiguous technique than that using contiguous technique with the same data rate and hop rate therefore the four designed FFH/SSS using noncontiguous technique had good performance and most economical for the contiguous type, see Table (5.1).

f. To find out the difference in BER performance for all the four designed proposed FFH SSS, see Figures (5.74), (5.75) and (5.76) and Table (5.2).
g. Noncoherent detection is designed and implemented in the receivers of the two types of BFSK FFH/SSS due to Doppler effect.
h. ASK demodulator is designed and implemented for the receivers of two types of ASK FFH/SS transceiver system.

6.2 Recommendations for Future Work

The results of the current work can be extended as a future work as follows: -

a. It is clear that there are two factors can reduce the effect of jamming and noise, these factors are the numbers of channel (number of digital BPF) and the number of hops per channel, that means increasing the process gain (Gp) and this can be done by increasing the frequency band of spread spectrum to be hopped.
b. With exceeding hop rate more than data rate by many factors (more than the one), the FFH/SSS can overcome the threat of the follower jammers easily. Even the fastest follower jammers may be relatively close to the system to affect it because of the propagation speed of the electromagnetic waves.
c. Using longer PN, Gold PN sequences to add more complication to the jammer.
d. Because the four proposed designed FFH/SS transceiver systems are operated successfully, this work can be implemented by using FPGA.

References

[1] P. Heydari, "A Study of Low-power Ultra- Wide band Radio Transceiver Architectures", IEEE Communications Society / 0-7803-8966-2/2005© wcnc 2005 E-mail: payam @ eecs. uci.edu.

[2] G.Stayanov and M.Kawamata, " Variable Digital Filters ", J. Signal Processing. Vol. 1, No.4, PP.275-289, July 1997.

[3] C.W. LEON, "Digital and Analog Communication System", 5th ed.1997, prentice Hill, Inc.

[4] J. Proakis, "Digital Communication", McGraw-Hall, Inc., 2002.

[5] R.L.Picholtz and D.L.Schilling, and L.B.Milstein, "Theory of Spread – Spectrum Communication – A tutorial", IEEE Trans. Commun., Vol. COM-30, No. 5, pp.855-884, May 1982.

[6] A. J.Viterbi, "Spread Spectrum Communication –Myths and Realities", IEEE Commun. Mag., Vol. 17, No.3, PP. 11-18, May 1979.

[7] S. Haykin, "Communication System", Forth Edition, John Wiley and Sons, Inc., 2001.

[8] T.S.D.Tsui and T.G. Clarkson, "Spread Spectrum Communication Techniques", Electronics and Commun. Eng. Journal Vol.6, No.1 PP.3-12, Feb.1994.

[9] C.E.Cook and H.S.Marsh, "An Introduction to Spread Spectrum", IEEE Commun. Magazine Vol.21, No.2, PP. 8-16, Mar. 1983.

[10] H.N.AL-shammary, "Design and Implementation of Direct Sequence Spectrum System Using Field Programmable Gate Array", Msc. Thesis, Department of Electrical Eng., University of Technology, 2004.

[11] S.K.Gharkan, "Performance of Direct Sequence Spread Spectrum Signal", Msc. Thesis, University of Technology, ALRasheed College of Engineering and Science, Electrical and Electronic Department, 2005.

[12] R.C.Dixon, "Spread Spectrum System", New York: John Wiley and Sons Inc. 1984.

[13] C. E. Shannon, "Communications in The Presence of Noise", Proceedings of the IRE, Vol.37, No.1, PP.10-21, Jan.1949.

[14] R. A. Scholtz, " The Origin of Speared Spectrum Communication", IEEE Trans. Comm., Vol. 30, No. 5, PP. 822 – 854, May 1982.

[15] P. J. Munday, and M. C. Pinches, “Jaguar-V Frequency-hopping Radio System”, Proc. of IEE, Vol.129, No.3, PP.213-222, June 1982.

[16] S.J.M.AL-Muraab, “Implementation of Frequency Hopping Spread Spectrum Technique in Communication System”, M.Sc. Thesis, Department of Electrical Engineering, University of Baghdad, 1986.

[17] C. Meng, and L.B.Milstein, “Channel Equalization and Performance Analysis of A Coherent Frequency Hopped Spread Spectrum System”, IEEE Journal on Selected Areas in Communication, Vol.7, No.4, PP.548-560, May 1989.

[18] S. G. Glisic, and L.B.Milstein, “Discrete Tracking System for Slow FH; Part I-Algorithms with Distributed Synchronization Group”, IEEE Trans.Commun., Vol.39, No.2, PP.304-313, Feb.1991.

[19] S. G. Glisic, and L.B.Milstein, “Discrete Tracking System for Slow FH; Part II- Algorithms with Distributed Synchronization Group”, IEEE Trans.Commun., Vol.39, No.2, PP.314-322, Feb.1991.

[20] L. E. Miller, and J.S.Lee, “Analysis of an Antijam FH Acquisition Scheme”, IEEE Trans. Communication., Vol.40, No.1, PP.160-170, Jan.1992.

[21] D. E. Borth, P.D.Rasky, G.M,Chiasson and J.F.Kepler, “Frequency Hopped System for PCS” Proc.of IEEE, 3rd International Symposium on spred Spectrum Techniques and Applications,Vol.1, PP.105-114, Finland, 4-6 July 1994.

[22] X. Chen, Y.Li, and S.Chng, “Frame Synchronization by De-Correlation Detection,” International Conference on Communication Technology, Chia, Oct.22-24, 1998.

[23] J. Min, H.Samuel, “Analysis and Design of A FH/SS Transceiver for Wirless Personal Communications”, IEEE Transaction on vehicular Technology, Vol.49, No.5, PP.1719-1731, September 2000.

[24] M. R. Subhi, “practical Implementation of Frequency Hopping Synchronization System”, M.Sc.Thesis, Department of Communication

and Electronic Warfar, Military Engineering Collage, 2002.

[25] H. K. Hammed, "Design and Implementation of a Frequency Hopping Communication System for Both Speech and Data at High Bit rate", M.Sc.Thesis, Department of Communication and Electronic Warfar, Military Engineering Collage, 2002.

[26] H. K. Chail, "Design and Implementation of Branch Hopped Wavelet Packet System", Ph.D. thesis, University of Technology, ALRasheed College of Engineering and Science, Electrical and Electronic Department, 2003.

[27] A. M. AL-FHAAM, "Fast and Multicarrier Frequency Hopping Signals Over Frequency Selective Rayleigh Fading Channel". MSc. Thesis, University of AL-Mustansyriah, Baghdad, 2004.

[28] Khalid Awaad Humood, Adham Hadi Saleh, Wa'il A. H. Hadi "Theoretical Design of MIMO Transceiver &Implementation Its Transmitter Using FPGA "Diyala Journal of Engineering Sciences, Vol. 07, No. 04, PP. 115-131, December 2014.

[29] Khalid Awaad Humood, Saad Mohammed Saleh, Wisam Najm Al-din Abed," Design of 2 ×4 Alamouti Transceiver Using FPGA," International Journal of Engineering Research & Technology (IJERT) ISSN: 2278-0181 IJERTIJERT www.ijert.org Vol. 3 Issue 11, November-2014.

[30] Hayder Khaleel AL-Qaysi, Tahreer Mahmood, Khalid Awaad Humood," Evaluation of different quantization resolution levels on the BER performance of massive MIMO systems under different operating scenarios", Indonesian Journal of Electrical Engineering and Computer Science. Institute of Advanced Engineering and Science (IAES), Vol. 23, No. 3, September 2021, pp. 1493~1500.

[31] Tahreer Mahmood, Omar Abdulkareem Mahmood & Khalid Awaad Humood. "An efficient technique to PAPR reduction for LTE uplink using Lonzo's resampling technique in both SC-LFDMA and SC-DFDMA systems". Applied Nanoscience,14 September 2021.

[32] M.Ahmed , Z. Hanli,M.Sumit and D.Babak, " Wireless Field Trail Results of a High Hopping rate FHSS-FSK Testbed ", IEEE Journal on selected areas in commun . Vol.23, No.5.PP 1113 - 1122 May 2005 .

[33] F. William Utlaut , " Spread Spectrum Principles and Possible Application to Spectrum Utilization and Allocation ", IEEE Commun .Society Magazine Vol.16, No.5 PP 21-31Sep.1978.

[34] G. R. Cooper, and C.D.McMillan, "Modern Communication and Spread Spectrum", New York: McGraw- Hill, 1986.

[35] S. Anokh and A. K. Chhobra, "Principles of Communication Engineering", S.chand and Company Ltd Ramnagar, New Delhi, Sixth Revised Edition 2004.

[36] F.Behrouz, C.Catherine, and F.C.Sophia, "Introduction to Data Communications and Networking ",Ch.5, WCB McGraw-Hill Companies, Inc., 1998.

[37] S.M.AL-shammary, "Designed and Simulation of Low Setting Time Digital Synchronization",M.Sc.Thesis, University of Technology AL-Rasheed College of Engineering and Science, Electrical and Electronic Department ,2005 .

[38] J.R.Smith, "Modern Communication Circuits", Second Edition, McGraw-Company, 1988.

[39] A.Rofougaran, "A Single-Chip Spread-Spectrum Wireless Transceiver in CMOS", Final Report, Integrated Circuits and Systems Laboratory Electrical Engineering Department University of California Los Angeles, A 90095-1594, December 1998.

[40] Chapter III: CDMA, University of Applied Sciences, (http:/www2ing.puc c1/~ iee 3552 spread- spectrum pdf, 2000).

[41] T.S.Rappaport, "Wireless Communications Principle and Practice", Second Edition, prentice-Hall, Inc, 2000.

[42] D.L.Nicholson, "Spread Spectrum Signal Design and A.J. System", Computer Science Press, Inc. Copy right 1988.

[43] M.P.Ristenbatt, J.L. Daws, JR., " Performance Criteria for Spread Spectrum Communication", IEEE Transaction on Communication, Vol. 25, No.8,PP.756-763, Aug.1977.

[44] L. B. Milstone, "Interference Rejection Techniques in Spread Spectrum Communications", Proc. IEEE, Vol. 76, No.6, PP. 657-671, June 1988.

[45] E. B. Felstead, "Follower Jammer Considerations for Frequency Hopped Spread Spectrum", Communications Research Center, Ottawa Canada, emil: barry.felstead@crc.ca 1998.

[46] S. Rappaport and D.Grieco, "Spread Spectrum Signal Acquisition: Methods and Technology", IEEE Communication Magazine, Vol. 22, No. 6, PP.6-21, June 1984.

[47] Hussain K. Chaiel,Mohhamed H Ali, Saad M.AL-Shammary, "FastDirect Digital Synthesizer", University of Technology ,Baghdad , Iraq , emil:hankamel -2005@ yahoo.com. 2005.

[48] Johanthan Min, "Analysis and Design of Frequency-Hopped Spread-Spectrum Transceiver for Wireless Personal Communications" Final Report, University of California, Jan.1996.

[49] Z. Galani, R.A.Campell, "An Overview of Frequency Synthesizers for radar", IEEE Transactions on Microwave Theory and Techniques, Vol.39, No.5, PP.782-790 May 1991

[50] J.R. Alexovich and R.M. Gagliardi, "Effect of PLL frequency synthesizerin FSK frequency–Hopped Communications", IEEE Transactions Vol.37, No.3, PP 268-276, Mar. 1989.

[51] J. Min and H.Samuel, "Synchronization Techniques for a Frequency – Hopped Wireless Transceiver", Vehicular Technology Conference, IEEE 46th, Vol.1, PP 183-187, May 1996.

[52] Khalid Awaad Humood, Adham Hadi Saleh, Wurod Qasim Mohamed, "Design & Implementation of OP-AMP RC Sine Wave Oscillator", Diyala Journal of Engineering Sciences, ISSN 1999-8716, Vol. 08, No. 01, PP. 89-901, March 2015.

[53] Khalid A. Humood, Omar A. Imran, Adnan M. Taha, "Design and Simulation of High Frequency Colpitts Oscillator Based on BJT Amplifier" International Journal of Electrical and Computer Engineering (IJECE), Vol. 10, No. 1, February 2020, PP. 160-170.

[54] "Simulink Block Library of The Communication Tool Boxes Reference", The Math Work Inc. 2002.

[55] S.K.Mitra, "Digital Signal Processing: A Computer-Based Approach",

McGraw-Hill, 1998.

[56] C. Marven and G.Evers, "A Simple Approach to Digital Signal Processing", Copyright © 1996, John Wiley and Sons, Inc.

[57] C. T. GHEN, "Digital Signal Processing", Copyright © 2001 by Oxford University Press, Inc.

[58] L. C. Ludeman. "Fundamentals of Digital Signal Processing", Copyright 1986 by Harper and Row, publishers, Inc.

[59] E. Strom, and Tony, ''An Introduction to Spread Spectrum System, Technical Report Department of Signal and System, Chalmers University of Technology, SE-4296 Goteborg, Sweden,2nd Corrected Printing, January ,7 2004.

[60] Khalid Awaad Humood, Wurod Qaism &Farah Hammed, "Design Analog RC- Active 2nd Order Audio Low Pass Filter (LPF)", First engineering scientifc conference college of engineering- university of diyala 22-23 December 2010, PP.485-498, issn 1999-8716.

[61] Khalid A. Humood ," Design Second order Switched Capacitor Band Pass Filter " , Scientific Journal of The Bulgarian Academy of Sciences , Engineering Sciences, XLIX, 2012, No. 3 , PP.38-54.

[62] "Introduction to Spread Spectrum Communications", http:/www.course.ie.cuhk.edu.hk/~ieg30109/ch5pdf, 2000.

[63] K. C. Teh, Alex C. Kot and K. H. Li, "Multitone Jamming Rejection of FFH/BFSK SELF-Normalizing Receiver", School of Electrical and Electronic Engineering Nanyang Technological University,2001, Singapore 639798 E-mail: eackot @ ntu.edu.sg.

[64] NIIT, "Introduction to Digital Communication Systems", Prentice-Hall of India Private Limited, 2004.